Papers presented at

UNDERWATER WET WELDING AND CUTTING

International seminar and workshop
TWI North, Middlesbrough, UK
17-18 April 1997

TWI (UK)
in conjunction with
PWI (Paton Electric Welding Institute, Ukraine)

ABINGTON PUBLISHING
Woodhead Publishing Ltd in association with The Welding Institute

Published by Abington Publishing
Woodhead Publishing Ltd, Abington Hall, Abington
Cambridge CB1 6AH, England
www.woodheadpublishing.com

First published 1998

British Library Cataloguing in Publication Data
A catalogue record for this book is available from the British Library.

ISBN-13: 978-185573-388-6
ISBN-10: 1-85573-388-9

Printed by Victoire Press, Cambridge, England.

PWI activities in the field of underwater welding and cutting technologies

B E Paton, E O Paton Electric Welding Institute

We cannot say now that underwater welding and cutting of metals is nothing but an idea. Far from that, many famous institutions and companies of the world worked hard and not without a success in this field of science and technology. Their efforts resulted in having an early insight into the essence of the phenomena taking place during the above processes, in a number of efficient devices developed for underwater welding and cutting and, which is not less important, in identification of difficulties to be handled to have a fundamental progress in this area.

The Paton Electric Welding Institute of the National Academy of Sciences of Ukraine also made a substantial contribution into the advancement of the underwater technology.

The continuous progress in the R & D conducted with the purpose to repair and fabricate off-shore metal structures is no mere chance. Underwater welding finds an increasingly wide application. Erection and construction of rigs for production of oil, gas and other mineral resources from the sea bottom, lifting and repair of ships, salvage and rescue operations, laying down of underwater pipelines, periodic servicing and repair of port structures and bridges - by no means this is a complete list of examples of the application of underwater welding. The requirements to the quality and reliability of welded joints which were made and are operating under the water become more and more stringent. Welds made in the up-to-date critical-application off-shore metal structures should not be inferior in the level of their properties to those made on earth, nor should they have any significant difference from the latter. At the same time, physico-chemical and metallurgical processes which occur during underwater welding take place under the most severe, extreme conditions. These conditions are characterized by an intensive heat removal, considerable saturation of molten metal with hydrogen and an increased ambient pressure. This requires that the comprehensive theoretical and experimental research be conducted, which would allow for peculiarities of the underwater welding conditions. The R & D efforts in this area should include investigation of the effect of cooling rate, hydrogen saturation, hydrostatic pressure and other factors upon the process of welding and the quality of resulting joints. Studies should be made of weldability of steels. It is necessary to develop special welding consumables, methods and procedures. The above efforts should also include elaboration of the basic principles for mechanization and automation of the process and development of the systems for remote control and monitoring.

Underwater welding is traditionally subdivided into wet and dry welding depending upon conditions under which it is carried out. Wet welding is performed directly in the water, i.e., without any isolation of an electrode, the arc or a workpiece from the environment. Dry welding is performed under conditions where the welding zone is fully isolated from the water. Specialists in underwater welding are well aware of these aspects of the process. But an important point here is that

the development of underwater welding in all the industrialized countries, including the former Soviet Union, began from the wet method.

The USSR undertook its pioneering studies in the field of underwater welding as early as in the 1930s. The technology for manual underwater arc welding using a consumable electrode was developed by K.K.Khrenov in 1932. This technology found its way into practical application for conducting repair, salvage and rescue operations.

The first post-war years were characterized by the use of only manual arc welding. The initial attempts to upgrade the method were aimed at the improvement of the existing electrodes and the development of the new ones, primarily those which could neutralize the adverse effect of hydrogen absorbed by a weld and provide an increase in the capacity of the process. The outcome of these efforts was the development of the EPO-55 grade electrodes for welding low-carbon steels, which allowed the productivity of labour of a welding diver to be raised by about 15 %. Such electrodes, however, could not be used for welding in the positions other than the flat one.

The experience accumulated by the middle of the 1950s revealed drawbacks of the manual arc welding used at that time. The method could not ensure the consistent strength of welded joints. For instance, the spread of the tensile strength values amounted to 60-70 %. The capacity of the process estimated from the welding speed remained low and did not exceed 2 m/h. Skills and personal qualities of a welding diver had a high effect on soundness of a weld.

These problems were characteristic of the type of the works conducted in other countries as well. Western companies, having faced an apparent impossibility of ensuring the full-strength welded joints by the wet method, preferred then the dry welding and did achieve the high-quality joints in those types of the operations where the dry welding was feasible. Nonetheless, the method of manual wet welding was not rejected, although it could not help resolve the problem in principle. Till now this method is used primarily to repair only the non-critical off-shore objects or in emergency situations.

At the same time, the former USSR, mostly Ukraine and Russia, continued their exploratory works, fundamental and applied research only in the field of the improvement of wet underwater welding. Since 1965 the Paton Electric Welding Institute has been very active particularly in this field. With time we established a special laboratory for the technologies of underwater welding and cutting of metals. The basic achievements of the laboratory will be described in the other presentations that will follow. Currently the laboratory is equipped with the chambers that simulate the deep water, used for the research, with a water tank, the specialized welding equipment and the computer facilities. Also the laboratory incorporates a diving station. Our welding divers participate both in the research and in practical works the demand for which gradually increases. An active role in the establishment of the laboratory, its equipping and training of the scientific staff was played by Prof. A.E.Asnis and Dr. I.M.Savich. For the developments in the field of underwater welding they were awarded a title of laureates of the State Prize of Ukraine. At present the laboratory is headed by Prof. Yu.Ya.Gretsky.

Now we will dwell in more detail on the activity of the laboratory. From the very beginning its purpose was to mechanize the welding and cutting processes. The initial experiments we conducted resulted in formulation of our own criteria. We concluded that semi-automatic welding using solid steel wire and CO_2 shielding of

molten metal presented great difficulties but held no promise (the bending angle of welded joints could not exceed 50 deg). Manual welding seemed not promising either, especially for critical applications because of low ductility of weld metal (elongation - not more than 9 %). It was then that we had an idea of developing a basic technology of wet welding using self-shielding flux-cored wire.

This idea was favoured by the evident advantages of such an approach. The nature of the flux-cored wire is such that its chemical composition can be varied over the wide ranges. This offered us a possibility of having dense and strong welds without any additional gas or flux shielding of metal. The reliable shielding could be provided by the wire itself, i.e., by the proper selection of its chemical composition. We believed that the problem of hydrogenation of weld metal and the heat-affected zone, as well as the consequences of this phenomenon, which were already well-known, could be handled if not completely then at least partially, through a special design of the flux-cored wire. Whereas an electrode coating is in a direct contact with water and, hence, is moistened, the core of the flux-cored wire is protected by a sheath. It is an advantage of this wire with regard to one of the sources of the hydrogen saturation. Then, the development of the self-shielding wire meant elimination of extra devices which made the torch heavier and the work of a welding diver more difficult and which eventually greatly simplified the basic operations. Handling the above problem on the basis of using the flux-cored wire provided a combination of manoeuvrability and versatility of manual welding with the advantages characteristic of the semi-automatic welding. It was evident that with this method we could solve the problem of continuity of welding operations, provide a fundamental increase in the productivity of labour of a welding diver and reduce the time of a stay of a human being under the water. Additionally, it was known that the semi-automatic welding could be mastered under conventional conditions much quicker than the manual welding. This advantage must also show itself under the underwater welding conditions. Therefore, the above idea accounted also for a human factor. This could simplify choosing and training of people for performing the underwater welding.

Validity of these assumptions was proved in the process of the work that followed.

The fundamental research aimed at the development of the method of wet welding based on the above assumptions comprised the following efforts. Our associates studied peculiarities of the arc burning under the fresh water and water having different salinity. They identified conditions for ensuring the stable arc burning process under different hydrostatic pressures and determined a composition of waste gases and their interaction with molten metal at the high oxidation potential of the atmosphere in a vapour-gas bubble. They studied the effect of alloying upon a structure and properties of weld metal and peculiarities of transfer of alloying elements from a consumable electrode to weld metal directly in the water. The laboratory staff determined conditions for elimination of porosity and non-metallic inclusions in weld metal, the effect of hydrostatic pressure and welding parameters upon the level of mechanical properties of welded joints and upon the quality of a cut and economical indices of mechanized underwater arc cutting of steels and non-ferrous metals. Much attention was given to selection of an optimal wire diameter, rational parameters of underwater welding and cutting and a procedure for making butt, fillet and overlap joints in all spatial positions. We could continue listing the works done at our lab. We hope, however, that what was said above is enough to show that the developments of the technologies for underwater welding and cutting done at the Paton Welding Institute are based on the results of the comprehensive and purposeful research.

As a result of the efforts made in the field of consumables now we can offer a flux-cored wire for wet welding of low-carbon and low-alloy steels with a tensile strength to 500 MPa intended for the depth down to 20 m and a flux-cored wire for arc cutting of steels and alloys at the depth down to 60 m in the fresh and sea water. Under the said conditions the developed self-shielding flux-cored wire provides a sufficiently high level of strength of welded joints and, what is most important, the level of ductility of weld metal which meets the requirements of Class A of the commonly recognized underwater welding ANSI/AWS-23.6 Specifications worked out by the American Welding Society in collaboration with the world-leading specialists.

We never stopped investigations in the field of manual welding. So, now we can offer the new electrodes which we developed and manufactured ourselves. They are characterized by a possibility of performing welding in any spatial position. Unlike other existing electrodes, they provide a sufficiently high level of ductility of weld metal. With these electrodes the value of elongation is stable and equal to 12-14 %, while the bending angle both on the side of a weld root and on the face side of a weld is equal to 180 deg. Therefore, these electrodes guarantee the quality of welded joints on a level not lower than that required of Class B of the above Specifications. As far as our developments in the underwater arc cutting are concerned, three types of the flux-cored wires are available now and ready for commercial application. All of them are used without additional feeding of oxygen into the arc zone. Available also are rod and tubular electrodes and the so-called 'exothermic electrodes' which can be used not only for severing of steels, but also for cutting of non-metallic materials, such as plastics and wood.

In our opinion the equipment for underwater wet flux-cored wire welding and cutting developed by engineers and designers of the Paton Welding Institute can be called unique. A special feature of the developed semi-automatic device is that its wire feed mechanism is immersed into the water and, during operation, can be located as close to a welding diver as possible. Welding divers highly appreciated the positive features of this design from their many-year experience of operation with the model A-1660 device. Nevertheless, still there are the reserves for a further improvements to be made in this semi-automatic device. This subject will be covered in a separate presentation.

One of the lines of the research conducted at our Institute is underwater flash butt welding of steels. The Institute has been active in the R & D in this area for the last four years. By now we managed to demonstrate the possibility of using flash butt welding to join pipes under the water for the fabrication and repair of off-shore structures and pipelines.

We hope that the use of this technology will allow us:

- to eliminate a direct participation of welding divers in carrying out underwater welding and to fundamentally reduce the costs incurred to ensure the safety of their labour;
- to improve reliability of welding operations;
- to ensure the high and consistent quality of welded joints and to exclude the effect of the welder's skills and labour conditions on the quality of joints;
- to eliminate the effect of hydrostatic pressure on the quality of welded joints;
- to simplify the quality inspection procedures.

Being encouraged by the positive results of the pilot-commercial testing of the laboratory developments, we continue our work in this area.

Returning to the discussion of the wet arc welding and cutting, we have to dwell on the problems encountered when using these technologies. In the fluxcored wire welding this problem can be considered to be solved now for relatively simple (from the standpoint of weldability) low-carbon and low-alloy steels with the average yield strength of 350 MPa. Welded joints with a strength equal to that of parent metal can be made at the depth down to 20 m. However, the life is going on and now the demand has arisen for reliable welding of the increased strength steels at the larger depths (down to 50-60 m). We hope that the developed approaches and the accumulated knowledge and experience will allow us to solve these and even more complicated problems which may arise in repair of off-shore pipelines.

Another topical problem is underwater welding of stainless steels. In nuclear power stations, under the high radiation conditions, it is necessary sometimes to perform welding operations on metal structures from austenitic steel of the Kh18N10 type. To decrease the harmful radiation effect it is advisable to cover such structures with a layer of water so that welding could be performed under such a layer.

It is known from proceedings of international conferences that the USA and Japan are active in looking for a solution for this problem. The activity of these countries in this area includes evaluation of the existing electrodes from the point of view of their suitability for underwater welding of stainless steels. However, the problem of making sound welded joints free from pores and cracks has not been solved as yet. In case if the problem is handled by adapting the technology of manual welding to the given conditions, because of low productivity of this method and a limited time during which a welding diver can stay near a radiation source, a diver will have to go into the water too many times to perform the required amount of the works. Drawbacks of such an approach are evident. Evident also is the expediency of mechanization and automation of the process to minimize the human labour near the radiation source. We suppose that our experience could be helpful in this respect. The research done at the Paton Welding Institute proves the feasibility of underwater flux-cored wire welding of stainless steels. We believe that the success in finding a solution for this problem could be the onset of a breakthrough in the field of mechanized wet underwater welding and promote the progress in automation of the process on the basis of the current achievements.

Another point that should be mentioned in this connection is an extent of confidence people have in wet welding as a whole and underwater flux-cored wire welding in particular. We are glad that the International Workshop on Underwater Welding of Marine Structures held in New Orleans, Louisiana, USA, from 7 to 9 December 1994 recognized the underwater wet flux-cored wire welding as a very promising method. Of course, such an assessment is well grounded. This method, when used under conditions it was qualified for, i.e., directly in the water, provided ductility of metal on the level of requirements of Class A of the ANSI/AWS D3.6 Specifications. Pipelines repaired using the flux-cored wire at the bottom of some rivers in the CIS countries have been reliably operated for about 20 years. The method is successfully used for repair of the ships afloat. Investigation of the long-term fatigue strength of underwater welded joints subjected to cyclic loading shows that they are not in the least inferior to those made under conventional conditions using stick electrodes. These results confirm that the wet flux-cored wire welding is worthy of further development and upgrading to increase confidence in the process. This shows that the sphere of activity where we can apply our joint efforts is very wide.

Study of physico-metallurgical peculiarities of wet arc welding of structural steels

K A Yushchenko, E O Paton Electric Welding Institute
Yu Ya Gretskii, E O Paton Electric Welding Institute
S Yu Maksimov, E O Paton Electric Welding Institute

INTRODUCTION

By now we cannot declare that physical phenomenon and metallurgical peculiarities of underwater welding remain absolutely unknown. It is just the contrary: due to research and development of many investigators of well-known institutions, including the E.O.Paton Electric Welding Institute (PWI), the significant volume of works has been performed which allowed to obtain the valuable information in this field. Of course, at that moment we are interested more in scientific basis of wet welding, since the Underwater Welding and Cutting Seminar is devoted just to this problem. If shortly, the formed views of the wet welding peculiarities are in general as follows.

The physical properties of water that differ it from air mainly define a character of welding arc process proceeding. The necessary condition for arc existing is presence of vapour-gas bubble which is formed around the arc. It appears at the moment of electrode touching to base metal at the expense of heating the contact area by transmitted current. After an electrode breaking off, the arc appears inside bubble. The gas formed by the decomposition of electrode coating material, the evolution of gases from the base material and electrode, and the dissociation of water in the arc cause the bubble to grow. Owing to arc burning, the volume of bubble rises up to critical size, then a bigger part of bubble (80...90%) comes to the surface and a new bubble begins to form. The radius of bubble changes from minimum to critical sizes in the range of 0.7...1.65 sm in fresh water and in the range of 0.8...0.23 sm in salt water. Gas exchange process inside the bubble is rather intensive and gas bubble composition is considered to be renewed 8...10 times per second. The big amount of hydrogen in the bubble atmosphere, elevated hydrostatic pressure and cooling effect of peripheral gas flows cause a constriction of welding arc. Because of the arc constriction, the current density can reach value of 11200...14280 A/sm^2 that is of 5...10 times higher then the value of current density in welding with electrode of the same diameter in air. The temperature drops is suggested to be in the range of from 2560°C up to temperature of metal boiling.

The bubble gas is composed of 62...92 % hydrogen, 11...24 % carbon monoxide, 4...6 % carbon dioxide, oxygen, nitrogen and traces of gaseous metals. Because the arc atmosphere is high in hydrogen content, the susceptibility to hydrogen embrittlement becomes especially critical.

The cooling rate of weldment areas is an average of 2...3 times higher then that in air - of the order of 200...300 °C/s. The rapid cooling effect results in high HAZ hardness, low HAZ impact strength due to formation of quenching structures, weld metal porosity and slag inclusions, and unfavourable weld shape.

Hydrostatic pressure of surrounding water has a marked influence on the thermodynamics, kinetics and equilibrium of all of the many complex reactions

proceeding in the arc and weld pool. Water pressure increases the solubility of gases in molten metal, and so, underwater wet welds contain more hydrogen and oxygen with water depth increase. As the result, porosity and non-metallic inclusions become a more serious problem when welding in deeper water.

Therefore, in underwater wet welding, the above said reasons create the significant difficulties in obtaining in-air-quality welds.

Developing the wet welding consumables and technological processes, the research workers of the PWI has investigated a number of above questions applying to flux-cored and manual welding. The main results of these investigations are reported bellow.

ELECTRO-PHYSICAL PECULIARITIES

In spite of specific conditions of underwater electric charge, the physical processes taking place in the arc are in a high degree similar to ones occurring on open welding arcs. So, using the high speed filming (1) and x-ray-filming (2) simultaneously with voltage and arc current oscillography, it has been established that the electrical regime of arc is constant at invariable distance between electrodes in spite of significant vapour-gas bubble pulsation occurring periodically. That fact confirms the negligible dependence of processes taking place in the arc on distance between arc column and bubble wall. The results of the high speed filming and x-ray filming show that sizes of bubble are bigger then sizes of arc column. Therefore, it is possible to consider the underwater arc as a free one, if its development in the bubble is not limited by electrode sizes or the arc is not blown by gas jet and is not constricted by special nozzle (3). On this base the equations of channel model of open arc can be used for estimation of main arc characteristics by underwater welding if the number of additional peculiarities are taken into account (3). Calculation data and experimental results show that the arc voltage increases on the average by 1.5...2 V with depth increase per every 10 m in the range of 0...100 mwd and on the average by 4.5...5 V per every 100 m in the range of 100...300 mwd (3). Comparison of obtained voltage on operation depth Ua=f(H) with experimental data of Japan investigators (4) showed the good correlation.

The peculiarities of arc burning and metal drop transfer at underwater flux-cored wire welding were studied using specialised microcomputer-based analyser ANP-2 which permits the arc electric and time parameters to be measure and the information acquired a statistically processed form to be presented on graphic and digital displays. The investigation shown (5) that the duration and the frequency of short-circuits and arc extinction significantly grow with the increase of the operation depth; the process stability deteriorates. The observed rise of welding current is associated with the increase in the quantity of short-circuits. Addition of rare-earth metals into the charge of flux-cored wire provides the considerable improvement of arc stability and almost two times reduction of arc downtime (arc extinctions and short-circuits). These questions are considered more detail in the report about technological peculiarities of wet semi-automatic welding with flux-cored wire.

Changes of main parameters of arc and arc gap depending on water depth have been investigated theoretically with the help of physico-mathematical modelling. These calculations have been performed in the wide range of operation depths (see Table 1). The character of change of arc column temperature, arc length, arc column radius and drop radius is given in Fig.1. These data show that the most

significant changings of arc parameters are expected at the first 300...400 m of submerging. The process parameters are believed to be stable at further increase of hydrostatic pressure.

Table 1 Dependencies of arc parameters on operation depth

Operation depth, m	0	20	100	280	820	2440
Arc column temperature, K	8170	8550	8950	9370	9810	10270
Arc length, mm	2.5	2.08	1.73	1.45	1.2	1.0
Arc column radius, mm	1.1	0.92	0.76	0.63	0.53	0.44
Drop radius, mm	1.98	1.89	1.79	1.67	1.55	1.38

Estimation of the static volt-ampere characteristic is one of the basic questions of study of welding arc properties. The investigations have been performed as applied to wet MMA welding with stick electrodes of 4 and 6 mm in dia. and wet semi-automatic welding with thin solid wire. The static volt-ampere characteristics of arc burning under water proved to be of concave form (Fig.2). The minimum value of Ua corresponds to current value in the range of 130...200 A depending on electrode diameter and arc length. Proceeding from concavity of volt-ampere characteristic, underwater burning arc is submitted to common lows of arc charges. The concavity of volt-ampere characteristic of arc burning under water is explained by constriction of the arc: 1) at the expense of cooling action of hydrogen and hydrostatic pressure; 2) at the expense of cathode spot constriction with welding current increase because of scantiness of geometrical size of electrode tip.

Oscillography of welding processes performed in fresh and sea water permitted to determine an increase in stability of process and reduction of arc ignition time with water salinity rise. The ignition time is equal to 0.98 s in fresh water, and it is equal to 0.56 s and 0.36 s at water salinity of 30‰ and 41‰ correspondingly (6). According to obtained data, it is more difficult to provide arc process stability and high quality of welded joints when welding in fresh water than in sea water. The stabilising effect of sea water is explained by presence of dissociated salts. The point of view about negative influence of chlorine as not mobile anion on arc charge stability has been corroborated. Due to the specific conditions and low-mobility of chlorine ions the letters have not time to exhibit their depressing influence on arc or the influence of chlorine is not enough to disturb the stability of arc burning in sea water. It is also suggested (6), that chlorine ions partly re-combinate with hydrogen being in water and escaping because of dissociation, forming the very volatile HCl compound. In such a way the ions of chlorine are carried away from arc zone.

By now the power sources for underwater welding are installed on the board of ship. Due to that, it is impossible to bring the power sours nearer to place of work performance. As the result, the length of external electric circuit, especially when welding at the large depth, is of significant sizes. Due to that the arc voltage drops significantly and flatness of power source external characteristic decreases. As the result, the arc stability is deteriorated then welding with semi-automatic machine having constant rate of electrode wire feeding. In this connection, analysis of possibility of following to indicate the typical disturbances on arc length by self-regulating system in underwater mechanise welding had been performed (7). The calculations of total electric resistance of external welding circuit as applied to semi-automatic welding conditions had shown that the rigidity of external volt-ampere power source characteristic decreases essentially with depth increase (Fig.3). As the result, coefficient of stability of system "power source-arc" (Ks)

increases essentially. Therefore, the duration of action in response to arc length change (τa) increases with depth increase and, so, the self-regulation severity decreases. However, the system of self-regulation of underwater arc remains stable for all the depths investigated (Table 2).

Table 2 Calculation data of arc self-regulation intensity at different depths

Depth, m	Electric resistance of external circuit, Ohm.	Open circuit voltage, V	Steepness of external power source characteristic, V/A		Coefficient of stability Ks, V/A	Duration of action τa, S
			Power source	Arc		
0	0.049	39...41	-0.01	-0.059	0.059	0.292
40	0.108	62...65	-0.01	-0.118	0.118	0.429
100	0.167	80...84	-0.03	-0.197	0.207	0.619
160	0.226	100...104	-0.04	-0.266	0.306	0.811
220	0.285	118...120	-0.06	-0.345	0.435	1.013

These investigations have shown that the velocity of transition processes proceeding in the system of self-regulation at the semi-automatic underwater welding depends on the steepness of external volt-ampere power source characteristic, on the field strength of arc column, and on the field strength of arc column, and on the values of self-regulation coefficients for welding current and arc voltage. These facts are known for welding in air. But, the peculiarity of self-regulation process in underwater welding is that the resistance of external circuit is so large and its influence on reduction of self-regulation severity is so significant that effect of field strength of arc column and coefficient of current self-regulation on the self-regulation are less noticeable than those in air welding. Therefore, the reduction of resistance of external welding circuit is the most effective method for increase of response of arc self-regulation (and for improving of weld quality), especially in welding at the large depths.

One of the most significant aspects of underwater wet welding problem is interaction of molten metal with gases, in particular the unavoidable saturation of liquid metal by hydrogen up to 55...60 $sm^3/100$ g (8,9). Hydrogen amount in departing gases is determined by value of 62...95% depending on welding conditions (8, 10, 11, 12).

To reduce the hydrogen amount in vapour-gas bubble atmosphere and, therefore, in the deposited metal, or to neutralise partially its harmful effect is possible by several ways: introduction of such components into flux-cored wire charge or into stick electrode coating, which reduce a hydrogen partial pressure at the expense of bubble atmosphere dilution by another gases; a use of special shielding gas; variation of welding parameters (current, voltage, arc length and so on); application of the consumables providing formation of weld metal structure characterised with negligible sensitiveness to hydrogen saturation.

At the wet welding, the hydrogen partial pressure can be reduced in two known ways: 1) with obtaining different gases in atmosphere of arc in the process of consumable melting and 2) with combining of insoluble hydrogen in strong chemical compounds, insoluble in liquid metal. Both of these methods have been evaluated under conditions of manual welding.

The first method has been investigated, changing the ratio of amounts of rutile and marble (9). As seen from Fig.4, dissociation of marble results in increase of CO and CO_2 concentrations and, correspondingly, in decrease of hydrogen concentration in the composition of departing gases. The partial pressure of hydrogen proved to be the controlling factor at his amount upward of 60% and the presence of another gases does not influence on the degree of saturation of molten metal with hydrogen (Fig.5).

According to the second method, we tried to reduce the hydrogen amount at the expense of interaction of hydrogen and water vapour with fluoric compounds and formation of thermostable hydrogen fluoride. With this aim, fluorite was added to rutile base coating (13). It has defined that the hydrogen concentration in weld metal decreases monotonously with rising of calcium fluoride amount in the all range (0...86% CaF_2) of investigated coating compositions (Fig.6). Such result is an evidence of hydrogen and water vapour interaction with calcium fluoride, the formed hydrogen fluoride exuding from molten metal.

The obtained data concerning influence of fluorite on composition of escaping gases are indirect evidence of rightfulness of above said point of view related to mechanism of interaction of compounds in the arc atmosphere (Fig.8). Because the ratio of concentrations of gases consisting the bubble atmosphere remains practically constant in the all range of investigated coating compositions, it can be declared that the decrease of diffusible hydrogen amount with increase of calcium fluoride takes place due to binding of hydrogen in insoluble chemical compound HF rather than at the expense of arc atmosphere dilution with another gases.

From comparing of the results obtained in the both of series of experiments (Figs. 5-7), it is followed that the introduction of CaF_2 into rutile base electrode coating decreases the diffusible hydrogen amount in the deposited metal more essentially than addition of $CaCO_3$. So, even at 20% $CaCO_3$ in electrode coating, the diffusible hydrogen amount remains the same how it is in the case of purely rutile coating (54 $sm^3/100$ g). At the same time, the equal quantity of CaF_2 (20%) gives the $[H]_{diff}$ amount less by 26%. Therefore, the method for reduction of weld metal hydrogen content at the expense of its combining with fluorine for underwater takes place in underwater conditions as well and is more effective than the method of arc atmosphere dilution with gases evolving due to decomposition of carbonates being in electrode coating.

Proceeding from obtained data, it was naturally to expect that the electrodes with basic coating will allow to obtain welds having less diffusible hydrogen content as compared to the electrodes with rutile coating. Therefore, the assessment of $CaF_2/CaCO_3$ influence on the diffusible hydrogen content was performed. Figure 8 shows the obtained results. It is seen that the maximum content of diffusible hydrogen corresponds to approximately equal amounts of CaF_2 and $CaCO_3$ in coating. Increase of parts of every components results in decrease of hydrogen content, It can be noted that the adding of limestone to fluorite base coating essentially weakens the positive effect of CaF_2. This statement arises from comparison of data about hydrogen contents (Fig.8) and obtained results in influence of the coating composition on H, CO and CO_2 amounts in departing gas (Fig.9). With carbonate content rising up to ratio $CaF_2/CaCO_3$ approximately equal to 1, the hydrogen content in departing gases decreases intensively, but the diffusible hydrogen amount increases. This seeming contradiction can be explained with rising of CaO in slag as the result of carbonate content increase in coating composition, that, in turn, rises the basicity of welding slag and decreases activity of SiO_2. In doing so, the intensity of hydrogen binding in compound HF sinks.

Apparently, the amount of carbonate dissociation products is insufficient to compensate weakening of positive calcium fluorite influence, if the ratio $CaCO_3/CaF_2 > 1$.

The outcome of performed investigations shows that, from point of view of overcoming harmful hydrogen effect the rutile electrodes with fluorite addition to coating are of the most interest. The assessment of level of weld metal hydrogen content has been performed as applied to semi-automatic welding with flux-cored wires. The influence of weld metal type and welding parameters has been studied (10). The relationships of $[H]_{diff}$, $[H]_{res}$, and $[H]_{tot}$, to arc voltage and welding current arc plotted in Fig.10. These data relate to wet welding in fresh water with experimental cored wires of ferritic and austenitic types.

We know that hydrogen diffuses from weld metal into the HAZ with either ferritic or austenitic structures. If the weld metal structure is ferritic, hydrogen diffuses into the HAZ at high and room temperatures, while if it is austenitic it mainly diffuses into the HAZ at high temperatures. In the case of a ferritic structure the concentration of hydrogen close to the fusion zone at first rises, then drops. The degree to which diffusionally mobile hydrogen is concentrated in the HAZ when quenching steels are welded is greater than in the case of those which cannot be quenched. When welds are made using austenitic type wires, as time passes there is no appreciable increase in the concentration of hydrogen in the HAZ close to the fusion zone. In the case under consideration (Fig.10), the concentration of diffusionally mobile hydrogen in welds with an austenitic structure is several times less than in the case of a ferritic structure. Since the amount of hydrogen which has diffused through the HAZ is proportional to the amount of it in the deposited metal, changing to using austenitic welds can be taken as one of the measures for reducing the embrittling effect of hydrogen in the HAZ. In view of the lower initial concentration of diffusionally mobile hydrogen in welds with an austenitic structure, the flow by diffusion towards the HAZ is restricted, and moreover the coefficient of diffusion of hydrogen in welds with an austenitic structure is lower than the coefficient for the parent steels of the grades selected. This evidently makes it possible to avoid the formation of a concentration 'threshold' in the fusion zone. Since there is as yet no reliable procedure for measuring the hydrogen content of the HAZ, we measured the relative rates of evolution of diffusionally mobile hydrogen from the weld metals with austenitic and ferritic structures in the initial period following welding (Fig.11). In the former case hydrogen diffuses much slower, and the amount diffusing is smaller, and this means that the HAZ is in a less stressed state.

The results obtained in our experiments by measuring the hydrogen content of weld metals make it possible to suggest, that within the range of mechanised welding conditions employed a state of equilibrium saturation is not reached. In order to explain the nature of the $[H]_{diff}=f(V_{arc})$ and $[H]_{diff}=f(I_w)$ relationships which were obtained, it can be taken into account the features of melting and transfer during welding with cored wire in the air. As known the droplet temperature rises with the current rising. With certain critical values of the current the droplet dimensions decrease abruptly and transfer acquires a small droplet or stream nature; droplet temperature approaches boiling point. When the welding was carried out in our experiments (high current densities), the critical values of the current were 150 and 200 A with the electrode negative and positive respectively. When critical values of the current are reached, the partial pressure of the iron vapours rises abruptly, while the partial pressure of hydrogen drops. Herein probably lies the reason for the dropping nature of the curves in Fig.10b for currents in excess of 150 and 200 A. Rise in droplet temperature leads to a

substantial oxidisation of the metal, and this is also conducive to reducing the hydrogen content of the weld. This is confirmed by measurements of the oxygen content when welds are made using ferritic type cored wire, since as the voltage and current rise this increases up to 0.13%. The slight increase in concentration of hydrogen in the weld metal when the arc voltage is increased is due to increase in the partial pressure of the hydrogen as the arc becomes longer. It can be taken that metal vapours which lower the partial pressure of hydrogen predominate in the atmopshere in a short arc; as the length of the arc is increased, vaporisation of metal in the active arc spot zone has less effect on the composition of the arc atmosphere, and the partial pressure of the hydrogen is raised.

The curve representing the diffusionally mobile hydrogen content of the metal in austenitic welds plotted against the arc voltage has a maximum, and this is in agreement with the results of measurements made during welding in air. The obtained results allow to make the following conclusions:
1. Comparison of the diffusionally mobile hydrogen and residual hydrogen contents of weld metals deposited under water by manual and mechanised welding with cored wires providing ferritic and austenitic structures has shown that welds with an austenitic structure contain the smallest amounts of diffusionally mobile hydrogen. This makes it possible to make underwater joints in steels with a poor weldability.
2. Raising the arc voltage slightly increases [H]diff for welds with a ferritic structure, while this remains practically constant in welds with an austenitic structure. Raising the current to the point at which stream metal transfer sets in increases the diffusionally mobile hydrogen content of welds with both ferritic and austenitic structures. Further raising the current, causing transition to stream transfer, lowers [H]diff.

Influence of water salinity of the gas behaviour is of interest not only from scientific point of view, but is useful for practical aims. The data obtained in welding with flux-cored ferritic type wire are shown schematically in Figs 12 and 13 (14). With the higher water salinity the hydrogen content of weld metal decreases by 5...10% and the oxygen content increases by 5...15%. In welding under the sea water the additional quantities of potassium, sodium, magnesium and calcium salts get into the arc gas. Hence, it can be assumed that, as in welding in air, the higher concentrations of the said elements in the arc gas change the character of heat transfer to a droplet causing the increase in the degree of its overheating. Elevation of the temperature of a droplet causes, in its turn, its more intensive oxidation. The higher oxidation of droplets inhibits the metal absorption of hydrogen, since oxygen, while being a surface-active element, blocks the interface and decreases hydrogen solubility. Here, the total hydrogen content of a welded joint decreases. It should be also noted, that oxygen content of weld metals obtained directly in water by using the wires with rutile-based core is by 3-5 times as high as the oxygen content of welds made in air.

It is known that the steel susceptibility to ageing is considerably higher with the increase of nitrogen content above 0.008%. In welding under common conditions the protection of the molten metal from the contact with ambient air nitrogen is one of the main problems. However, this problem is not completely solved, because some amount of the atmospheric nitrogen is dissolved in the molten steel. Besides, the nitrogen from the parent and electrode metal also transfers into the weld. The air welded joints contain about 0.02% of nitrogen that specifies their susceptibility to ageing. In the conditions of the wet semi-automatic welding the arc atmosphere does not contain any nitrogen and moreover contributes to its partial removal from the molten metal. Nitrogen, dissolved in steel, forms NH_3 compound with

The control of weld metal properties depends to a large measure on the possibility to provide necessary level of its alloying. This, in turn, directly connects with questions of transfer and assimilation of carbon, silicon, manganese and another elements under wet welding conditions. The high degree of burn-off of the said elements is unavoidable because of large oxidation potential of gas-bubble atmosphere as the result of water steam dissociation. This fact is confirmed with results of study this peculiarities in the case of flux-cored rutile base wire using (Tab.3). The degree of transition of said elements has been determined using the series of experimental wires in which each element was changed at constant middle amount of the rest two elements. The dependencies obtained are given in Figs. 17, 18, 19.

Table 3 The degree of carbon, manganese and silicon assimilation in flux-cored wire welding

Element	Ranges in wire composition	Transition coefficient	Ranges in weld metal
Carbon	0...0.60	0.168...0.227	0.050...0.075
Manganese	0...4.12	0.169...0.211	0.01...0.52
Silicon	0...1.35	0.015...0.036	0.01...0.03

As seen, the possibilities of weld metal alloying with elements having high oxygen affinity are hardly limited at wet FCA welding. In this respect, the possibility of alloying with nickel are more prospective, and our investigations have confirmed this idea. If the high active elements present in electrode material, the losses of nickel are negligible.

As to alloying at MMA welding, this question is considered in detail in separate report "Development of MMA electrodes for manual underwater welding of steels in all positions". Here it is enough to notice only, that the obtained relationships between carbon, silicon and manganese amounts in weld metal and their contents in the coatings are considered to be of the same character. However, in a quantitative sense, it is the essential difference as to silicon: when MMA welding its transition coefficient is higher and averages 0.3...0.5.

Metallography questions and steel weldability assessment. The conditions of proceeding of oxidising-reducing reactions mainly with carbon, silicon, manganese and iron defined, directly or indirectly, quantity and composition of non-metallic inclusions (17). The results of study of interdependence between the graphite, ferrosilicium and ferromanganese amount in the flux-cored wire charge and quantity of non-metallic inclusions are given in Table 4.

In the weld metal deposited with flux-cored wire without alloying components, iron monoxide forms the main mass of inclusions. The rest of inclusions consists of silicon dioxide (the greater part) and other oxides of complex composition 55% of common quantity of inclusions are of sizes from 0.5 to 7μm and 42% are of sizes from 1 μm to 2.5 μm.

As seen from Table 4, the addition of alloying components to flux-cored wire charge causes the non-metallic inclusions quantity to decrease on the whole. As the carbon, content rises, the quantity of non-metallic inclusions decreases. The character of manganese and silicon effect is contrary.

hydrogen, easily dissolved in the surrounding water. The nitrogen content in the welds, made under the water, does not exceed 0.001%. This, in turn, is the favourable factor for providing the high cold-resistance of the welds because of absent of ageing susceptibility.

Given above data testify that one of the essential advantages of wet flux-cored wire welding as compared to welding with stick coated electrodes is less weld metal hydrogen amount. External flux coating of the stick electrode cannot prevent moisturization even if the varnish is carefully applied. Increasing humidity penetrates the flux in respect to depth and exposure time to the surrounding water. This leads to additional hydrogen contamination of the weldment. Hydrogen contamination generated by the water surrounding the burning arc cannot be avoid at all so that it is essential to reduce the humidity penetration of the consumable. This is possible with a flux-cored wire, because the wire tube is an additional protective means. However, even in FCA welding, the hydrogen concentration in weld metal exceeds the equilibrium one. Taking into account the specific wet welding conditions, that creates a dangerous of intensive pore formation.

The probability of blowhole formation has been studied by specially originated at the PWI phisico-mathematical model. The modelling of process has been performed with due regard for influence of moving liquid-solid interface, that differs our investigations from the analogous research of the Japanese scientists (15,16). The study of hydrodynamic parameters and principal behaviours of bubble evolution in liquid metal permitted to obtain the following expression for the radial rate of bubble surface movement:

$$\dot{r} = \frac{2RT\dot{m} - 2\rho g V_s \mu V}{6RTm\, r^2/V - \rho g \mu V(1+\cos\theta_0) - 4\gamma\mu V/r^2},$$

where : $\dot{m}$ - rate of changing of gas mass in the bubble; μ - molar weight of gas; V - volume of the bubble; ρ - coefficient of surface tension; R - gas constant; T - absolute temperature; θ_0 - initial contact angle of bubble.

The analysis of the gas bubble evolution using the said model shown, that characteristics of the evolution depends to a great extent on velocity of solidification front movement in the all possible range of nucleus initial radiuses. Bubble growth dynamics is determined with the moment of bubble nucleation and, therefore, with the degree of saturation with hydrogen of liquid layer before the solidification front. The hydrostatic pressure increase results in deceleration of diffusion processes and, finally, in decrease of bubble growth velocity, but not in stopping of this process (Fig14).

In accordance with theoretical calculations, the conditions of nucleation and growth of bubble are determined mainly with three factors, closely intercommunicated: hydrogen concentration before the solidification front, external (hydrostatic) pressure, and solidification speed (Figs. 15, 16) As seen, the influence of hydrogen concentration and pressure on the bubble critical radios is contrary, especially at low solidification speed values. Therefore, under wet welding conditions, the control of solidification speed is the only means to considerably affect on the weld metal susceptibility to porosity formation. The effectiveness of this approach rises as the solidification speed decreases. So, the practicability of this conclusions is to use the welding technique characterised by maximum possible input and weaving.

Table 4 Effect of flux-cored wire charge composition on quantity of non-metallic inclusions

№	Components, wt, %			Content of weld metal, %			$N \times 10^5$	V, %
	C	FeSi	FeMn	C	Si	Mn		
1	0.5	-	-	0.05	-	0.0850	10.93	0.7
2	1.0	-	-	0.06	-	0.1	7.19	0.49
3	1.5	-	-	0.065	-	0.07	7.06	0.45
4	2.0	-	-	0.075	-	0.08	6.96	0.41
5	-	-	4.0	0.065	-	0.19	5.03	0.42
6	-	-	8.0	0.07	-	0.28	5.57	0.44
7	-	-	12.0	0.075	-	0.33	6.12	0.49
8	-	-	16.0	0.07	-	0.52	7.03	0.52
9	-	1.0	-	0.06	-	0.085	5.32	0.51
10	-	2.0	-	0.07	0.01	0.095	6.51	0.60
11	-	4.0	-	0.06	0.02	0.01	6.84	0.78
12	-	6.0	-	0.072	0.03	0.17	7.24	0.87
13	-	-	-	0.06	-	0.095	11.76	0.96

In parallel with chemical composition the cooling rate of weldment influences the weld structure formation. The cooling rate of HAZ metal is substantially higher in underwater welding than that in common conditions. According to (18), such difference is approximately of 3-times when manual welding. At the same time, when welding with flux-cored wire this difference depends essentially on welding velocity (19). Comparing the data obtained at the equal welding velocity under water and in air (Fig.20), it can be seen as follows. At welding with small velocity (0.19 sm/s), existing duration of welding pool in liquid state is significantly less at underwater welding than that in air conditions. With welding velocity rising, the welding pool length values of both underwater and air environments are drowing together. However, the width of heat-affected zone at underwater welding remains some narrower than that in air, Table 5. Therefore, the differences between air and underwater semi-automatic welding thermal cycles, especially at the high temperatures, are practically run a level with welding velocity increase.

Table 5 Width of HAZ and of HAZ overheat area, mm

Welding technique	Overheat area at welding velocity		Heat-affected zone on the whole at welding velocity	
	0.19 sm/s	0.47 sm/s	0.19 sm/s	0.47 sm/s
Underwater	0.65	0.40	2.5	1.5
In air	1.60	0.65	7.0	2.0

The cooling rate proved to be in dependence on the water salinity (20). The data given in Table 6 confirm that fact. As seen, with water salinity increase from 0 to 30‰ the cooling rate of HAZ metal also increases 1.25-1.43 times because of weaking of protective role of vapour jacket at sample surface due to the presence of compound HCl in sea water. Owing to that, the hardness of HAZ metal increases by HV 30...40 when welding in water of 30‰ salinity comparing with data for fresh water. Microstructure of HAZ and weld metal becomes less homogeneous at the expense of increase of the areas with quenching structure.

Underwater weld metal structure is considered in papers (17, 21). It is shown that the structure is preferably ferritic if contents of alloying elements and carbon are negligible. In contrast to structure of weld performed on air, microstructure is

Table 6 Cooling rate of HAZ metal at wet semi-automatic FCA welding

Current, A	Environment	Cooling rate in the temperature interval, °C/s	
		from 800 °C to 500 °C	from 500 °C to 300 °C
230...250	Air	6.8	2.1
300...320		2.1	1.6
200...210	Fresh water	30.0	20.0
300...320		16.6	14.7
200...220	Sea water (10 ‰)	31.0	22.6
300...320		19.6	16.5
200...220	Sea water (30 ‰)	37.5	26
300...320		23.8	20

Note: Ua=29...32 V, Vw=6.3 m/h

more fine-grained and has areas with bainite and even with martensite. In welds performed in shallow water the microstructure consists mainly of primary grain-boundary ferrite and upper bainite. With increase of water depth a some quantity of Widmanstatten ferrite appears. Alloying of welds by nickel up to 3...4% significantly influences microstructure character (21). By addition of 0.8% Ni the structure consists mainly of coarse grain ferrite. If the nickel content is some more than 1%, the subgrain structure with lengthened grins of polygonal ferrite forms and areas of acicular ferrite appear. The quantity of these areas increases with increase of nickel content (up to 2.5%). Further increase of nickel content results in formation of zones with structure of lath martensite (especially in root part of weld), Fig. 21.

The questions of weldability of steels with different strength level are closely connected with a peculiarities of structure formation under underwater conditions. Here, the weldability problem consists mainly in a underbead cracking prevention as well as in increase of the weld metal ductility and in decrease of the hardness of heat-affected zone.

As the results of evaluating of weldability of low-alloyed steels under wet underwater conditions, it has been shown the sharp decrease of their resistance to cold crack formation (22). It is well known that the main reason is unfavourable combination of high hydrogen amount and HAZ quenching structure formation. In our experiments we tried to specify the localisation and the mechanism of formation of underbead cracks employing the widely applicable tube steels of 17G1S (0.23% C, 0.42% Si, and 1.33% Mn) and X60 types.

The furnished 17G1S steel is characterised with the lineage structure typical for manganese steels. The such structure formation is connected with manganese, phosphorus and sulphur segregation.

When welding the steel in air with commercial flux-cored wire, the structure of weld metal is ferritic with dispersed oxide inclusions dislocated mainly along grain boundaries. The width of heat-affected zone is in the range of 2...3 mm and has structure with different grains. Its phase composition depends on distance from fusion line. The structure is of mainly perlitic and, only immediately near the weld, the microstructure is of the upper bainite.

The HAZ sizes of samples welded under water decreases, the hardness increases. Directly near fusion line the base metal hardens up to 2800 MPa, i.e. not less than 1.5 times relative to initial level. The structure consists of coarse grain martensite,

the sizes of austenite grains are on the average approximately 0.1 mm. In these areas of HAZ metal, the cracks of considerable sizes appear. They are located along of austenitic grains. Location character of cracks allows to suppose that their formation is connected with the stop of fast-growing martensitic crystals inside austenitic grain.

Like welding in air, as the distance from weld increases, the austenite grain sizes decrease and the coarse-grain martensitic structure consecutively changes to structure of more dispersed martensite, then to bainite and, at least, to pearlite on the peripheral part of HAZ. By means of X-radiography, only the lines of body-centered cubic lattice of iron solid solution are fixed. This result confirms the data of metallography study about primary character of martensitic transformation in steel at underwater welding.

In the cooling process of steel X60 weldment, the acicular bainite forms in the HAZ. The maximum hardness value does not exceed 284 HV. The formation of thin layer of martensitic structure was observed sometimes near the fusion line. Namely here, the cold cracks were found.

Trajectory of crack corresponds to the most weakened areas of HAZ as the result of weldment fracture. On the boundary between weld and heat-affected zone, the considerable quantity of non-metallic inclusions form. These inclusions are located in sells (Fig.22). Microsounding with X-ray pencil showed that the main elements of these inclusions are manganese and silicon. In the zone of their location, the inclusions occupy about 75% of volume and, decreasing the effective cross-section of sample, they decrease essentially the mechanical strength of metal. As this takes place, the fracture of this area occurs toughly according to fractography.

Consistent study of the fracture permits to suppose, that namely this area with weakened strength is one of the main seats of failure. The ductile cracks of 0.5...2.0 mm in length arising under external loading in this area can be as effective stress concentrators and initiate the rapture of brittle areas of the heat-affected zone.

The second zone of welded joint failure is zone with coarse grain martensite structure. The fracture occurring in said zone is only brittle. Presence of embryonic micro cracks in the zone, complex stress state, and high defectivity of structure essentially facilitate the propagation of main crack. Initiation of welded joint failure directly in the zone of martensitic crystals is possible, too.

The important peculiarity of fractograms is presence of specific micro cracks located at angle to the main crack direction. They occur the most often in the areas with bainitic structure and close by the HAZ boundary. The formation of such cracks can be connected with phenomenon of hydrogen brittleness.

Therefore, knowing the main reasons of cold cracking of HAZ, it is possible to make out the concrete measures of their prevention. Because the performing of heat treatment under wet welding conditions is practically impossible, to avoid the quenching structure formation in weldment is hardly probable. It means that the necessity of prevention of hydrogen entering into heat-affected zone from weld in the large quantities becomes of very important and the only really precaution for the time being.

In this connection, we see the prospect in development of research direction characterised by austenitic type flux-cored wire application as to high strength

steel very sensitive to quenching structure formation and cracking under hard wet welding conditions. These considerations are grounded on the statement that with lower weld metal initial concentrations of diffusible hydrogen the "local" concentrations of it in the regions of raised hardness of the HAZ will also be lower, this predetermining that the welded joints will be resistant to cold cracking.

Our primarily experiment showed that above peculiarities are correct as to wet welding as well. The question of diffusible hydrogen was discussed above. Here we want to only illustrate some results of welding high strength steel of X60 type in respect of its weldability (23).

The susceptibility to cold cracking in the HAZ was determined in welding of restrained V-grooved test specimens. In one-pass X60 steel plate welding, the cracks were not revealed.

Figure 23 shows the distribution of hardness in the cross-section of the X-60 steel plate butt joint made by using the wire providing the austenitic weld metal structure. It should be noted that the distribution of hardness in the joints welded by using the austenitic and ferritic type wires is similar; the maximum values of hardness in the HAZ are approximately the same.

The sound base metal-weld metal fusion is provided in austenitic type flux-cored wire welding. The interlayer, characteristic of austenitic steel stick electrode welding, i.e. decarburized diffusion zone, is, as a rule, absent. The weld structure is a purely austenitic one with etched polygonization boundaries. Austenite grains in the overheating zone are surrounded by a ferritic network, the maximum grain being No. 3-4 (0.125 - 0.111 mm), at the weld root - No.6. Separate regions of martensitic structure, their hardness being 400 Hμ , are formed in the fusion zone of some specimens.

At present there is no doubt that hydrogen together with structural factors contributes to cold crack formation. The fact, that in the considered case with comparatively high values of hardness the cold cracks are not detected must be accounted for different behaviours of hydrogen in austenitic and ferritic welds (structures). Actually, under other conditions being equal, there are no cold underbead cracks in the welds having the austenitic structure, while in the ferritic structure welds they are observed.

According to the results of determining of diffusible and residual hydrogen, it may be noted that hydrogen in the welds of austenitic structure in the bound state, its diffusion movement is to a great degree blocked. It may be assumed that there occur no increase of the diffusible hydrogen concentration dangerous from the cold cracking point of view, in the HAZ higher hardness regions. This, probably accounts for the underbead cracks being absent in HAZ of the underwater welds of the austenitic structure with relatively high hardness of structural components.

The preliminary experiments showed the possibility to reach the next level of mechanical properties of weldments when welding with austenitic type flux-cored wire: ultimate and yield strength -623 and 346 MPa correspondingly, elongation - 38...40%, reduction in area- 55.6%. Therefore, the values of ultimate strength and of yield strength are in relationship characteristic of austenitic metal, the values of elongation and reduction in area are of a rather high level.

The problem weldability solution includes inseparably the questions of structural strength of underwater welded joints. They include, first of all, such

characteristics as fatigue strength and cold resistance. With the aim to compare these characteristics possessed to weldments made by flux-cored wire under water and by commercial coated electrodes in air, the series of corresponding experiments were performed (24).

The fatigue tests of low-carbon steel specimens cut across the weld of 14 mm thick butt joints were carried out at alternating bending. Two batches of flat and notched cylindrical specimens were manufactured. The latter can give comparative information on weld metal sensitivity to stress concentration. Test base was 5,000,000 cycles. As is seen from Fig.24, the fatigue strengths in underwater and air welding both of flat and notched specimens were practically similar.

Tensile tests of joints at vibration loads were carried out at the alternating bending in the Afanasjev type machine, until their complete fracture (Fig.25).

It was established that the fatigue strength of joints made in air and under the water, is practically identical. However, the results of the underwater welding conditions within the whole range are higher.

The joint resistance to impact loads at negative temperatures was determined on the 400x80x60 mm T-beam specimen. The specimens were manufactured of 12 mm thick welded butt joints. The tests were performed in the pendulum impact testing machine of the design of the E.O.Paton Welding Institute, the impact energy being 1.5 kJ. As is seen from Table 7, all the specimens withstood practically a similar number of impacts at the temperature up to 233 K.

Table 7 Results of impact testing

	Number of impacts till fracture of joints made by:	
Ttest, K	manual welding in the air	underwater FCA welding
273	13	12...13
253	11...12	8...13
233	5...6	2...4

Note: 1. The numerator gives the minimum and maximum quantity of shocks till joint fracture, in denominator is the mean value of testing 3-5 specimens. 2. In air welding the specimen fractured in HAZ while in underwater welding in parent metal.

It was of interest to determine and compare the cyclic toughness of metal of low-carbon steel welds in air and under water. The cyclic toughness was determined at 2° twist angle on the cylindrical specimen.

It is established that the relative cyclic toughness of welded joints made with electrodes in air amounts to 8.8%, while that of welds made with FCAW under water is equal to 9.2%, it testifies to a higher ability of the metal of underwater weld to absorb the vibrations.

When evaluating the cold resistance of welded joints, made in air and under water, the test temperature of specimens and area of section between notches, occupied by a crack, were taken into consideration. As is seen from Table 8, the joints welded under the water are more resistant to brittle crack propagation.

The high cold resistance of specimens can be explained by the more narrow HAZ zone in the underwater conditions than in air welding, this reducing the effect of strain ageing of metal.

Table 8 Results of cold brittleness tests

T, K	Share of area between notches occupied by crack, %	
	in air welding	in underwater welding
213	96-100	44-49
233	95-99	no cracks
253	96-98	no cracks
273	no cracks	no cracks

Note: The results of testing 3-5 specimens are given.

CONCLUSIONS

As it is seen from above given data, the rather large volume of investigations has been performed at the E.O.Paton Electric Welding Institute with the aim to study the electrico-metallurgical peculiarities of wet underwater welding.

These investigations include the questions of interaction of gases and molten metal, weld metal porosity formation probability, alloying of weld metal, transition and assimilation of alloying elements, structure formation and properties level of weldments and steel weldability under wet underwater welding conditions.

These data became the scientific base of electrode materials and technological processes development for welding directly in fresh and sea water of mild and low-alloy structural steels with yield point up to 350 MPa. In addition, the reality of solving the problem of wet welding of high-strength steels has been shown and the real approaches as to semi-automatic flux-cored welding of these steels have been outlined.

REFERENCES

1 Melnik Yu P and Savich I M: 'Rapid Filming Underwater Welding Process with Flux-Cored Wire', Avtomaticheskaya Svarka, No 8, 1974, p76
2 Madatov N M et al: 'Rapid X-Ray Filming an Welding Arc Under Water', Svarochnoe Proizvodstvo, No 9, 1965, p37
3 Lebedev V K et al: 'Calculation of Basic Characteristis of Arc in Underwater Mechanised Welding', Underwater Welding and Cutting, Kyiv, 1980, p29
4 Hamasaki M et al: 'Underwater MIG Welding - High Pressure Experiments', Metal Construction, Vol 8, No 3, 1976, p108
5 Pokhodnja I K et al: Some Peculiarities of Arc Burning and Metal Transfer in Wet Underwater Self-Shielding Flux-Cored Wire Welding', Avtomaticheskaya Svarka, No 9, 1990, p1
6 Madatov N M: About Influence of Sea Water Salinity on Underwater Welding Process with Consumable Electrode', Svarochnoe Proizvodstvo, No 4, 1961, p8
7 Lebedev V K et al: 'Analysis of Possibility of Following to Indicate Typical Disturbances on Arc Length by Self-Regulating System in Underwater Mechanized Welding', Underwater Welding and Cutting, Kyiv, 1980, p10
8 Gretskii Yu Ya and Maksimov S Yu: 'Metallurgical Peculiarities of Wet Underwater Welding with Coated Electrodes', Avtomaticheskaya Svarka, No 1, 1995, p10

9 Gretskii Yu Ya et al: 'Influence of Marble in Rutile Electrode Coating on Hydrogen Content in Weld Metal in Underwater Welding', Avtomaticheskaya Svarka, No 7, 1993, p51
10 Asnis A E et al: 'Measure of Decreasing of Hydrogen Content in Heat-Affected Zone in Heat-Affected Zone in Mechanized Underwater Welding', Avtomaticheskaya Svarka, No 8, 1983, p1
11 Kononenko V Ya: 'Effect of Water Salinity and Mechanized Underwater Welding Parameters on Hydrogen and Oxygen Content of Weld Metal', Avtomaticheskaya Svarka, No 3, 1991, p69
12 Kononenko V Ya: 'Oxygen and Hydrogen Content in Weld Metal in Wet Underwater Welding with Flux-Cored Wire, Avtomaticheskaya Svarka, No 11, 1993, p18
13 Gretskii Yu Ya et al: 'Influence of Fluorite in Rutile Electrode Coating on Hydrogen Content in Weld Metal in Underwater Welding', Avtomaticheskaya Svarka, No 8, 1993 p54
14 Kononenko V Ya: 'Effect of Water Salinity Mechanized Underwater Welding Parameters on Hydrogen and Oxygen Content of Weld Metal', Proce Welding Under Extreme Conditions, IIW, Helsinki, Finland, Sept 1989, p113
15 Suga Y and Hasui A: 'On Formation of Porosity in Underwater Weld Metal - Effect of Water Pressure on Formation of Porosity (the 1st Report)', Transactions of the JWS, Vol 17, No 1,1986, p58
16 Suga Y: 'On Formation of Porosity in Underwater Weld Metal - Study on Mechanisms of Blowhole Formation by Hydrogen- (the 2nd Report)', Transactions of the JWS, Vol 18, No 1, 1987, p61
17 Savich et al: 'Structure of Weld Metal Performed by Underwater Welding', Avtomaticheskaya Svarka, No 10, 1975, p24
18. Hasui A and Suga Y: 'On Cooling of Underwater Welds', Transaction of the JWS, No 1, 1980, p21
19 Melnik Yu P et al: 'Peculiarities of Termic Cycle of Welding of Low-Carbon Steel under Water', Avtomaticheskaya Svarka, No 1, 1976, p17
20 Savich et al: 'Structure of Weld Metal and HAZ When Welding under Water of Different Salinity', Avtomaticheskaya Svarka, No 4, 1984, p50
21 Gretskii Yu Ya and Maksimov S Yu: 'Effect of Nickel on Structure and Properties of Welds in Underwater Welding with Flux-Cored Wire', Avtomaticheskaya Svarka, No 8, 1995, p56
22 Savich I M et al: About Assessment of Weldability of Low-Alloy Steels with Regard for Rapid Cooling in Underwater Welding Conditions', Avtomaticheskaya Svarka, No 12, 1988, p48
23 Ignatushenko A A et al: 'Mechanized Underwater Welding Using Austenitic Consumables', Underwater Welding, IIW, Trondheim, Norway, June 1983, p227
24 Asnis A E et al: 'Structural Strength of Underwater Welded Joints', Underwater Welding, IIW, Trondheim, Norway, June 1983, p319

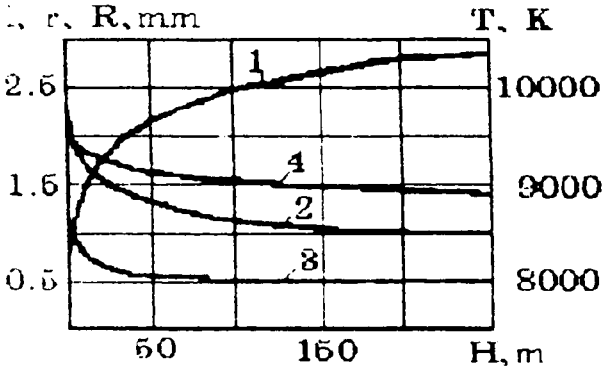

Figure 1 Dependence of temperature T (1), arc length l (2), arc column radius r (3) and drop radius R (4) on submerging depth

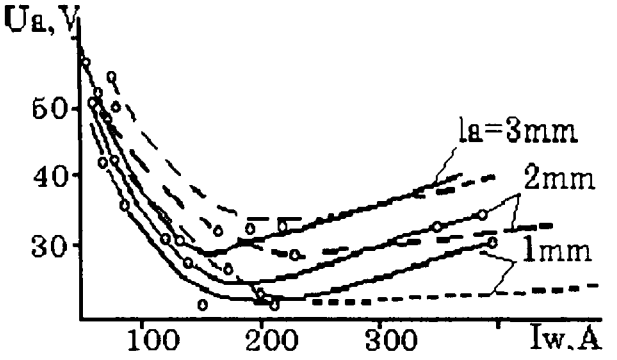

Figure 2 The volt-ampere characteristics of arc, burning under water at welding:
----- - with electrodes 4 mm dia
-- -- - with electrodes 6 mm dia
DC, electrode negative, fresh water

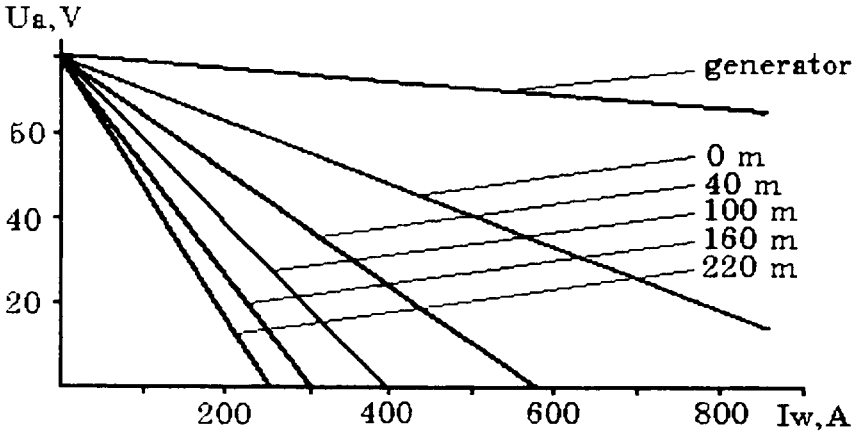

Figure 3 Changing of rigidity of external characteristics with operation water depth increase

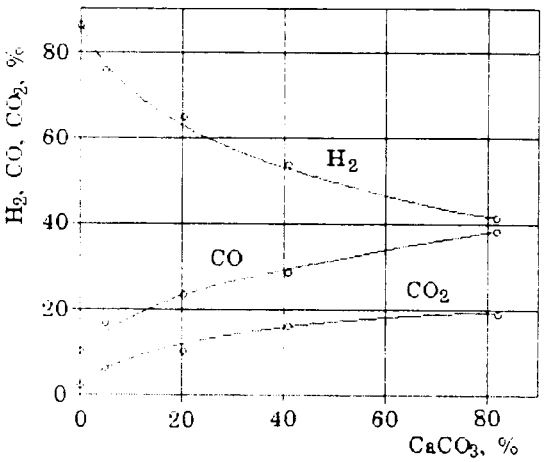

Figure 4 Influence of $CaCO_3$ amount in charge on hydrogen and carbon oxides content in departing gases

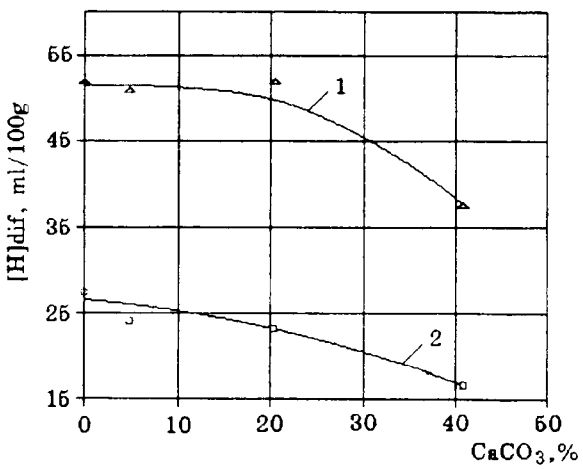

Figure 5 Influence of $CaCO_3$ amount in charge on diffusible hydrogen concentration in deposited (1) and fused (2) metal

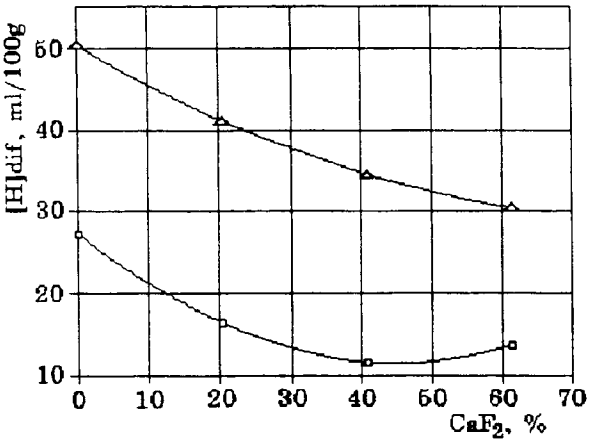

Figure 6 Influence of CaF_2 amount in charge on diffusible hydrogen concentration in deposited (1) and fused (2) metal

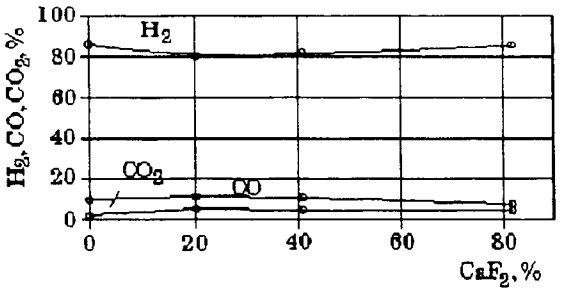

Figure 7 Influence of CaF_2 amount in charge on hydrogen and carbon oxides content in departing gases at wet welding with experimental electrodes

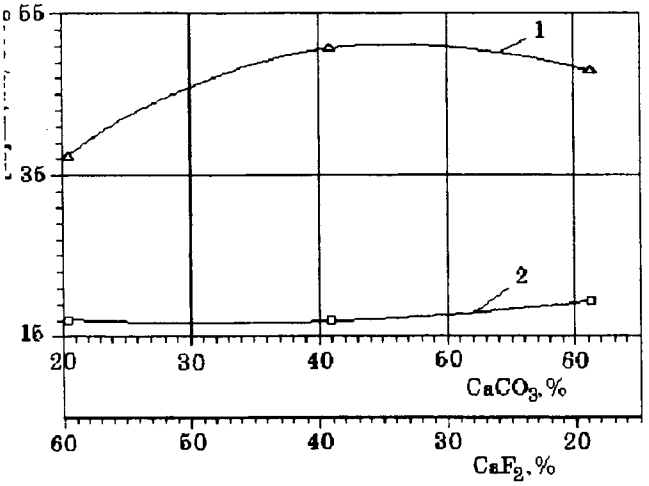

Figure 8 Influence of the percentage amount ratio CaF_2 and $CaCO_3$ in electrode coating on diffusible hydrogen content in deposited (1) and fused metal (2)

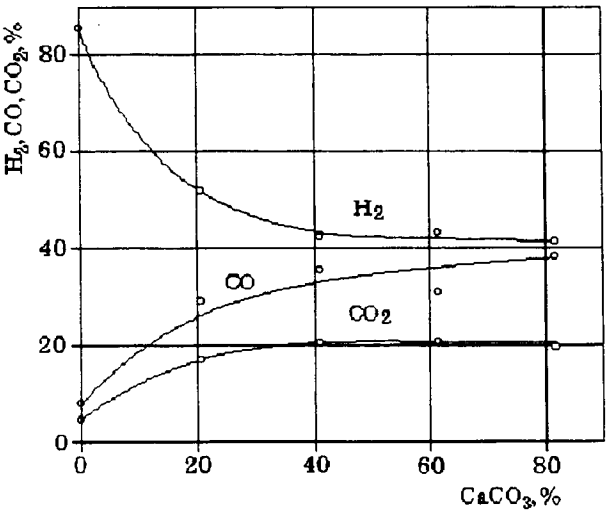

Figure 9 Influence of $CaCO_3$ amount in lime fluorspar coating on hydrogen and carbon oxides content in departing gases at wet underwater welding

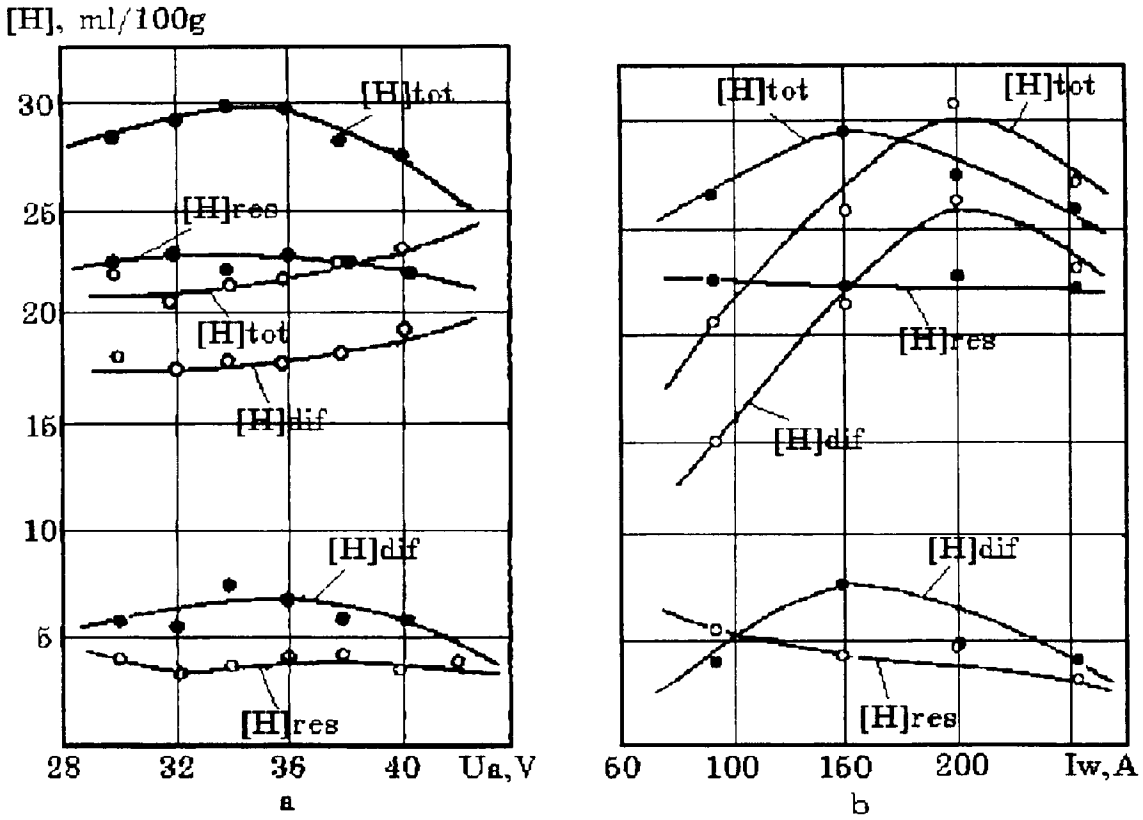

Figure 10 Dependencies of [H]dif, [H]res, [H]tot on arc voltage (a) and on welding current at welding (b): o - with wire of ferritic type ;
• - with wire of austenitic type

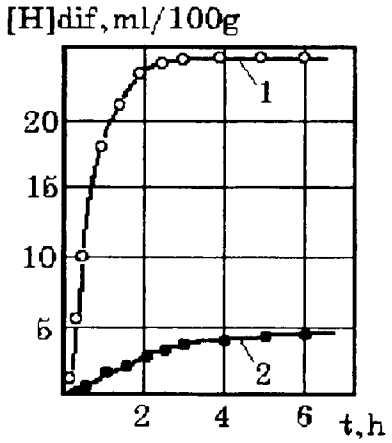

Figure 11 The relative velocities of diffusible hydrogen evolution from weld metal of (1) austenitic and (2) ferritic structure

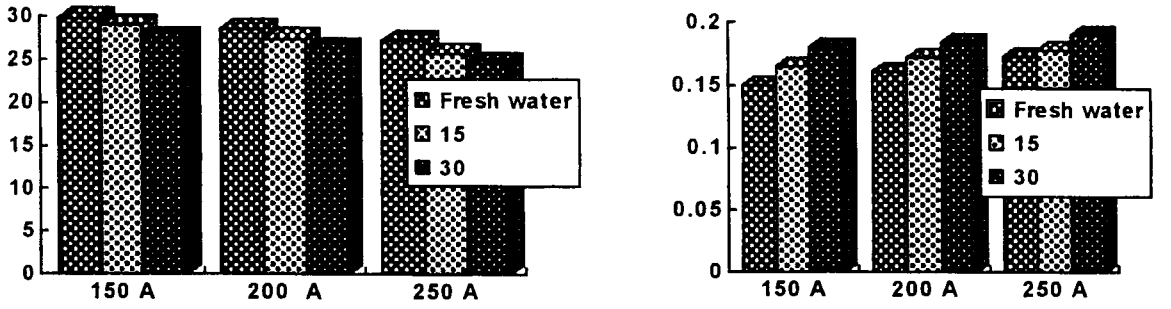

Figure 12 Effect of water salinity on hydrogen and oxygen content in weld metal at different welding current values

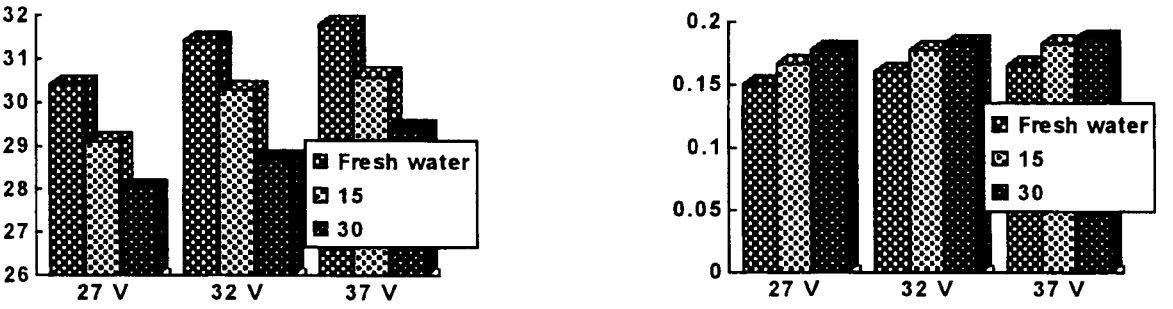

Figure 13 Effect of water salinity on hydrogen and oxygen content in weld metal at different arc voltage values

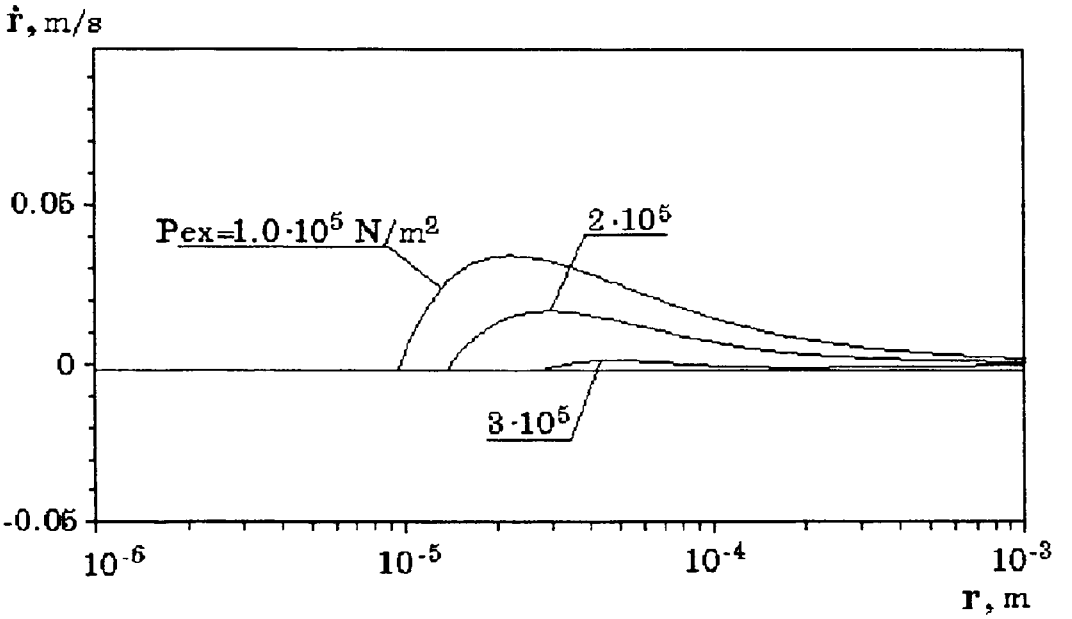

Figure 14 Influence of excessive pressure on bubble growth rate

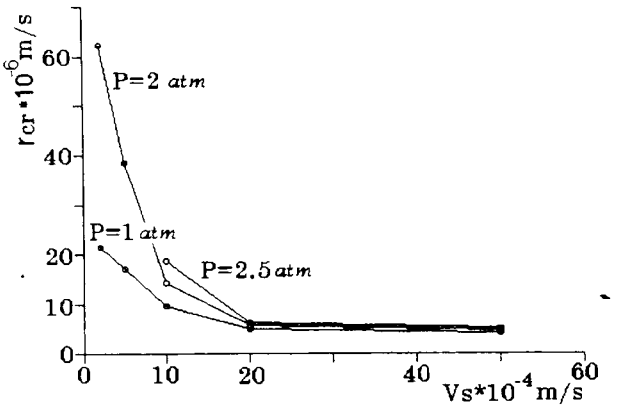

Figure 15 Influence of pressure on gas bubble critical radius

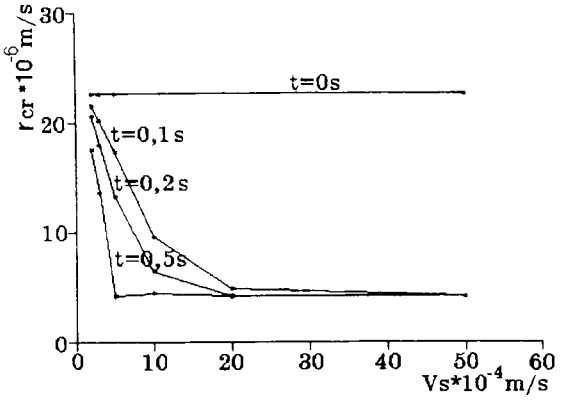

Figure 16 Influence of bubble formation time on its critical radius

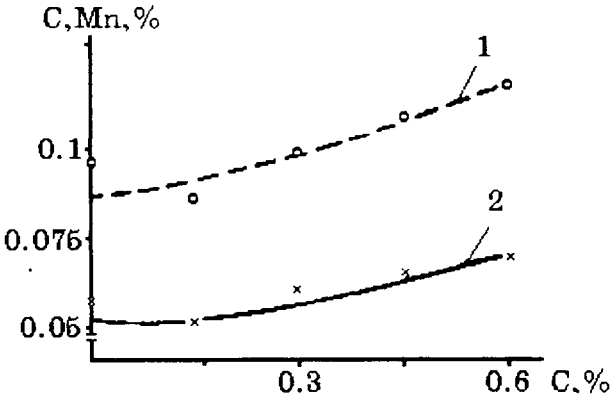

Figure 17 Content of manganese (1) and carbon (2) in weld metal depending on carbon content in wire

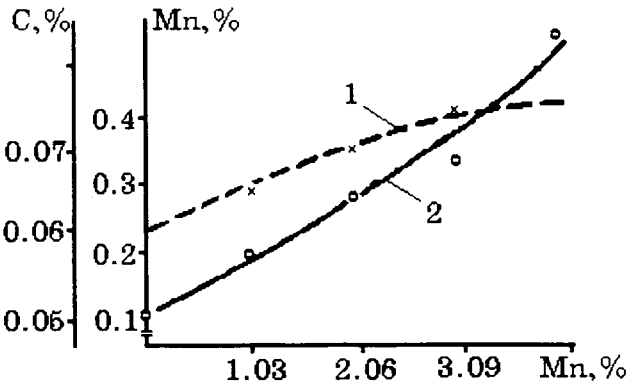

Figure 18 Content of carbon (1) and manganese (2) in weld metal depending on manganese content in wire

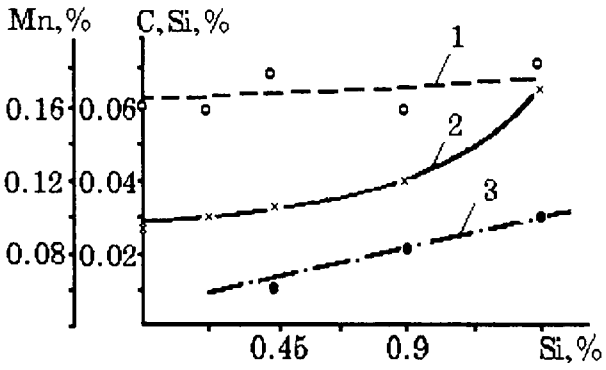

Figure 19 Content of carbon (1), manganese (2) and silicon (3) in weld metal depending on silicon content in wire

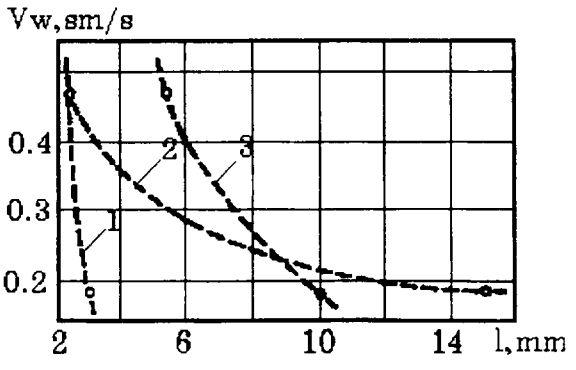

Figure 20 Dependence of liquid pool sizes on welding velocity: 1 - pool length (under water); 2 - the same (in air); 3 - width of pool in both the environments

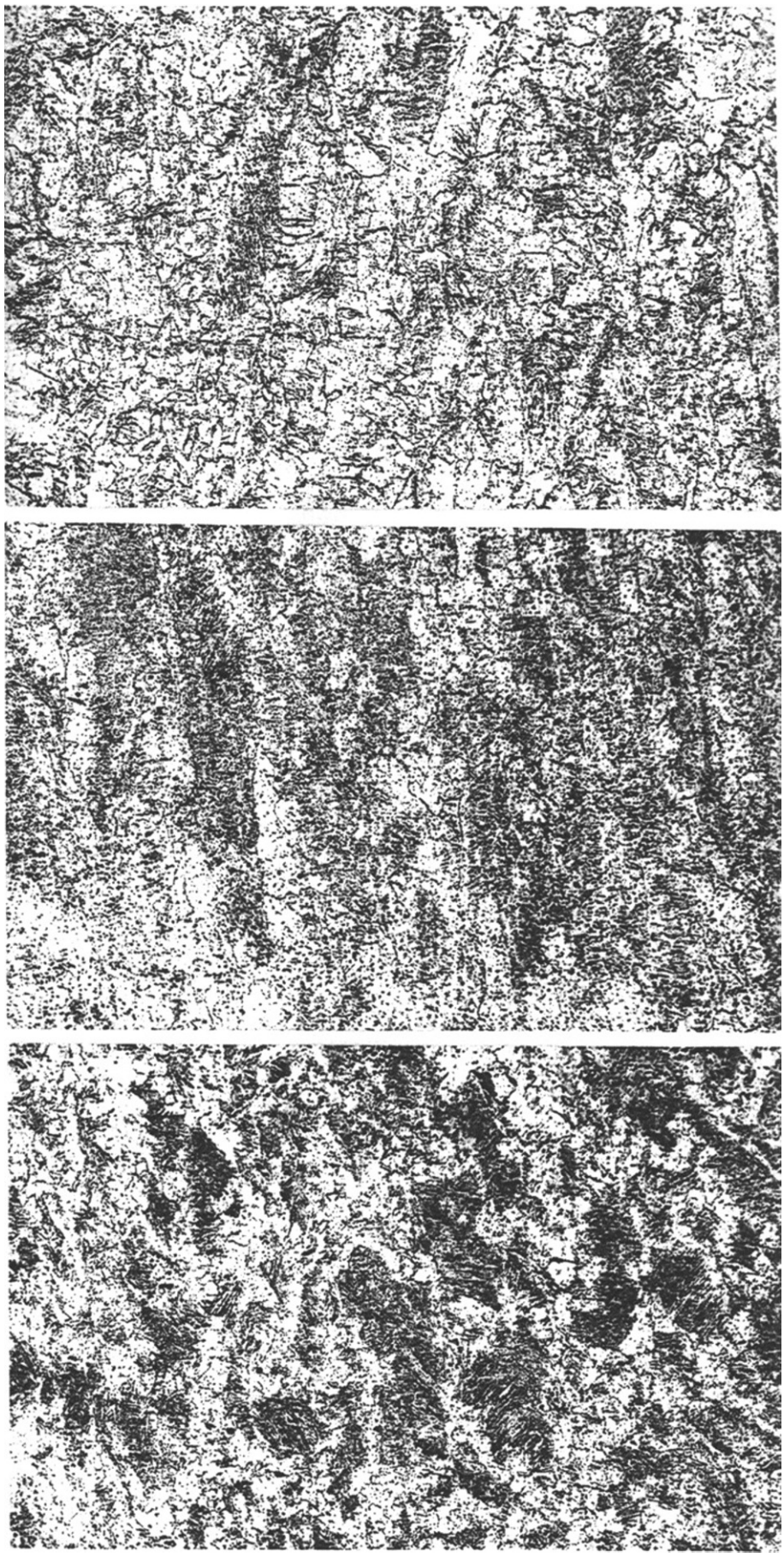

x100

Figure 21 The typical microstructure of welds with different content of Ni: a - 0.75%, b - 1.95%, c - 3.3%

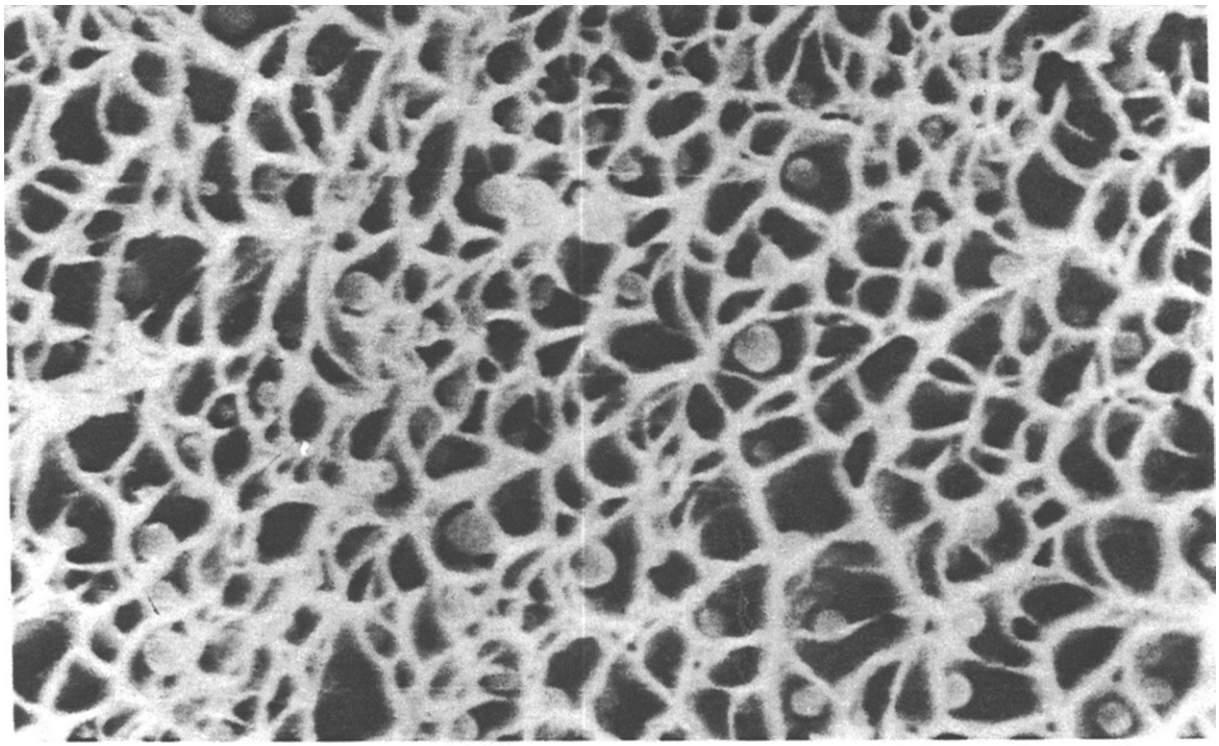

x2300

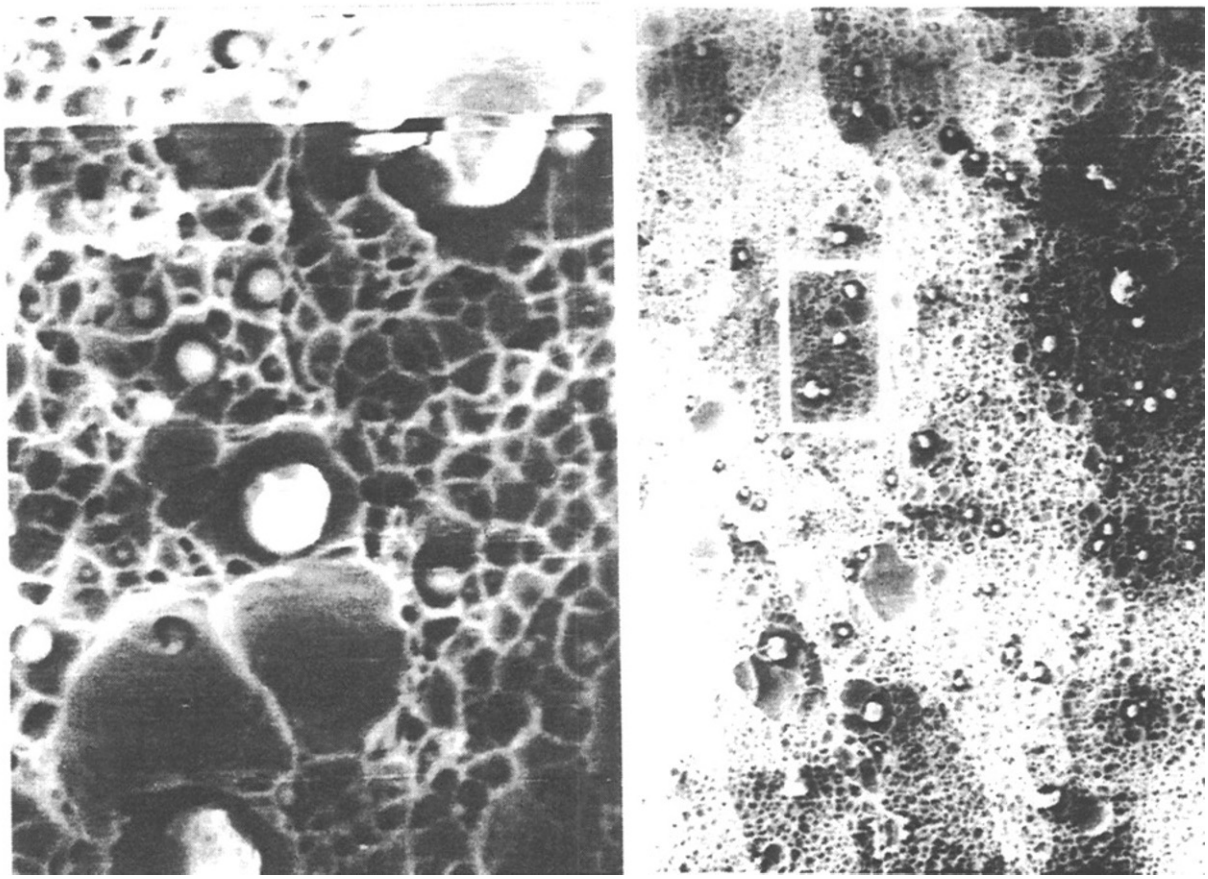

x1500

Figure 22 Non-metallic inclusions in weld metal

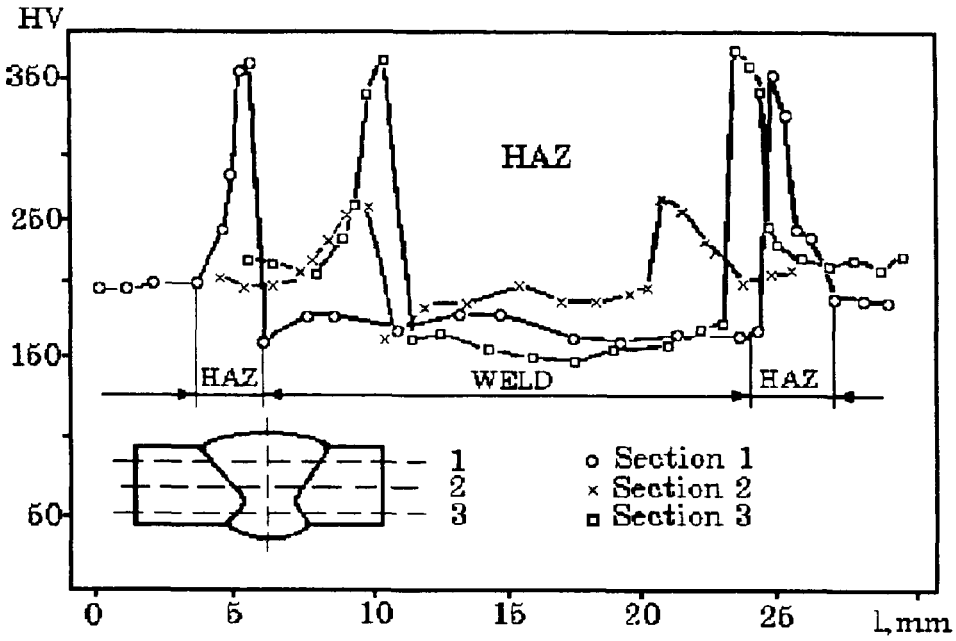

Figure 23 The distributing of hardness in a butt joint made of steel X-65 by using the austenitic type flux-cored wire

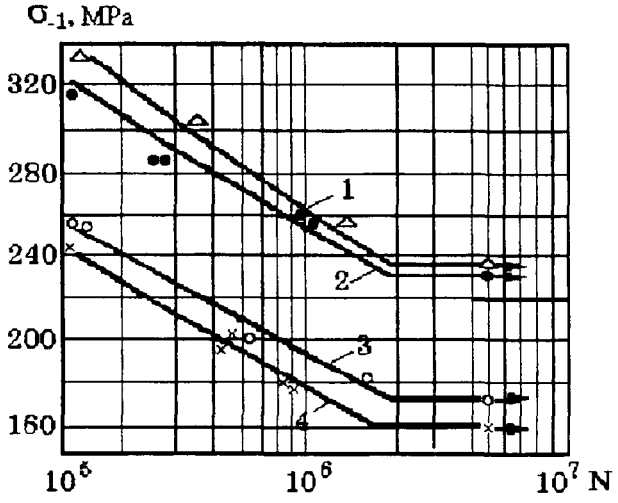

Figure 24 Fatigue strength at alternating bending 1,3 - underwater welding with flux-cored wire; 2,4 - welding with UONI 13/45 electrodes in the air; 1,2 - flat specimens

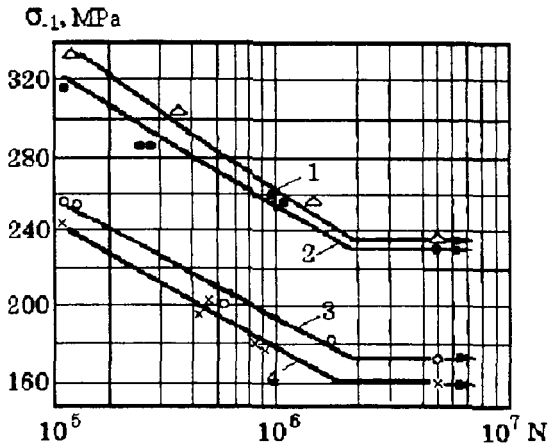

Figure 25 Vibration strength of welded joints: 1- welding under water; 2 - welding in air

Development of MMA electrodes for manual underwater welding in all spatial positions of steels

S Yu Maksimov, E O Paton Electric Welding Institute

The specific conditions of wet underwater welding, when arc burns directly in water, create a large difficulties in ensuring equivalence of base and weld metal. In this respect, the wide introduction of wet welding into service is restrained over many years. Working out of the semi-automatic flux-cored wire arc welding technique was the essential hitch in this field. However, this method did not solve all the technological problems of underwater arc welding. The industrial demand for manual welding has remained up to now. Nevertheless, there are no such special coated electrodes which would provide the satisfactory bead appearance, the possibility of performing of wet welding in all spatial positions and equality of base metal and weld metal operational safety even on widely applied carbon and low-alloyed structural steels.

In the majority of cases, the underwater welding works are performed traditionally with commercial electrodes worked out for common air purposes. The only feature of these electrodes is presence of additional waterproof coating preventing the mineral part of the coating from direct contact with water. In doing so, the strength of weld metal is, as a rule, almost equal to that of base metal, but the level of ductility remains low (elongation does not exceed 9 per cent) (1).

In the CIS countries, development of wet MMA welding stopped in the 1960-s at a stage of working out of electrode with iron oxide coating. The weld metal mechanical properties, especially ductility, are considerably lower than those required for welding of carbon and low alloyed steels for mass application. The electrodes do not allow weldments of the satisfactory quality to be made, especially in position other than the flat one.

In this respect, the scientific task appeared to found the solution for an increase in the weld metal quality level, so that welding-technological electrode properties allowed to welding to be performed in all spatial positions. With this aim, metallurgical and technological peculiarities of wet welding have been studied.

Bead appearance. First of all, the smooth transitions between weld and base metals should be ensured because elimination of such defect as overlap or excessive undercut makes difficulties or is impossible on the whole. The comparative testing of electrodes having coatings of different type has shown (2-5) that the electrodes with rutile type coating have better welding-technological properties in this respect. This result can be explained with lower melting point, narrow interval of freezing, and good wettening base metal with slag on the rutile base.

For choice of base coating composition with the aim of such electrode formulation, five of three-component composition were investigated: TiO_2-SiO_2-CaF_2, TiO_2-SiO_2-$CaCO_3$, TiO_2-CaF_2-$CaCO_3$, TiO_2-CaF_2-Fe_2O_3, TiO_2-CaF_2-$FeO*TiO_2$. The welding-technological

properties of experimental electrodes were estimated on amount using the follow criteria (see Table 1).
The character of component influence on welding-technological properties was estimated proceeding from analysis of regression models built up from experimental data.

Table 1. Criteria of expert estimation of experimental stick electrode properties under underwater wet welding conditions

Bead appearance	The slag crust character and peeling-off ability	Assessment, in amounts
Small-ripple weld surface with smooth transition to base metal	Thick slag crust peeling-off spontaneously and completely	9-10
Weld of a large convexity, there are no undercuts	Thick slag crust, removes-off at light hammering	7-8
Weld of a large convexity, non-uniformity over its entire length, there are undercuts	Thick slag crust removes-off satisfactory with metallic brush	5-6
Bead appearance is bed, there are overlaps and excessive undercuts	Thin slag crust covers weld surface only partly, removes-off very badly	3-4
Weld is not shaped	-	2

As it is seen from Fig.1, the area of acceptable compositions is adjacent to "rutile" corner of the diagrams. In the all systems excluding TiO_2-$CaCO_3$-SiO_2 system, the addition of third component widened these areas, but the level of welding-technological properties did not rise. The TiO_2-SiO_2-$CaCO_3$ system was preferable because it had the area of compositions providing the studied properties on the level of 9-10 amounts. In accordance with obtained data, the compositions corresponding the area of 56...80% TiO_2, 15...33% SiO_2, and 3...20% $CaCO_3$ was regarded to be the best available for search of optimum composition of coating.

Testing the system for goodness of fit was performed using the experimental electrodes with coatings mineral part of which was taken from above said area. Weld metal was obtained when wet welding the low-carbon steel of St3 type in our laboratory tank, the welding current value was in the range from 120 to 200 A.

The typical photograph of cross-section performed at minimum and maximum current value is given in Fig.2. As seen, the smooth transition from beads to base metal was provided. In addition, there were the small-ripple surface of beads and thick slag crust peeling-off spontaneously and completely as well. Therefore, it was possible to consider the electrode with coating of rutile-feldspar-limestone base as meeting the highest requirements of assessment criteria in accordance with Table 1.

Arc stability. The investigations of peculiarities of arc burning and molten metal transfer were performed with the help of information-measurement system on the base of PC/AT-386. The system provided the possibility of automatic analysis of arc electric and time

parameters of underwater MMA welding and the presentation of the information acquired in a statistically processed form (6).

Figure 3 gives the fragment of current and voltage oscillogram of wet welding with experimental electrode having rutile base coating with addition of 10% feldspar. The process is demonstrated to be stable, with momentary short circuits. The current and arc voltage histograms of typical appearance are given in Fig.4. It can be seen, the distribution of said parameters is of two-modal character, one of both modes being considerably bigger than another. The lesser mode displays the current and voltage at the moments of short-circuits. Interruptions of the arc are absent.

The above data concern downhand position and welding at current value of 190 A. Decrease of current down to 150 A and transition to overhead welding position caused some worsening of process stability that is confirmed with appearance of third mode (Fig.5), corresponding phenomenon of arc interruption. Nevertheless, the short-circuit duration (8 ms) remains more less then limit value of those (12-14 ms) typical for welding on air.

As the results of performed complex of investigations, it has been shown as follows. Under conditions of underwater welding with electrodes having coatings on the rutile base the arc stability is sufficient for welding in the all spatial positions. The additions of limestone to coating composition improve the stability at the expense of shortening duration and quantity of short-circuits. Introduction of fluorspar in coating necessary for decrease of diffusible hydrogen amount and for improvement of bead appearance does not worsen the arc burning process in contrast to welding under air conditions. This fact is explained with exceptionally high amount of hydrogen in the vapour-gas bubble atmosphere, because the negative hydrogen effect becomes negligible under such conditions. Therefore, with the point of view of underwater arc stability, it is not dangerous to add the fluorspar to coating, if it is necessary to improve welding-technological properties of rutile base electrodes.

Alloying, structures and properties. It was in question, in what ranges is possible an alloying weld with carbon, manganese and silicon to control of weld metal chemical composition and how is influence of such elements on structure and mechanical properties under unique underwater conditions.

Four series of electrodes have been employed in the experiments (Table 2). The obtained relationships between the carbon, silicon and manganese amounts in weld metal and their contents in the coatings are given in Fig.6. The relationships are considered to be of the same character as in common conditions. However, in a quantitative sense, the transition of said elements decreases drastically and characterises with next data: for carbon - 0.15...0.20, for silicon - 0.3...0.5, and for manganese - 0.06...0.15. The possibility for weld metal chemical composition control proved to exist for underwater MMA welding, too, the possibility depending closely on presence and kind of additional gas- or slag-forming component of mineral coating charge. The most favourable possibility of weld metal alloying are created if fluorspar and feldspar are added to rutile coating.

With the aim of assessment of alloying elements influence on weld metal structure and mechanical properties the electrodes with coatings of series 1 (see Table 2) have been chosen. While introduction such components as graphite, ferrosilicon and ferromanganese into coating decreases the share of mineral part of coating, welding-technological properties of electrodes deteriorate especially when welding root passes.

With this connection, the possibility of weld metal alloying under wet welding conditions are somewhat restricted. As the result, the upper limit of said component amount was not more than 10%.

For metallographic investigations and mechanical testing the butt joints of low-carbon steel St3 type of 12 in thickness were welded. The welds obtained were of six passes and contained silicon and manganese in the range of 0.09<Si<0.34% and 0.06<Mn<0.44%.

Table 2. Composition of the rutile-based coating of the experimental electrodes

№	Rutile,%	Feldspar,%	Fluorspar,%	Marble,%	Hematite,%
1	69...86	9...12	-	-	-
2	58...73	-	20...25	-	-
3	58...73	-	-	20...25	-
4	58...73	-	-	-	20...25

Note. 0.5...4% of graphite, 2...16% of ferrosilicon, 5...20% of manganese and 2% of carbonyl methyl cellulose are contained in coating of all series of electrodes

According to metallographic investigations, the microstructure of weld metal was practically identical in all samples and consisted in the cast ferrite-carbide mixture. The example of such structure is given in Fig.7. Note, the main feature of the microstructure is that it is fine grained. The hardness of weld metal did not exceed 201 HV at maximum content of alloying elements. The manganese and silicon influence on tensile strength, yield point and elongation of multipass weld metal is shown in Fig.8 and Fig.9. As seen, the addition of silicon in the above said range does not affect significantly on these characteristics. The influence of manganese was found to be more effective. Addition of manganese up to 0.2% raises the elongation only. If concentration of this element is more than 0.2%, both tensile strength and yield point rise but elongation decreases. Introduction of manganese and silicon simultaneously does not change really the level of mechanical properties. Proceeding from the aim of ensuring of elongation level not less than 14%, manganese content of weld metal must be up to 0.35%. In doing so, the value of tensile strength is in the range from 440 to 470 MPa and yield point exceeds 350 MPa. Such level of properties meets the condition for base and weld metal equivalence.

Waterproof coating. Presence and kind of waterproof coating of electrode are of important with respect to weld formation and convenience of diver-welder in operation. This part of electrode covering must meet a number of properties as to adhesion to mineral coating, hydrophobity, dielectricity and manufacturability in plotting. The most favourable combination of above properties proved to be when using polyethylene. The composition of colour waterproof coating has been found by us on the base of high pressure powder polyethylene. At the E.O.Paton Electric Welding Institute the corresponding technology of plotting such coating of 50...125 μm in thickness has been worked out on the base of vibro-vortical method and the unique laboratory plant has been designed (Fig.10).

The experimental plant consist of two chambers divided between one another with porous partition. The upper chamber is intended for filling up with the dispersed material, the lower chamber includes the electromagnetic vibrator and channel for supply of air or inert gas under pressure into first chamber. Plotting of waterproof layer on an electrode having still mineral part of coating and heated up to certain temperature is performed in pseudo-liquid polyethylene powder environment of upper chamber.

Serious testing of the electrodes with fully made coating have been performed both in fresh and sea water. The tests shown the correspondence of the electrodes with above demands. Elimination of getting wet of mineral coating part and its electric erosion in the water of salinity up to 18‰ are ensured. Hydrophobic layer burns uniformly, without formation of fringe or bushing which would make the difficulties in diver-welder operation.

The new developed electrodes took the grade EPS-AN1 (Electrode for underwater welding of Academy of Sciences, type 1) and for the time being are manufactured at the Experimental Department of E.O.Paton EWI according to technical code number PWI 835-92.

Some technical data concerning melting of the electrodes are given in Table 3.

Table 3. Base characteristics of electrodes EPS-AN1 type melting

Kind of current, polarity	Coefficient of deposition, g/A*h	Coefficient of spilling, %	Outcome of fit metal, %	Expenditure of electrodes per 1 kg of deposited metal
DC, negative	8.2...8.5	up to 3.5	60	1.7
AC	8...8.5	3.5...5	60...65	1.7

The electrodes of EPS-AN1 type have been examined according to the requirements of AWS D3.6 Specification (7), type B. The mechanical properties of weldments performed using base metal of low-carbon steel St3 type and low-alloy steel 09G2 type are given in Table 4. The bend tests of electrodes were performed both from root and face sides. They have shown, that the bend angle is equal to 180 degrees in either case. The photograph of tested sample is given in Fig.11.

Table 4. Mechanical properties of weldments

Steel	Yield strength, MPa	Tensile strength, MPa	Elongation, %	Impact Energy, J	
				20°C	-20°C
St3	330...350	420...460	14...18	35...43	25...33
09G2	340...370	430...470	14...18	39...47	26...37

Therefore, we have right to declare that the electrodes meet the requirements of Class B in accordance with AWS D3.6 Specification.

Figure 12 is evidence of porosity absence in multipass welds. Figure 13 confirms the possibility of welding performance even in overhead position.

In addition, the testing of corrosion resistance have been performed in synthetic sea water during 1000 hours, water temperature being 32...35 °C and velocity of solution moving being 10 m/s. As the result, it has been determinated that the average values of corrosion velocity were as follows: base metal - 1.50...1.55 mm/year, HAZ - 1.46...1.50 mm/year, and weld metal - 1.30...1.33 mm/year. As seen, the weld metal obtained with electrode EPS-AN1 is inferior to base metal in this respect.

Worked out electrodes are applied in repair of demaged metallic structures. Welding of cracks, corrosion defects being on surface and through the all metal thickness, welding

with putting in patches - these and other works are performed in water environment and under thin water layer, Fig.14.

CONCLUSIONS.

At the E.O.Paton Electric Welding Institute the complex of research and development works on finding the principles of coated electrode creation for wet underwater welding has been performed. The investigations were directed to study of conditions for obtaining of deposited metal with good appearance, providing of arc burning stability and ensuring of mechanical properties level demanded. On the base of obtained fundamental results the new coated electrodes of EPS-AN1 grade for wet underwater welding of structural steels for mass application having yield point up to 350 MPa were developed. The electrodes ensure the value of weld metal elongation not less than 14%, the weld metal being of the same strength as base metal. The important feature of the electrodes is that they permit the wet welding to be performed in all spatial position. The created electrodes meet the requirements of class B of AWS D3.6 Specification. Broad field testing shown the fitness of the electrodes of EPS-AN1 grade for performing a number of works in actual practice.

REFERENCES

1 'Underwater Repair Procedures for Ship Hulls (Fatigue and Ductility of Underwater Wet Welds)', SSC-370, 1993, p8

2 Grantham J 'Development of an Underwater SMAW Electrode for Improved Fatigue Strength in Wet Welded Joints', Abstr. Pap. Present. 71st AWS Annu. Meet. and 21st. Int AWS and Solder. Conf., Miami, Fla, Apr. 22-27, 1990. p290

3 Liu S 'Underwater Welding Consumables Research', Welding Research Council Progress Reports, No 9/10, 1990, p18

4 Loebel P at al: 'Underwater MMA Welding', Jahresber., 1986, GKSS-Forschungszent., p 50

5 West T C at al: 'Wet Welding Electrode Evaluation for Ship Repair', Welding Journal, Vol69, No 8, 1990, p46

6 Korotynskii A E at al: 'Computer-based System for Control of Underwater Welding Processes', Automatisation of Methods of Non-destructive Quality Control, Kyiv, Ukraine, June 2-4, 1992, p30

7 Specification for Underwater Welding, ANSI/AWS D3.6, p51

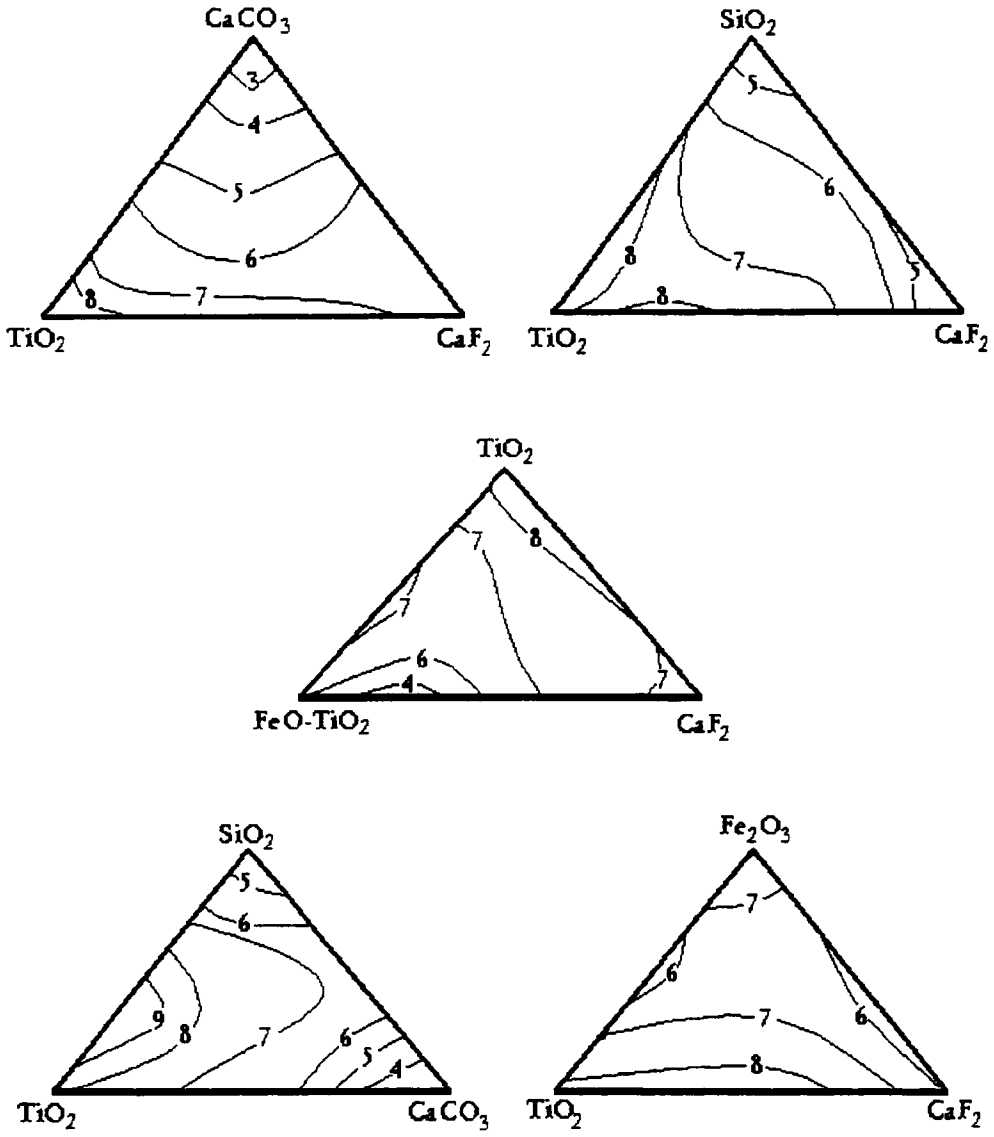

Figure 1 Influence of coating component On welding-technological properties

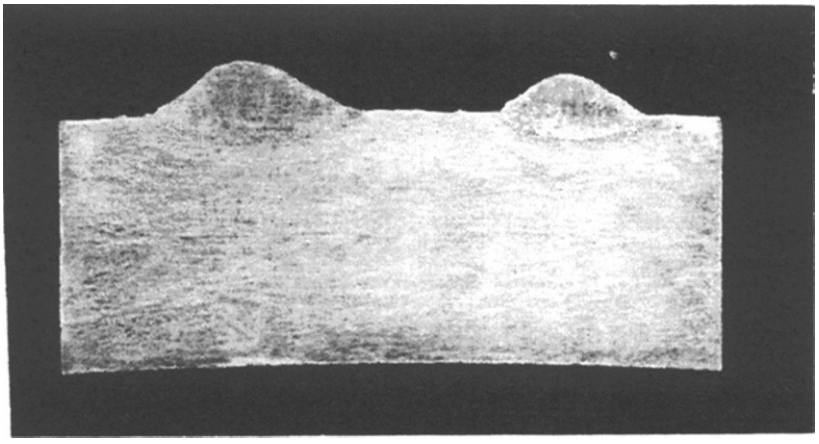

Figure 2 Typical photograph of cross-section performed at minimum and maximum current value

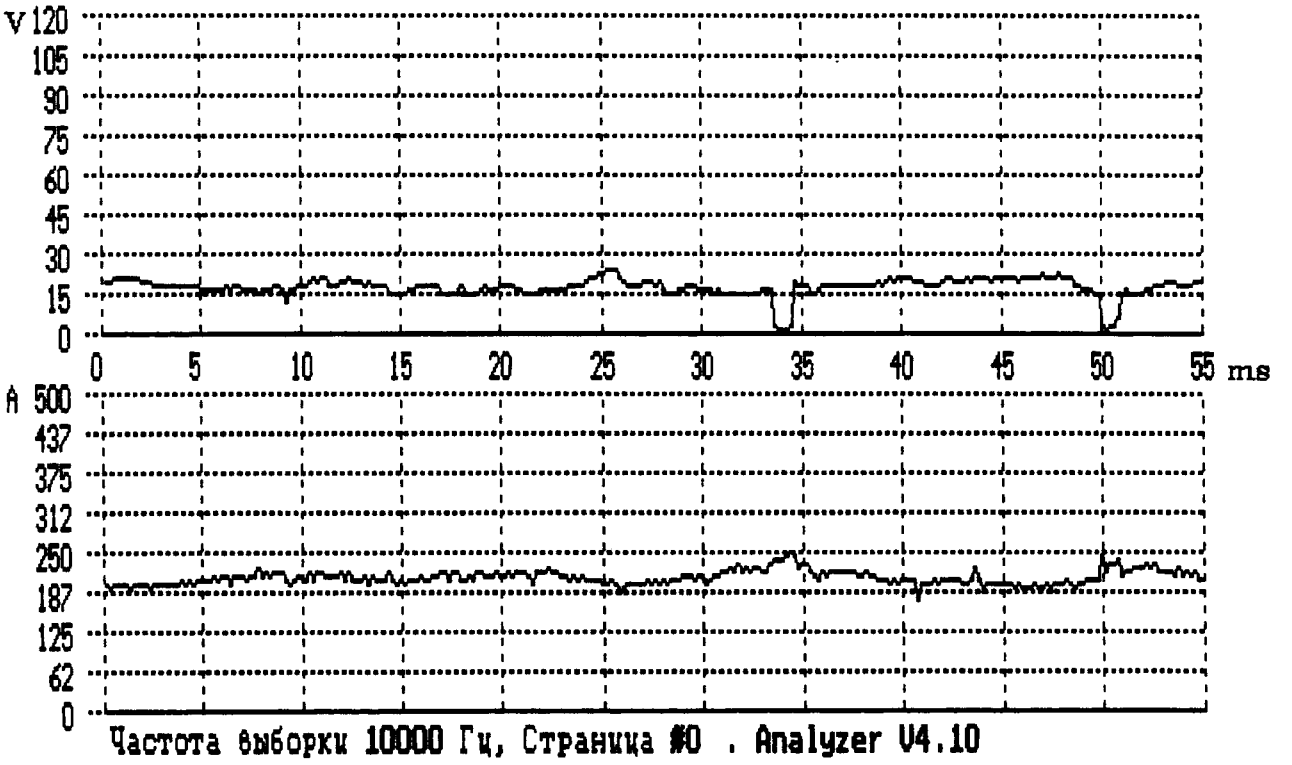

Figure 3 Fragment of current and voltage oscillogram

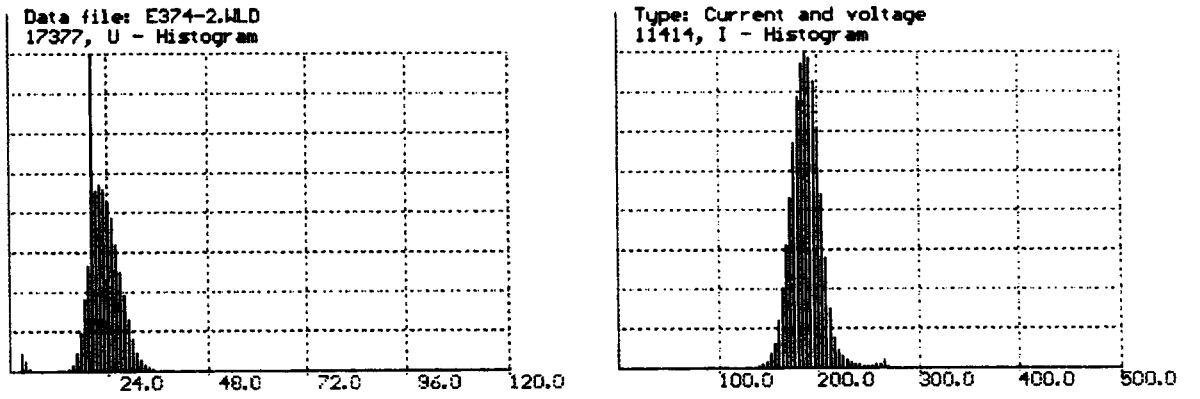

Figure 4 Welding current and arc voltage histograms, downhand position

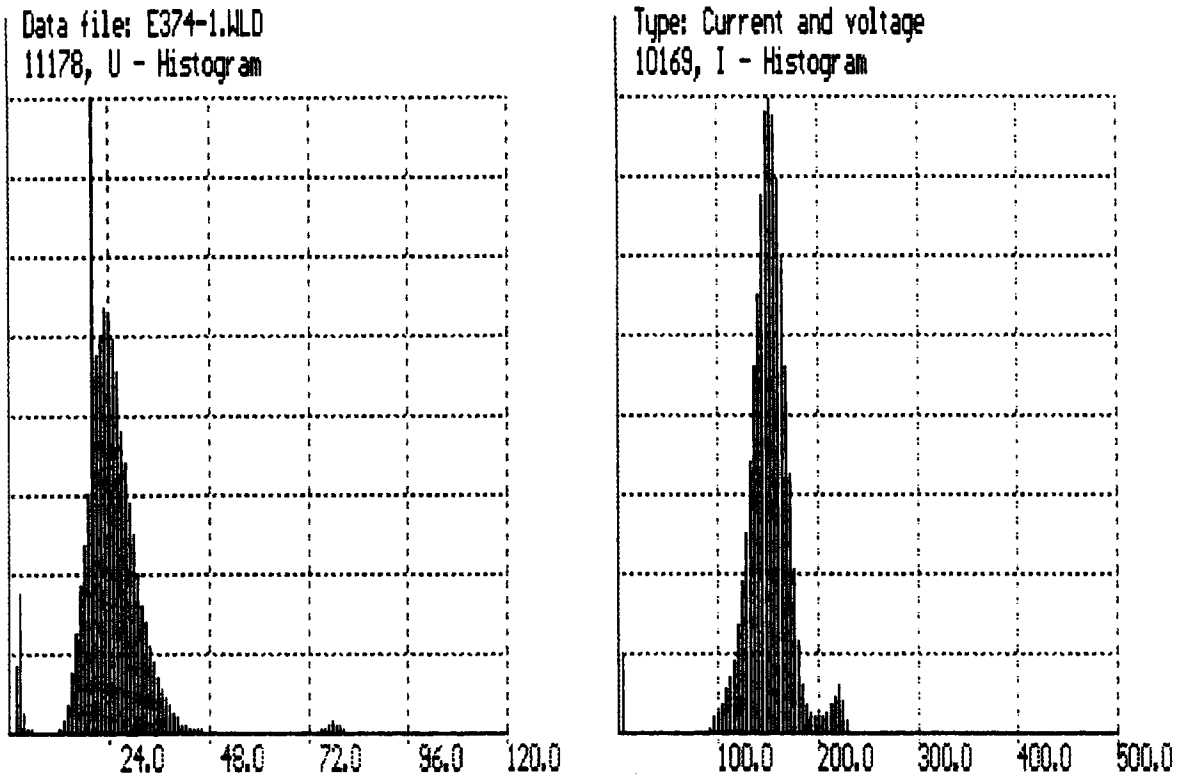

Figure 5 Welding current and arc voltage histograms, overhead position

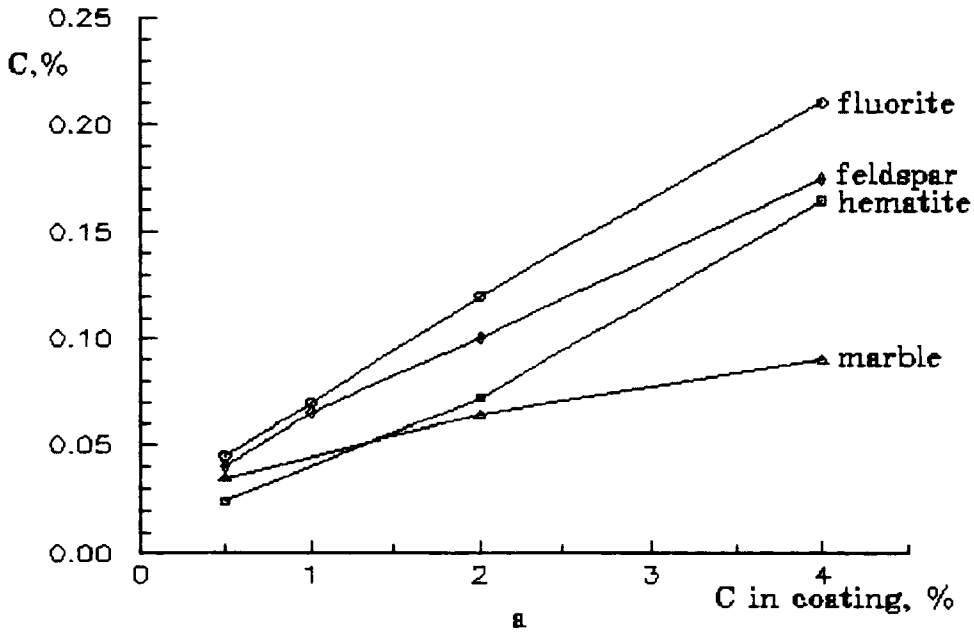

a

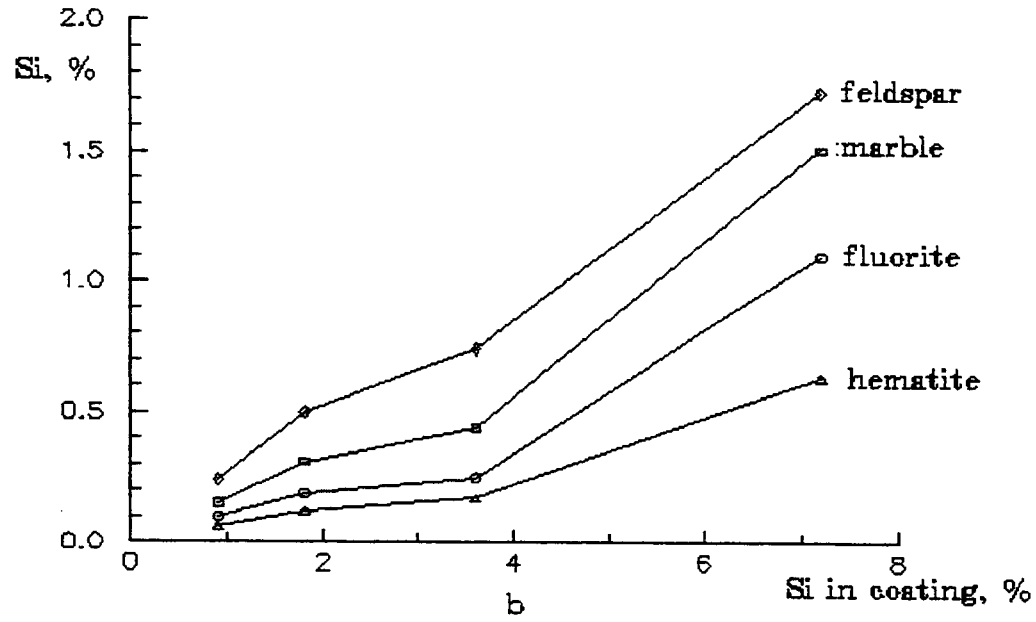

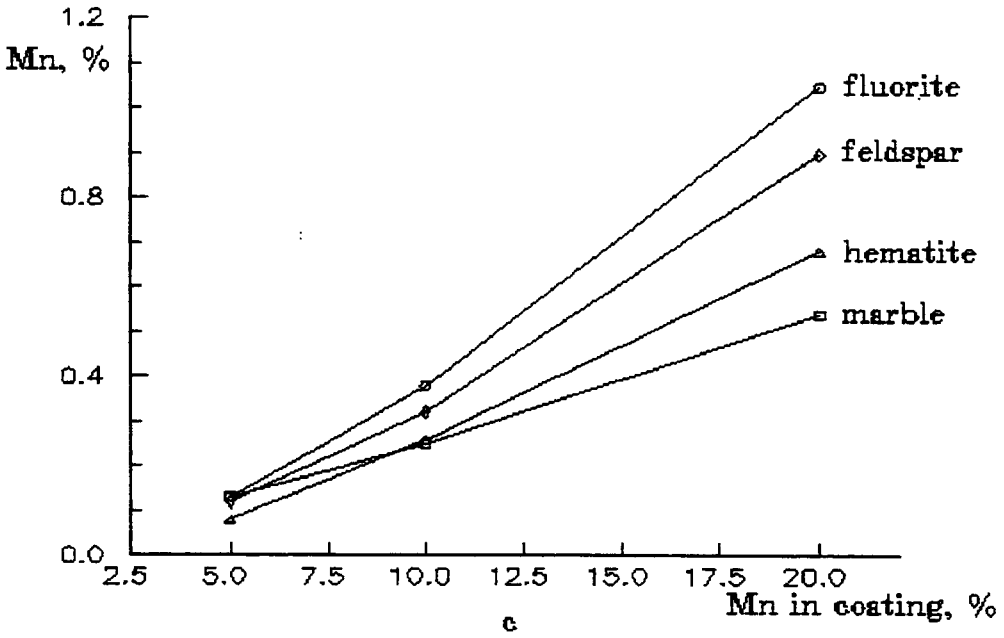

Figure 6 Relationships between the carbon (a), silicon (b) and manganese (c) amounts in weld metal and their contents in the coatings

Figure 7 Microstructure of weld metal

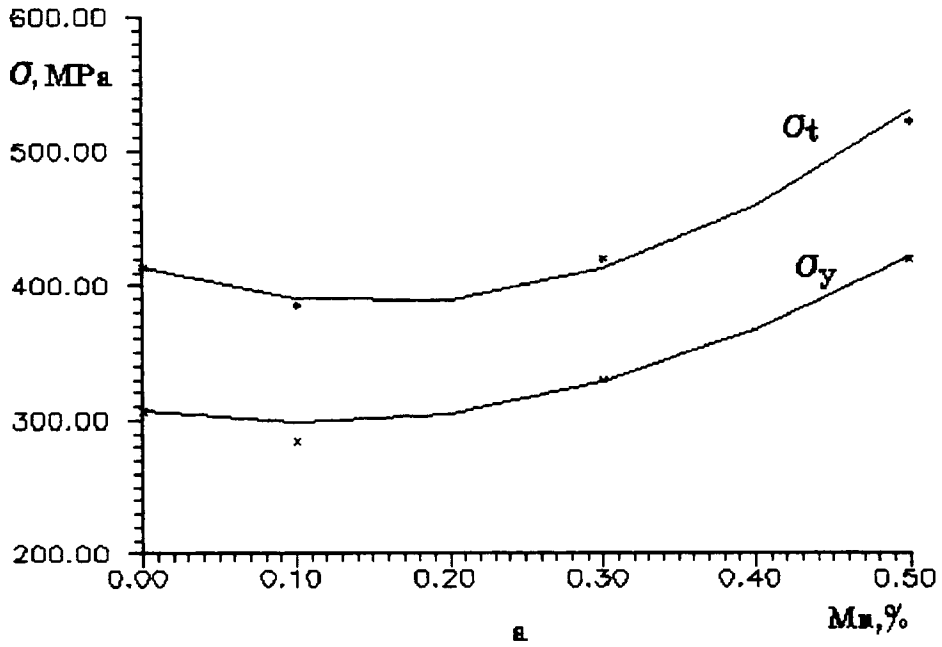

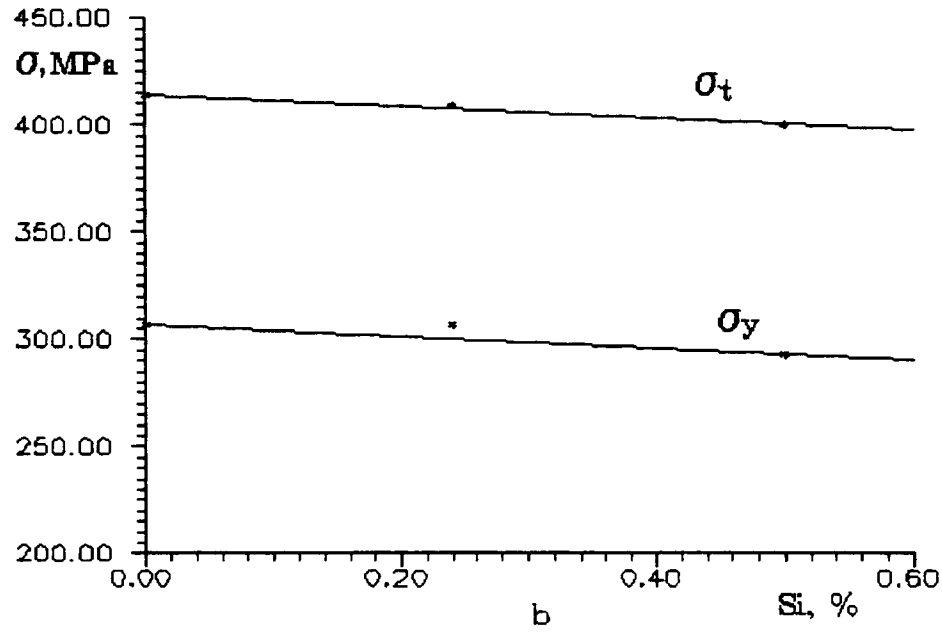

Figure 8 Manganese (a) and silicon (b) influence on tensile strength and yield point of weld metal

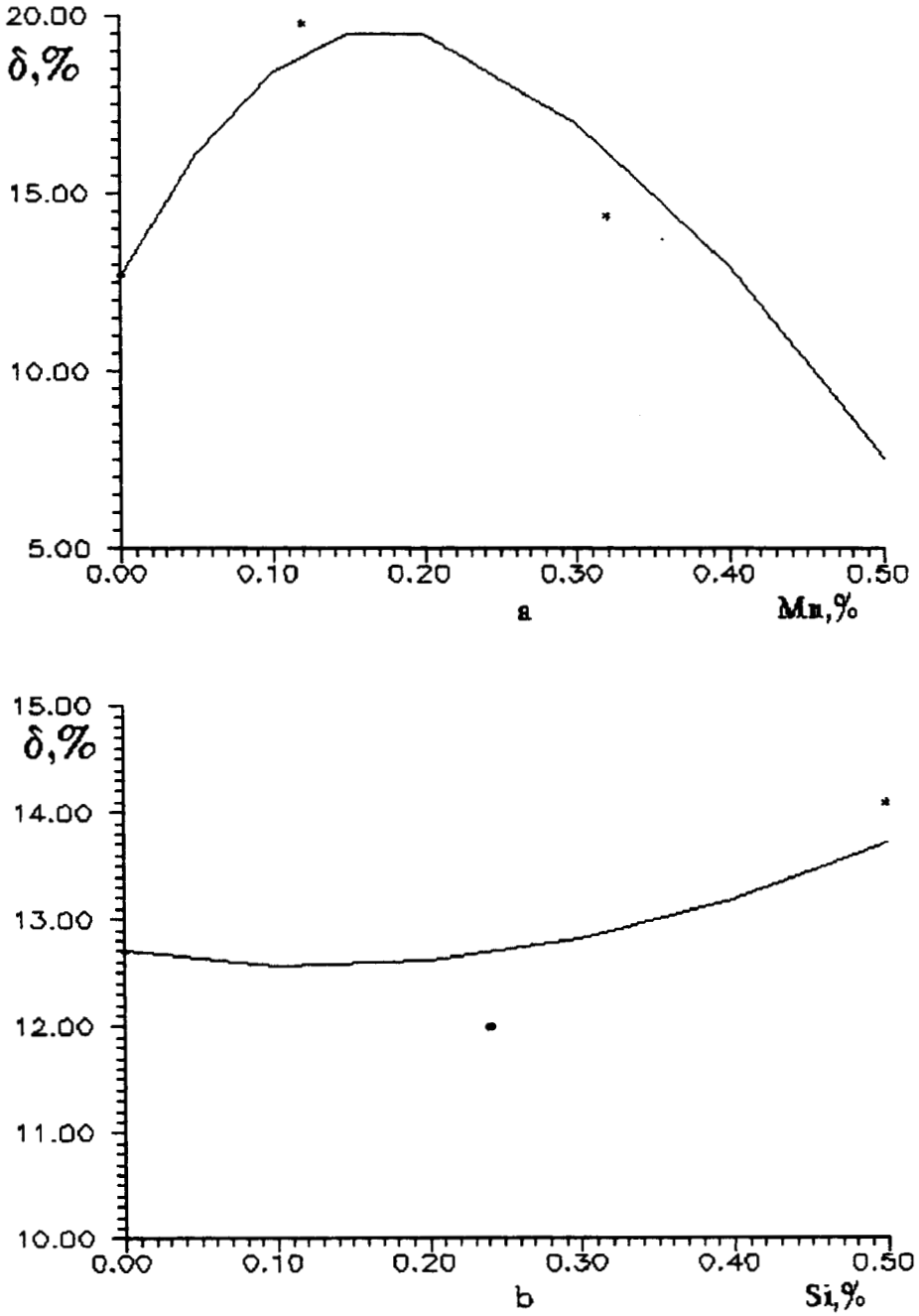

Figure 9 Manganese (a) and silicon (b) influence on elongation of weld metal

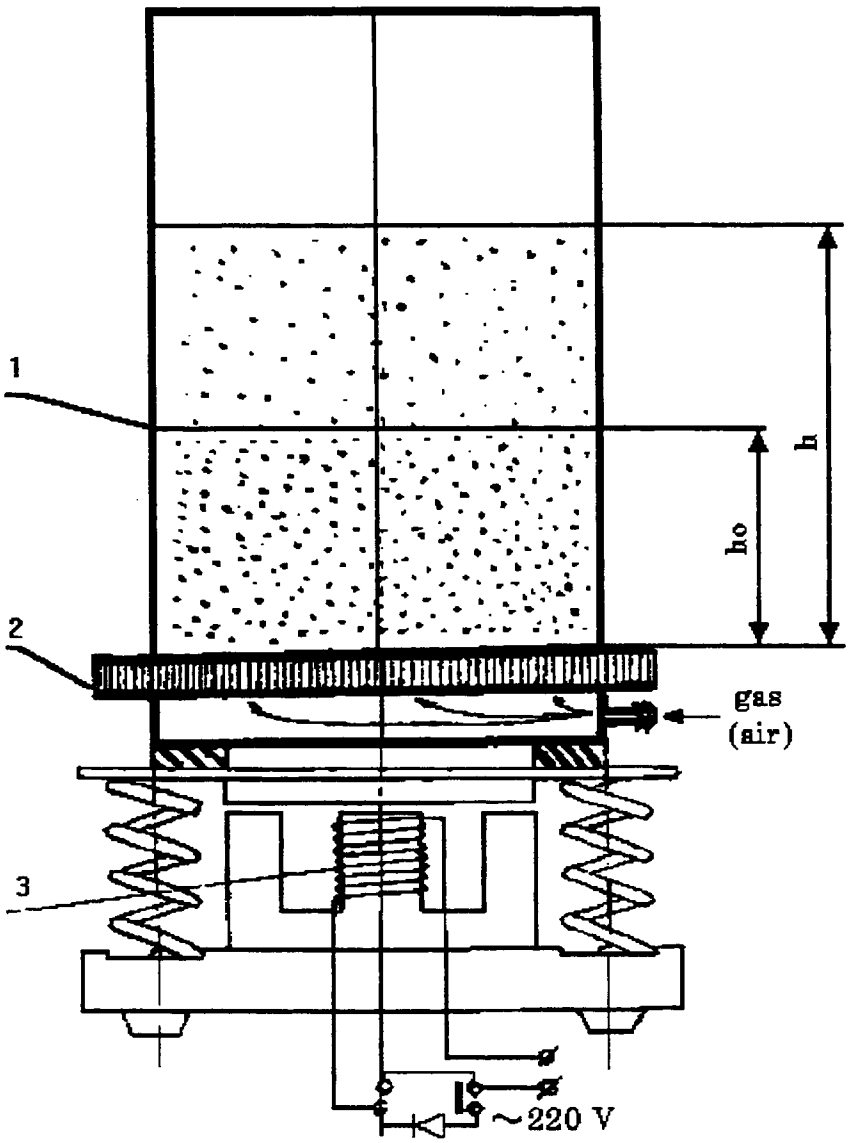

Figure 10 Laboratory plant for plotting the waterproof coating: 1 - chamber for powder whirling, 2 - porous partition, 3 - electromagnetic vibrator

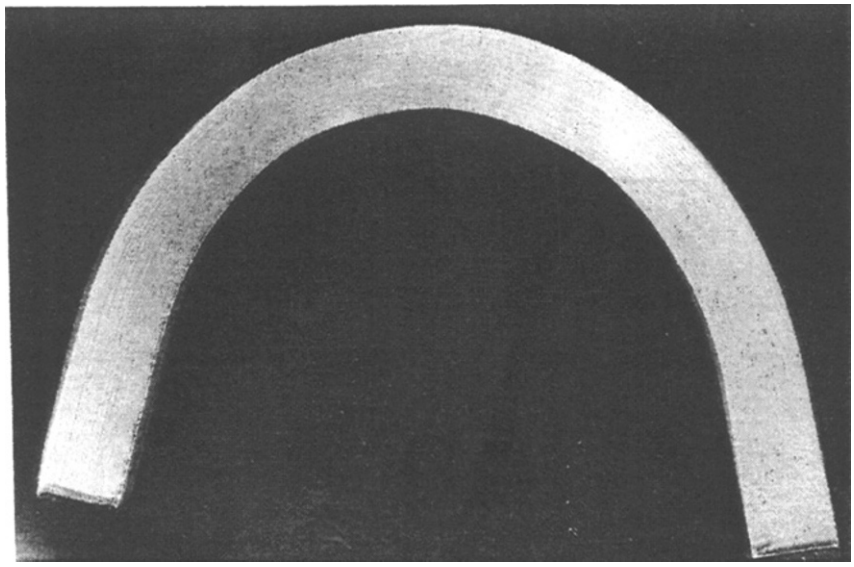

Figure 11 Sample after bend test

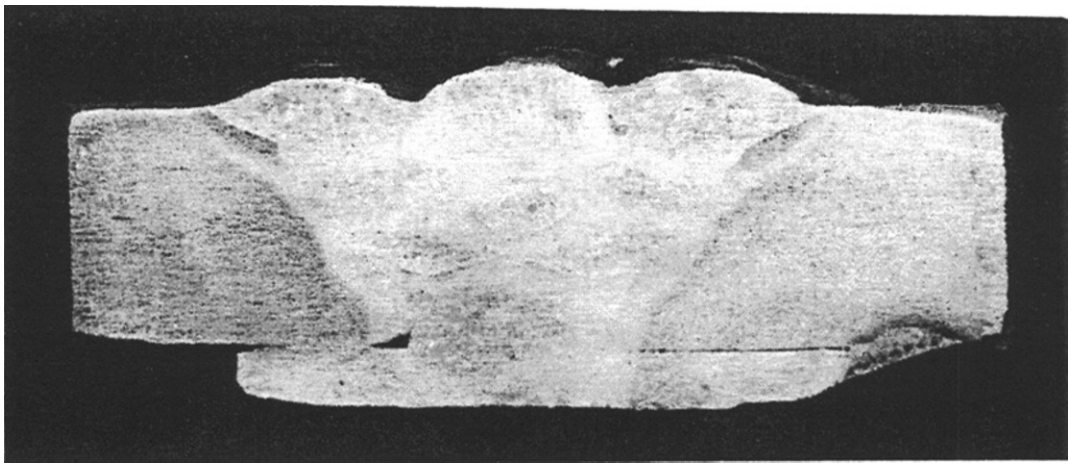

Figure 12 Cross-section of multipass weld performed with electrode EPS-AN1 type

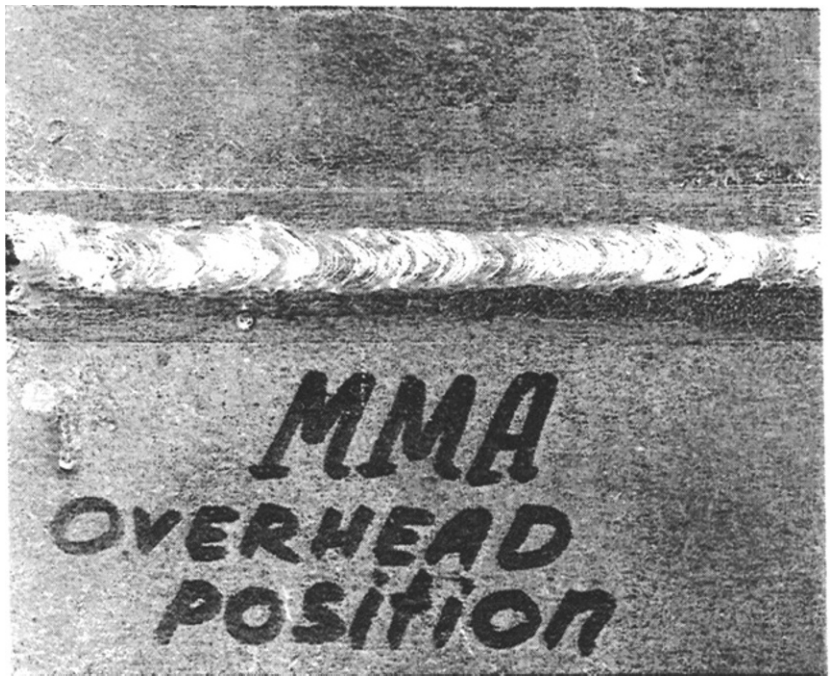

Figure 13 Root weld appearance. The weld has been performed in overhead position with electrode EPS-AN1

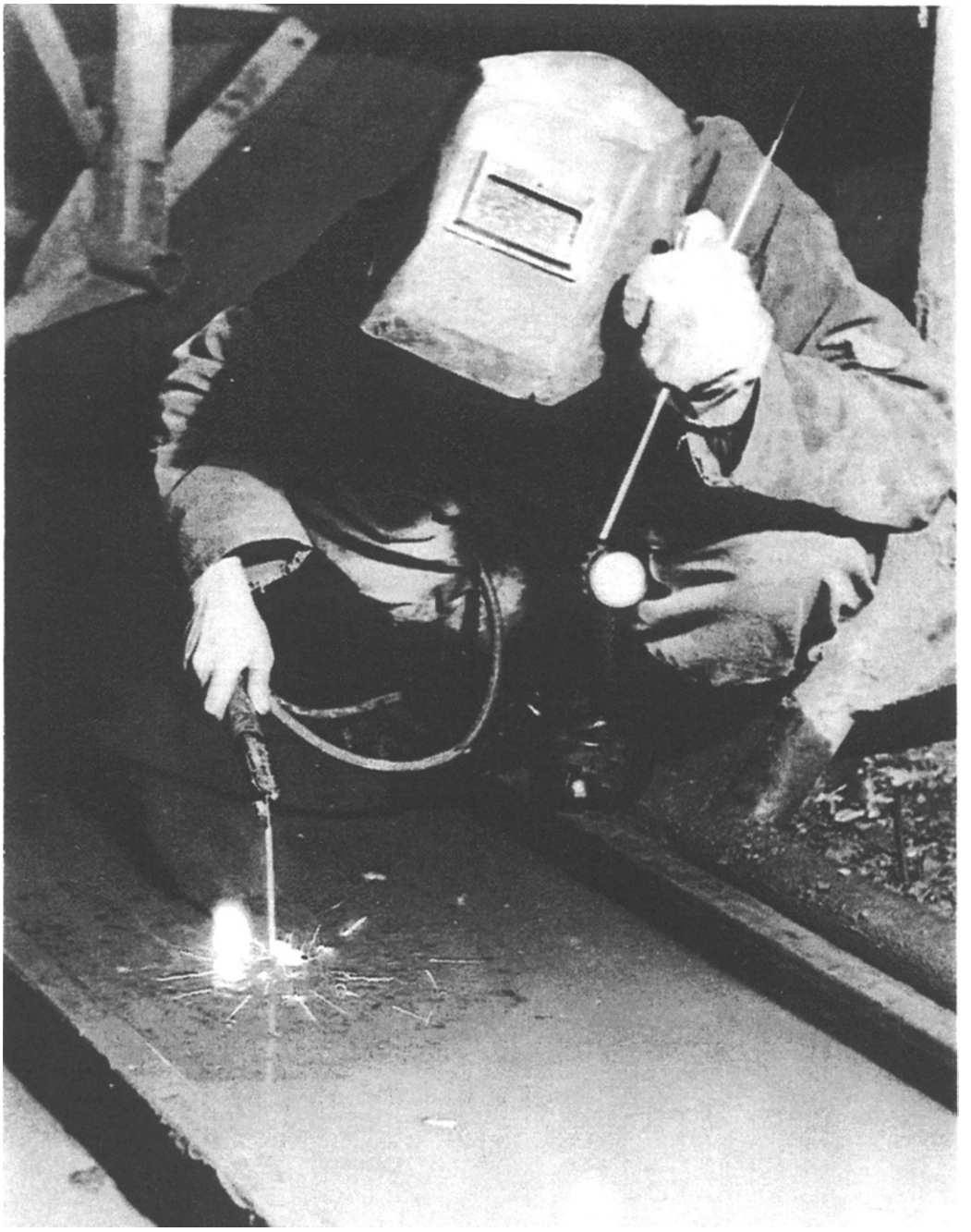

Figure 14 Performance of arc welding under thin lay of water

Special equipment of PWI design for underwater welding and cutting

I M Savich, E O Paton Electric Welding Institute

To realise the advantages of semi-automatic welding and cutting processes it is necessary use the special equipment of unique design. At the E.O.Paton EWI, development of such equipment was originated almost simultaneously with beginning of research works on development of these methods. It was clear that the semi-automatic system should operate for a long time under water. If the wire feeder is located on the ship deck, it will be possible to perform the arc welding in the water-line region only, because it is not possible to feed the flux-cored wire to larger distances.

The first submersible device was the commercial semi-automatic machine, the feeding part of which was located in the plastic box. Presence of flexible welding hose did not allow to make the box as watertight and, therefore, it was necessary to feed air uninterruptedly into the box at pressure higher than hydrostatic one.

Obviously, the first semi-automatic machine had a number of disadvantages among which the main ones were as follows:
- in the case of breach of wire feeding, the diver-welder was devoid of possibility to open cover of the submerged box to eliminate the faults and push through the wire;
- the additional air hose made difficulties for moving of diver-welder near the object to be welded;
- air being supply into box went out the welding torch and created additional bubbles around the arc making worse in the arc zone visibility.

Such a circumstances forced us to continue the works on development more convenient device in service for operating in the wide range of depths. Over several years some models of device had been made. In every model the certain new idea was realised improving the service quality until, at last, the suitable semi-automatic machine meeting the requirements of lot production was created (Fig.1).

By now, the chosen constructive design of semi-automatic machine foresees the presence of control cabinet located on the ship deck and submersible block pulled down under water (Fig.2) The power source located on the ship deck as well, control cabinet and submersible block are connected with welding cables and with cable of control circuit.

The control cabinet consists of control equipment, test and measurement equipment, and indication equipment.

The control unit is a thyristorized electric drive. This unit allows gradual regulation of rotation speed of the electrode wire feed motor, automatic limitation of the armature current to a safe value under overloading and cutting off the power from the electric drive during short circuits formed in the armature and excitation circuits.

The front panel of the control cabinet comprises a control panel with the welding process controllers, knobs of the automatic switch and the welding wire feed regulator, as well as the indicating lights.

The submersible block of the last design (Fig.3) is container having a dielectric package which houses the wire feeder, the forcing against wire mechanism and the electrode wire reel.

The drive with forcing wire against mechanism serve to feed the flux-cored wire via a guiding hose and torch to the welding zone. Reduction gear and electric motor are located in a common sealed casing the cavity of which is filled up with dielectric liquid. The free space of inside the container is filled up with fresh water. The dielectric package of container permits to insulate the elements being under voltage during welding from contact with sea water. This measure provides the reduction of current dissipation up to minimum values and maintenance of said elements in operating state.

Hydrostatic pressure of surrounding water is freely transferred on the water inside the container and, owing to presence of compensator, inner pressure is kept up equal to external one. Any flexible element, for example sylphon or flexible enough membrane can be used as compensator. Equality of pressure in all the elements of submersible block permits to avoid deformations and fixing with a wedge of some parts.

Owing to such design, the semi-automatic machine can reliably operate for a long time at the wide range of depths, exceeding the diver-welder possibility.

The technical data of commercial semi-automatic machine of A1660 type are as follows:

Parameter designation	Standard value
1. Maximum value of welding current at duty cycle = 60%, A	400
2. Diameter of electrode wire, mm	1.6 - 2.0
3. Kind of welding current	direct
4. Polarity of welding current	straight, reverse
5. Electrode wire feed speed, m/h	100...600
6. Feed speed regulation	smooth
7. 50 Hz mains voltage, V	230
8. Capacity of electrode wire reel, kg, not less than	3.5
9. Consumed power, kV×A, not more than	0.6
10. Overall dimensions, mm:	
- immersion block	
length	500±5
width	330±3
height	350±3
- control cabinet	
length	400±5
width	320±3
height	425±4
11. Weight, kg:	
- submersible block	45
- control cabinet	35

As the power sources for semi-automatic underwater welding the welding converter having a flat external volt-ampere characteristic and increased open-circuit voltage can be used. In operating the semi-automatic machine is served by two persons: operator dealing with control cabinet at the ship deck and diver-welder being under water and performing the welding. Adjustment of electric parameters of technological regime including the beginning and ending of process is performed by operator. The diver carries out the welding and, in the case of necessity, can open the cover of container "in situ", replace the empty reel and install new reel with wire, and then continue his work.

Underwater semi-automatic cutting can be performed with semi-automatic machine worked out for welding provided the cutting current does not exceed 450 A. At the such current value, it is possible to effectively cut the steel sheets of up to 20 mm in thickness. In doing so, the special flux-cored wire of 2.0 mm in dia is applied. For cutting of steels of larger thickness (up to 40 mm), the semi-automatic machine of more simpler model has been created. The model is available for operating at the current value up to 800 A. Taking into account that the cutting process does not need gradual regulation of wire feeding rate, the drive with asynchronous electric motor has been applied in this model. The change of wire feeding rate was stepped. This was performed using two changeable gears. Such semi-automatic machine was very simple and reliable but had the significant disadvantage: either operator or diver could not change the cutting technological parameters during the operation. Accumulated experience and performed calculations permit to declare that it is possible to design the semi-automatic machine with the drive made on the base of asynchronous electric motor and having the reduction gear and the changeable gears. This design will allow diver to change the wire feeding rate "in situ". With increasing the quantity of changeable gears and widening the range of feeding rate, we will have the possibility to employ such semi-automatic machine for welding as well. Therefore, it is prospective to obtain the universal semi-automatic machine for welding and cutting under water distinguished with rather simple and reliable design.

Created semi-automatic machine combined with manipulator of inhabited or uninhabited deep-water apparatus will permit an operator to perform cutting of submerged objects or joining axialery structure parts to ship hulls in salvage situation. In addition, it will be possible, on the base of created semi-automatic machines, to work out the automatic installations to perform welding and cutting of metallic structures under water condition of increased radiation. In this case, the remote control panel can be located far from operating place up to 500 m. Such installations are expected to be used at repair and dismantling of nuclear power stations.

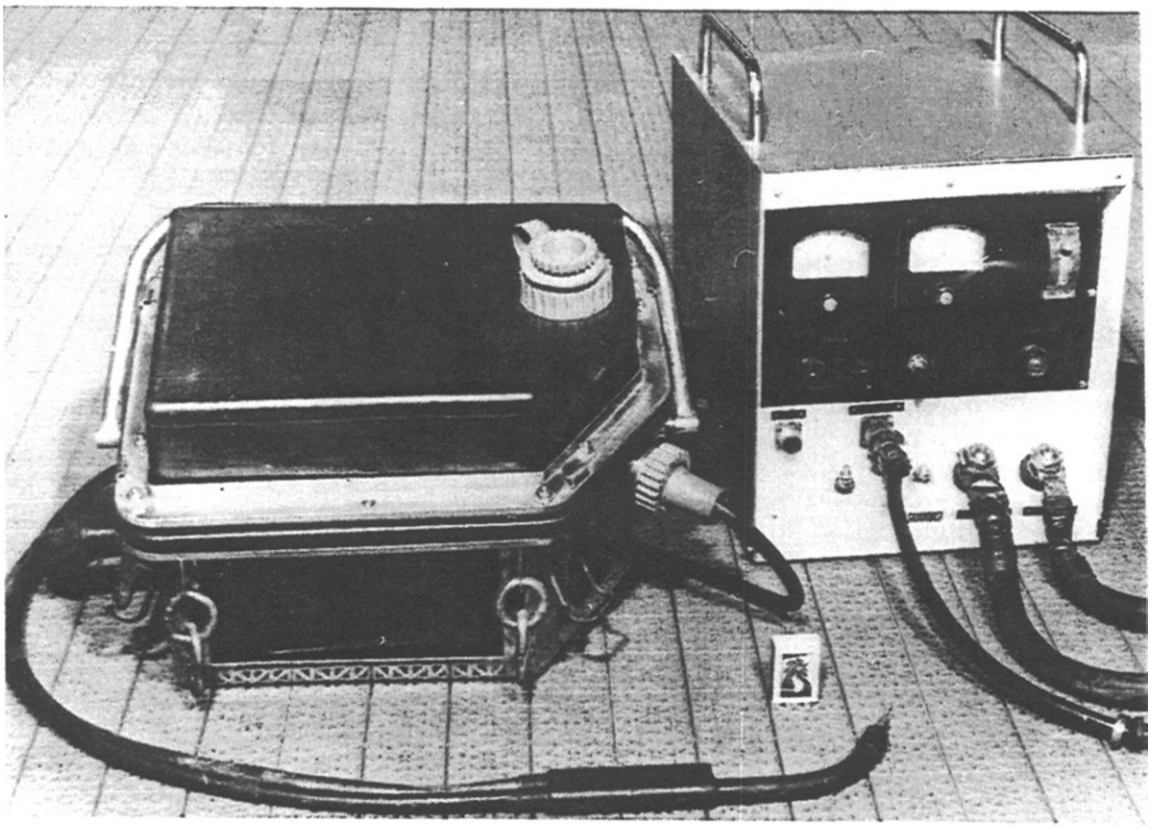

Fig.1. Semi-automatic machine for underwater arc welding.

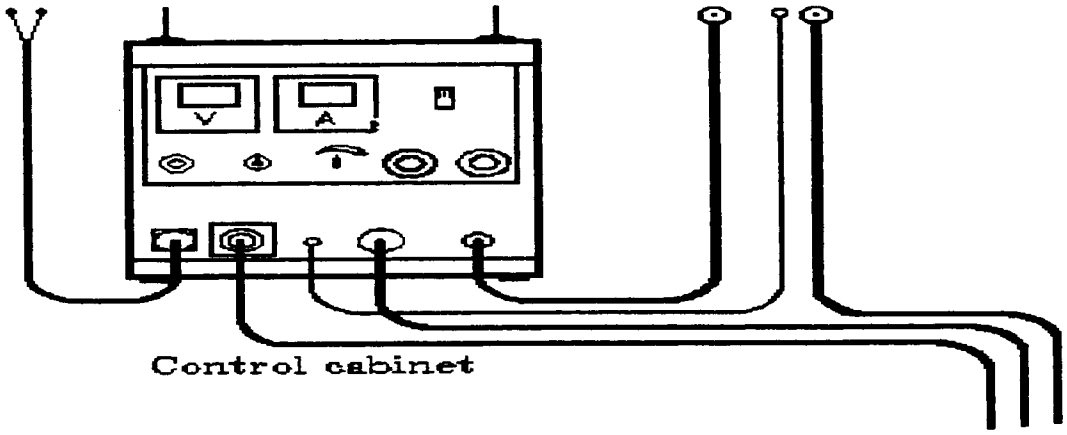

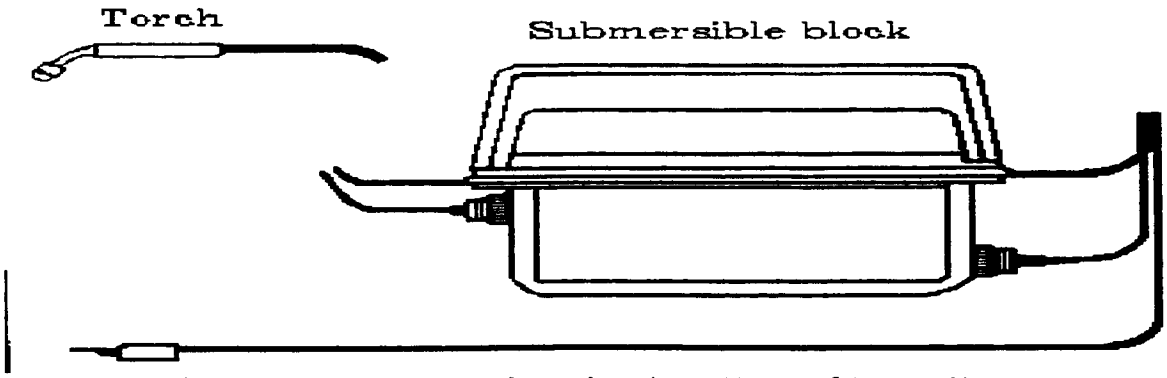

Figure 2 Scheme of connection of semi-automatic machine units

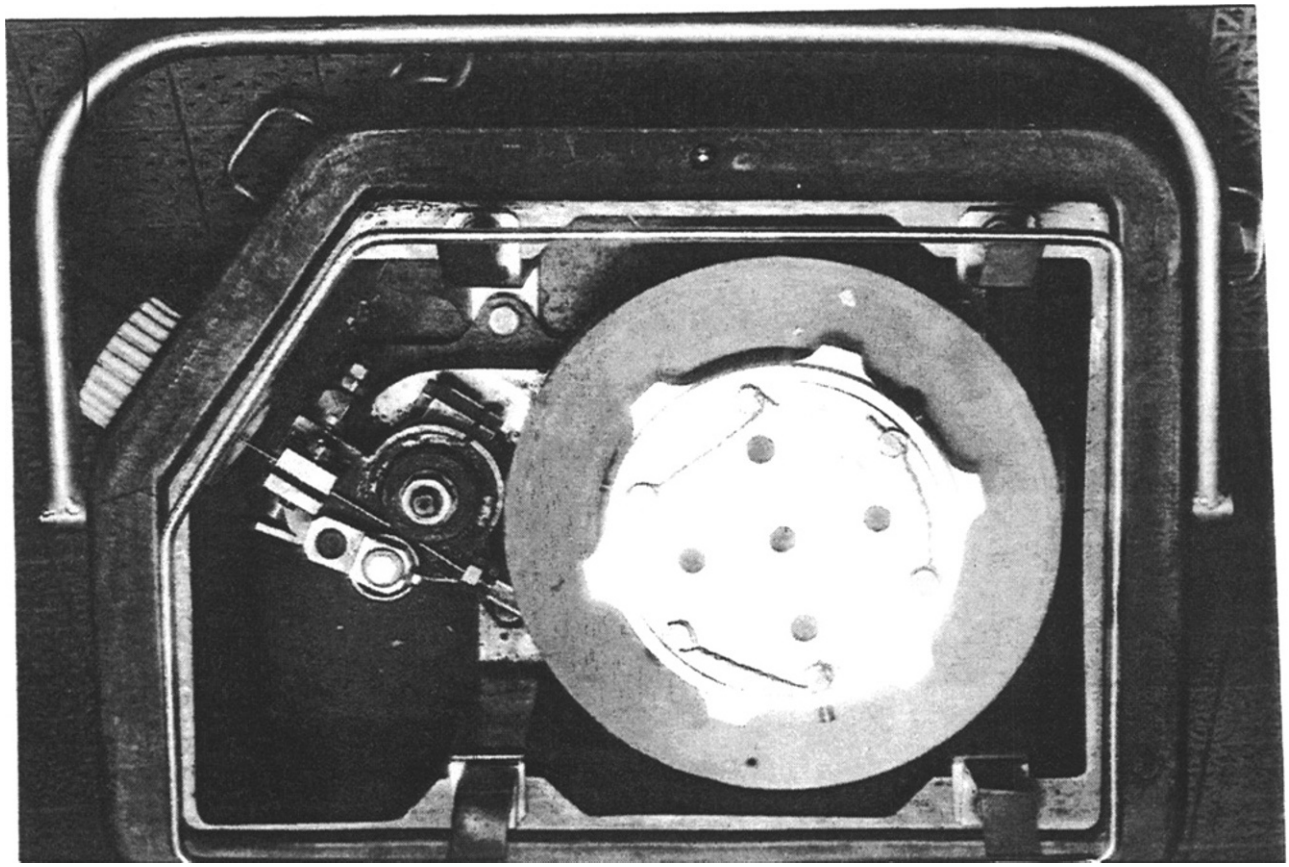

Fig.3. Submersible block of semi-automatic machine.

Wet underwater welding trials with commercial manual metal arc electrodes

D J Abson, TWI
M A Cooper, Ministry of Defence, UK

ABSTRACT

Six commercial wet underwater welding manual metal arc electrodes were evaluated in trials which simulated repairs to structures such as ships or piling in shallow water. Welding was carried out both vertically down and overhead, at a depth of approximately 5 metres. One of the electrodes was an austenitic stainless steel, and the remainder were ferritic steel, containing low levels of carbon and manganese. Two weld configurations were employed in 8 mm thick C-Mn steel plate, for which the IIW CE = 0.38. Simulating a patch repair, patch plates were welded onto each side of a pair of plates which were separated by a small gap, and a 550 mm long butt weld was deposited, to provide samples for testing both the weld metal and the heat-affected zone (HAZ). During welding, the welder/divers completed a questionnaire on the handleability of each electrode. Each weld was radiographed, and sectioned and examined metallographically. Tensile, Charpy and hardness testing were carried out.

The trials revealed significant differences in the handleability of the six commercial electrodes, which showed some correlation with the weld appearance and quality. Handleability was better when welding vertically than when welding overhead, and was also better for fillet welds than for butt welds. Worm-holes and porosity were common in the latter. Extensive cracking occurred in the panels welded with the stainless steel electrode, preventing the extraction of mechanical test specimens from them. For the weld metal of the ferritic steel butt welds, strength and hardness increased with increasing alloying, as measured by IIW CE. Weld metal Charpy toughness varied widely between the different deposits. HAZ toughness was higher than that of the weld metal, but followed the trend of the weld metal data.

On the patch plates, which were welded with three-pass fillet welds, failure occurred in the parent steel on cross weld tensile specimens for the ferritic consumables, and in weld metal for the panels welded with the stainless steel electrodes.

Viewed overall, two of the ferritic electrodes gave the best handleability and mechanical properties. However, fine-scale cracking was observed in the vertical butt weld deposited with one of them, and thus the other ferritic electrode gave the best all-round behaviour. The remaining electrodes showed poorer handleability and a higher incidence of weld defects, including the extensive cracking observed in the butt welds produced with the stainless steel electrode.

INTRODUCTION

Wet under-water welding has been employed for many years as a technique for the repair of steel structures and vessels.(1,2) It offers the prospect of effecting considerable cost savings, if it can replace the more costly options of changing the draught of a vessel or structure, taking it out of service, moving it to a dry-dock, or carrying out hyperbaric welding. Wet under-water welding is normally carried out by the manual metal arc process, although some continuous wire, semi-automatic welding has been reported in Russia (3) and the U.S.A. (4).

Following a survey of available commercial wet under-water welding electrodes by TWI (5), wet under-water welding trials have been carried out with six commercial electrodes. It was considered important that the welding of a patch, simulating a repair, should be included, as well as the deposition of metal in a butt weld, to provide material for all weld metal tensile and other tests. This paper presents the results of such trials, which were carried out in the wet under-water welding tank at TWI North.

The American welding code AINSI/AWS D3.6-93 (6) indicates that the salinity of the water is a non-essential variable, i.e. that welding procedures which are qualified in fresh water may be used in salt water, and vice versa. The trials were therefore conducted in fresh water.

EXPERIMENTAL DETAILS

Diving Facility

The diving facility at TWI North comprises a 6.5 m deep tank with support facilities to allow up to two divers to operate in the tank. The welding was carried out by each of two experienced welder/divers. The water temperature was 16°C. A backing plate, to which all panels to be welded were attached, was itself attached securely to a work bench on the bottom of the tank.

The initial trials, carried out with a 400amp diesel-powered DC generator, with a maximum open-circuit voltage of 80V, and stepped current range settings, revealed that arc stability was not good with this generator, and it proved to be unsatisfactory in not permitting continuous variation in the current settings. (This set was employed for the welding of both the vertical butt weld and the overhead patch weld panel deposited with the electrode coded H; see below). It was replaced with a 300amp diesel-powered Lincoln "Nomad" DC generator, with a maximum open circuit voltage of 95V, which allowed continuously variable current settings.

Electrodes and Parent Steel

The MMA electrodes which were employed all have rutile coatings; five were ferritic electrodes, coded B, L, H, D and G, and one was an austenitic stainless steel electrode, coded S. All these electrodes were 3.2 mm diameter. The electrodes coded B and S had been waterproofed by dipping them in wax. The coating was found to be damaged on receipt on approximately half of the electrodes, exposing the underlying flux coating. The remaining electrodes had polymer or lacquer coatings.

The steel plate employed in the trials, Table 1, was 8 mm thick NES 791 PT3 ISS2 1987(Admiralty grade B), which is equivalent to BS EN 10025: 1993 grade S355J2G3 (formerly BS EN 10025:1990 grade Fe 510 D1, and before that BS 4360: 1990 grade 50D).

Weld Configurations

Two configurations of test panel were employed, and each was used for both vertical and overhead welding. The first was a pair of patch plates, 170 mm x 120 mm, which were welded on each side of a gap between two slightly larger pieces of plate. This arrangement is similar to that employed in AWS D3.6-93. However, only one plate thickness (8mm) was used throughout in the present trials, whereas in AWS D3.6-93, the patch plates are each half the thickness of the main plate. The arrangement used in the present trials simulates more accurately the welding of a patch repair, but has the disadvantage that failure in cross-weld tensile tests will always occur in one of the main plates, unless the welds are extremely defective. The main wet welds in these panels were a pair

of multiple-pass fillet welds (which were each welded with three beads), on opposite faces of the test assembly. The corresponding pair of multiple-pass welds at the opposite end of the assembly were each welded previously in three passes, in air, by MAG welding with a C-Mn wire; short lengths of single-pass fillet weld were deposited, as tack welds, to hold each assembly together, prior to the wet welding. In addition to the multiple-pass fillet welds, up to four single-pass fillet welds were also deposited by wet welding, at the sides of the patch plates.

The second panel configuration was a 550mm long butt weld. The panel was restrained by strong-backs, and a 6mm thick, 40mm wide backing bar was employed. A 20 degree bevel was machined on each side of the preparation, with a 10mm root gap for the vertical panels and a 12mm root gap for the overhead panels.

Welding Details

The welder/divers stood on the bottom of the 6.5m deep tank. The welding depth was therefore approximately 5m. The polarity employed for each electrode was that recommended by the electrode manufacturer, namely DC +ve for electrodes H and S, and DC-ve for the remainder. It proved possible to hold an arc with each of the electrodes, rather than using them as contact electrodes. Careful adjustment to the current was needed. Some fluctuation in current occurred around the set value, although the tolerance on the optimum current setting was only approximately ±5 amps. Arc energies were not determined, but are estimated to be normally in the range 1.0 to 1.5kJ/mm. The butt welds were completed in nine passes, which were deposited in three layers, with the third pass in each layer being deposited in the centre. Inter-run slag removal was achieved with a chipping hammer and, where necessary, grinding with an air-powered burr grinder.

NDT, Photography, and Sectioning

Each of the multiple-pass butt and fillet welds was radiographed using a 200kV X-ray source and also photographed prior to sectioning. In order to radiograph the multiple-pass fillet welds so that both welds were revealed, the panels were tilted through an angle of 30°; two exposures of different duration were required, to accommodate the difference in effective thickness.

Mechanical Testing

From each of the patch plates, two 55mm wide lap weld tensile specimens were machined, spanning the whole panel, as in AINSI/AWS D3.6-93 (6), with the multiple-pass welds transverse to the tensile axis. These specimens were tested at room temperature. Transverse sections through the multiple-pass welds were used for Vickers hardness surveys, carried out with a 10kg indenter load.

The two cross weld tensile specimens, which were machined from each of the butt welded panels except S/B/V and S/B/O (which were welded with the austenitic stainless steel electrode, S, and which were not sufficiently sound), had an overall length of 145mm, a parallel length of 80mm, and a gauge width of 25mm. Any overfill was machined flush with the plate surface. They were tested at room temperature. Longitudinal, all-weld-metal tensile specimens were machined with an overall length of ~70mm, and generally had a gauge length of 28mm and a gauge diameter of 5.6mm. However, both were reduced, in proportion, when defects were found within the parallel portion during machining. They also were tested at room temperature. The tensile specimens from the butt welds were given a 100°C/10h hydrogen removal treatment prior to testing. All tensile testing was carried out according to BS EN10002-1: 1990.

Charpy V-notch specimens were machined from each of the butt welded panels except S/B/V and S/B/O (which were not sufficiently sound), and were notched in two different locations. Five specimens from each panel were notched on the weld central plane, and five were notched in the HAZ, although these HAZ specimens inevitably sampled some weld metal. Each set of five specimens was tested over a range of temperature, to give a partial transition curve. All the specimens, which were sub-size (5x10mm), were machined and tested according to BS EN10045-1: 1990. Overall, test temperatures ranged from -60°C to +40°C.

Transverse sections through the butt welds were used for Vickers hardness surveys, carried out with a 10kg indenter load. The cap, root and mid-depth regions were sampled, in the weld metal and the HAZ. In addition, the hardness of the parent plate was measured, at approximately the mid-depth.

Chemical Analysis and Metallography

The butt welds were each analysed on an optical emission spectrometer, sparking on to the weld cap, after it had been ground flush with the surface of the plate. Analysis for oxygen and nitrogen, by inert gas fusion, was determined on samples cut from an adjacent weld slice.

A transverse section was prepared from each of the butt welds, from the multiple-pass fillet welds on the patch plates and cut from one of the single-pass fillet welds. All the sections were ground and etched in nital to reveal the weld profile prior to hardness testing. Macrographs were taken of the butt welds and multiple-pass fillet welds, with some welds being polished to a 1μm diamond finish, prior to etching in nital. This polished finish was required in selected welds which were subjected to more detailed metallographic examination. The microstructures of the stainless steel welds were revealed by etching in a solution of 120ml HCl, 50g $FeCl_3$ and 480ml H_2O.

RESULTS

Electrode Handleability

Questionnaires were completed by the welder/divers on the performance of each electrode. The issues covered included arc striking, arc stability, spatter, slag fluidity, weld pool fluidity, fume level, and slag removal. The results of the questionnaires, for both the vertical and the overhead welding, indicate that the electrodes with the best handleability are B, H and L.

One feature of the behaviour of all the electrodes which was not revealed by the questionnaire is the restricted range of welding parameters over which each electrode operated satisfactorily. As noted earlier, the tolerance on the optimum current setting was typically ±5amps. In addition, the travel speed had to be sufficiently slow that the weld pool would spread, so that unduly peaky beads were avoided. However, at low travel speeds the slag flooded ahead of the electrode. The welding conditions were particularly critical for electrode S, where solidification cracking occurred down the central plane of the butt welds at travel speeds only slightly faster than the critical speed for avoiding the slag flooding ahead of the electrode, thereby further restricting the useable range. However, the benefit derived from selecting the correct travel speed for welding with this electrode was short-lived, as a crack developed all the way down one fusion boundary of each of the butt welds, before the weld was completed.

Weld Appearance and Quality

Photographs of two of the butt welds are shown in Fig.1(a) and 1(b). The most uniform profile of the vertical butt welds was that of weld H/B/V[1], in which the appearance was similar to that of a weld deposited in air, with uniform ripples. Welds, B/B/V, Fig.1(a), and L/B/V were progressively slightly less uniform. The surface profile of welds G/B/V and D/B/V was less uniform

[1] The coding scheme was:- electrode (B, L, H, D, G or S)/butt (B) or patch (P)/welding position (vertical, V, or overhead, O). still, and that of weld S/B/V, was extremely uneven.

By contrast, the surface appearance of the vertical single pass and multiple-pass fillet welds on the patch plates was generally good. Welds B/P/V and L/P/V had the smoothest profiles, with the remaining welds all having slightly less uniform appearance.

All the overhead butt welds had poorer surface appearance than their corresponding vertical deposits. Welds G/B/O, D/B/O and S/B/O, Fig.1(b), had particularly uneven profiles. Weld L/B/O was slightly more uniform, with both H/B/O and B/B/O having the best profiles.

The surface appearance of the overhead single pass and multiple-pass fillet welds on the patch plates was generally uneven. Weld S/P/O had the smoothest surface appearance. All the other welds had uneven profiles, with weld B/P/O having the smoothest profile of the remaining welds.

For the vertical butt welds, the uniform profile of welds H/B/V and B/B/V was apparent from the radiographs. Both welds, and also weld L/B/V, had some lack of penetration in the root, which was extensive in weld H/B/V. Such lack of penetration occurred also in weld G/B/V, and was found in one of the two radiographs from weld D/B/V. Worm-holes up to 4 or 5mm in extent and porosity ≤2mm diameter occurred in all welds, except H/B/V, which only contained fine-scale porosity. The most seriously defective weld was S/B/V, which was cracked all the way down one fusion boundary, and contained other, intermittent cracks.

All the vertical multiple-pass fillet welds contained a small amount of porosity, which was ≤2mm for welds H/P/V and B/P/V, both of which also had slight lack of fusion in the root. Weld G/P/V had a slightly uneven profile, and a 60mm long crack occurred at one end of weld S/P/V.

For the overhead butt welds, welds H/B/O, B/B/O and G/B/O all contained fine-scale porosity throughout the weld. Maximum pore sizes ranged from 4 to 6mm. In weld B/B/O, worm-holes were small, but the maximum size was ≤8mm in weld H/B/O and ≤7mm in weld G/B/O. The profile of weld G/B/O was uneven, and there was intermittent cracking; the same features occurred also in welds L/B/O and D/B/O, both of which had extensive porosity (≤4mm for weld L/B/O and ≤13mm for weld D/B/O). In addition, weld L/B/O contained some worm-holes (≤5mm). Finally, weld S/B/O contained severe cracking and gross worm-holes and porosity.

The multiple-pass overhead fillet welds generally contained small worm-holes and a small amount of porosity. The exceptions to this were weld S/P/O, where the porosity was more extensive and the worm-holes were larger, and weld G/P/O, where there were no reportable defects.

Overall, these observations show that defect levels assessed non-destructively were lower in vertical than in overhead welds and in fillet welds compared with butt welds. Cracking was extensive in butt welds S/B/V, L/B/O, D/B/O and S/B/O, and much less severe in weld G/B/O. The electrodes which gave the soundest welds were B and H, although lack of penetration in the root was seen in welds H/B/V, H/P/V and B/P/V.

Chemical Analysis

The chemical compositions of the ferritic weld metals in the vertical and overhead butt welds, Table 1, show that they are all carbon steel with a moderately low carbon content, low levels of Mn (0.25% to 0.72%), and generally minor variations in the levels of residual and trace elements. Silicon levels range from 0.11% in weld L/B/V to 0.59% in weld B/B/O. The highest levels, which probably reflect higher levels of silica in the slag, occur in welds produced by the electrodes which have the best handleability, namely electrodes H, B and L.

The weld metal oxygen levels range from 0.0700% to 0.1395%. The lowest oxygen levels occur in the vertical and overhead welds deposited using electrode B, with those deposited with electrode D having the next higher level, in each case. Both oxygen and sulphur contents contribute to non-metallic inclusion contents (7). Thus, welds H/B/V and G/B/O will have the highest inclusion contents among the vertical and overhead butt welds, respectively.

The weld nitrogen contents show appreciable variation. Electrode D produced welds with the lowest nitrogen levels, namely 0.005% for both the vertical and overhead welds. Corresponding figures for electrode G welds were ~0.009% higher.

The butt welds deposited with electrode S showed an appreciable difference in the level of Cr (26.6% in weld S/B/V, cf 19.5% in weld S/B/O). This difference is greater than would be expected from any possible losses due to oxidation, and is therefore attributed to a difference in dilution. While weld oxygen levels were similar to those found in the ferritic steel welds, the levels (of ~0.07%) were several times higher than those in the ferritic steel welds. However, in (predominantly) austenitic stainless steel weld metal, such levels do not give cause for concern.

Metallographic Observations

Macrographs of selected butt weld transverse sections are shown in Fig.2. (Figure 2(b) shows the Vickers hardness indentations.) The butt welds deposited in the overhead position were wider than the corresponding vertical welds, as the preparation was slightly wider for the former case (12mm cf 10mm for the vertical butt welds). The majority of the butt weld sections revealed reasonable profiles, both for individual beads and for the overall welds. The exceptions were the overhead welds D/B/O and S/B/O, Fig.2(b), which had poor profiles, and some gross porosity. The section from the stainless steel weld S/B/O also revealed the cracking which ran all the way down the fusion boundary at one side of the weld; similar porosity and cracking were found in the corresponding vertical butt weld S/B/V. The remaining welds generally had lesser defects, with some porosity in weld L/B/V, and some lack of penetration in the root for welds H/B/V, B/B/V [Fig.2(a)], L/B/V, H/B/O, D/B/O and S/B/O [Fig.2(b)].

The transverse sections of the multiple-pass fillet welds which were deposited vertically revealed a good weld profile for weld B/P/V. The profiles of welds H/P/V and L/P/V were not so good, with some porosity and undercut in weld L/P/V. In welds G/P/V and D/P/V, some of the beads had a concave surface, and that was true also of one side of the stainless steel weld, S/P/V.

The profiles of the ferritic steel overhead multiple-pass fillet welds generally showed uneven convex beads, the exception being weld B/P/V, which had only a slightly convex surface. The surface profiles of weld L/P/O and weld D/P/O, Fig.2(c), showed particularly convex surface profiles, and a small amount of undercut. The overhead stainless steel weld S/P/O had an uneven profile, some porosity, and some cracking.

Detailed examination of the weld microstructures of the ferritic steel butt welds revealed that they fell into two main groups. In the first group, deposited both vertically and overhead with electrodes G and D, the prior austenite boundaries in the as-deposited microstructures were lined with large colonies of ferrite with second phase (FS which often extended all the way across the prior austenite grains) and some large primary ferrite (PF) grains, Fig.3(a). There were only occasional individual (acicular) ferrite (AF) laths. In weld metal reheated by subsequent passes, the grain-coarsened regions, with constituents as for the as-deposited regions, were very narrow, and the extensive grain-refined regions consisted of uniform equiaxed ferrite grains. It will be noted from Table 1 that these welds have the lowest values of IIW CE.[2]

In the second main group, the as-deposited microstructures of both vertical and overhead welds deposited with electrodes H and B had prior austenite boundaries lined with narrow bands of PF and FS. The intragranular structure contained both large and small colonies of FS, and individual AF laths; see Fig.3(b). There were occasional patches of ferrite-carbide aggregate, but the small colonies of FS and the individual ferrite laths were surrounded by martensite. In weld metal reheated by subsequent passes, the grain-coarsened regions had microstructures similar to the as-deposited regions, and the grain-refined microstructure consisted of equiaxed ferrite grains with carbide films generally lining the prior austenite boundaries. The welds deposited with these electrodes have the highest values of IIW CE.

The microstructures of the butt welds deposited with electrode L were intermediate in character between the two main groups detailed above. These welds have values of IIW CE which are intermediate between those of the other two groups.

One feature which is worthy of comment is the occasional fine-scale cracking observed in as-deposited and reheated regions of welds B/B/V, Fig.3(b), and also in the HAZ of this weld. This cracking is readily identified as hydrogen-induced cracking.

In the welds deposited with the stainless steel consumable, electrode S, the microstructure differed from one bead to another, reflecting differences in dilution. In the early passes which are in contact with the parent (ferritic) steel, the microstructure was commonly non-uniform within each bead. In the butt welds, the microstructure close to the parent steel was up to 100% martensite. However, elsewhere in the early beads, visual estimates of the proportions of the various microstructural constituents are 80% martensite, 5 to 10% ferrite and 10 to 15% austenite. Such microstructures reflect not only high dilution of the parent steel into the first layer weld beads, but also show that the welding conditions, including the rapid solidification, allowed incomplete mixing to occur. In beads in the second layer, the proportion of ferrite had increased to 10 to 25% in weld S/B/O (where it was not clear if the remainder was entirely austenite) and to 30% in weld S/B/V. Corresponding figures for the capping pass are 15-25% ferrite in weld S/B/O and 60% ferrite (with the ferrite grains having very ragged edges) in weld S/B/V. These microstructural differences between the overhead and vertical welds show that dilution was greater in the former.

In the fillet welds, the microstructure in weld S/P/V changed progressively from 10 to 15% ferrite in the first bead to an estimated 40% ferrite in the second bead, and 60% ferrite in the third bead, with the other phase being austenite in this weld. Each of the beads in weld S/P/O appeared to contain an estimated 5 to 15% ferrite. However, the proportion of martensite changed abruptly in bands within the first bead on each side. The microstructure in the bands comprised either an estimated 5%

[2] This parameter was developed to characterise the risk of HAZ hydrogen-induced cracking, but is also used as a hardenability parameter.

ferrite and 95% martensite or 10 to 15% ferrite, with the remainder being austenite, Fig.3(c). The microstructure of the later passes was generally more uniform, with the proportion of martensite being ~80% in the second pass, falling to 50 to 60% in the last pass. The non-uniform microstructures in the early passes reflect incomplete mixing of weld metal with the parent steel. Fine-scale hydrogen-induced cracking was observed in the first two passes, a larger crack also ran from the gap between the two abutting pieces of plate in the root.

Weld and HAZ Hardness

The ferritic steel vertical butt weld metal Vickers hardness data, Fig.4(a), show that hardness increases with increasing carbon equivalent. Weld metal mean hardness was highest in the cap, except in weld D/B/V, where the root had the highest mean hardness. Overall, the mean hardness values ranged from 170 HV10 to 216 HV10 for the ferritic steel welds, with weld B/B/V showing the highest hardness in each of the three places sampled.

In the austenitic stainless steel weld S/B/V, the weld metal hardness ranged from 232 HV10 at the cap through 249 HV10 in the centre to 261 HV10 in the root.

The parent plate hardness measured at the plate centre showed a large variation namely (from a mean of 140 HV10 to a mean of 171 HV10), attributable to segregation at the plate centre. However, HAZ hardness, at the plate centre, showed an even wider variation (from 238 HV10 to 297 HV10), with no obvious correlation with the parent plate values. For the ferritic steel welds, the HAZ hardness was always highest at the cap, with mean values ranging from 394 HV10 to 422 HV10. However, the mean HAZ hardness for the austenitic stainless steel weld was greatest in the root, where the mean HAZ hardness (304 HV10) was greater than that of the ferritic steel weld HAZs. The situation was reversed in the cap region, where the mean HAZ hardness of the stainless steel weld was lower than that of any of the ferritic steel weldments.

The ferritic steel overhead butt weld metal Vickers hardness data Fig.4(b), once again show that the mean hardness increases with increasing carbon equivalent. For the ferritic steel welds, weld metal mean hardness ranged from 165 HV10 to 238 HV10. Mean hardness was generally highest in the cap region.

The stainless steel weld S/B/O had the highest weld metal hardness of any weld cap region, 246 HV10, and also had a substantially higher mean hardness in the root, namely 370 HV10; the mean hardness of the weld centre was 238 HV10.

Parent plate mean hardness values showed even greater variation than in the vertical weld panels (from 142 HV10 to 183 HV10), with again no correlation with HAZ values at the plate centre. For the ferritic steel welds, the mean HAZ hardness at the weld cap was up to 200 HV10 (but more usually ~150 HV), which is greater than the mean HAZ hardness in the root. Weld H/B/O had a surprisingly low mean HAZ hardness in the root (196 HV10), presumably as a result of effective tempering by later passes. Once again, the mean HAZ hardness in the cap region was lowest in the stainless steel weld (S/B/O) and, once again, the stainless steel weld had a higher mean HAZ hardness in the root than in the cap region (239 HV10 cf 230 HV10).

Weld metal hardness values determined on the weld metal of the multiple-pass fillet welds were generally comparable with those of the corresponding butt welds.

Tensile Tests

The all-weld-metal tensile test data for the ferritic steel vertical butt welds are presented in Fig.5(a), as a function of IIW CE. Yield strength values ranged from 385 and 395 MPa for weld D/B/V to 495 and 483 MPa for weld B/B/V. The same ranking (with strength increasing in the order D/B/V, G/B/V, L/B/V, H/B/V, B/B/V) occurred for the tensile strength values, which ranged from 471 and 462 MPa (for weld D/B/V) to 584 and 578 (for weld B/B/V). Welds H/B/V and B/B/V gave the highest elongation (13.5 to 20.0%) and reduction of area (30 to 45%), and welds L/B/V and G/B/V the lowest (namely 11.5 to 15.5% elongation and 10 to 30% reduction of area.) The yield strength values exceed those of the parent plate (355 MPa). However, because of a low work hardening rate and only modest ductility, tensile strength values for weld D/B/V fall below the specified range (490 to 640 MPa).

For the corresponding cross-weld tensile specimens, failure in the parent steel gave tensile strength values of 515 to 522 MPa. Failure at lower stress values (in the range 366 to 512 MPa) occurred at the fusion boundary, indicating the presence of fusion boundary defects in welds H/B/V, B/B/V and G/B/V; the tensile strengths for such failed specimens were lower than those for the corresponding all-weld-metal specimens. Failures in the weld metal occurred at tensile strength values in the range 529 to 534 MPa (in welds D/B/V and G/B/V). These values are larger than the tensile strength values measured in the corresponding all weld metal samples. The difference probably reflects not only differences in the weld beads which were included in the test specimen, but also differences in properties along the length of the weld.

The all-weld-metal tensile test data for the ferritic steel overhead butt welds are presented in Fig.5(b), again as a function of IIW CE. Weld H/B/O showed similar strength and ductility to the corresponding weld deposited vertically. Weld L/B/O had marginally greater strength (and also lower ductility) than weld L/B/V, while the differences were appreciable for weld B/B/O. By contrast, weld G/B/O had appreciably lower strength (but similar ductility) compared with the corresponding overhead weld. As for the vertical butt welds, yield strength values were greater than the specified values for the parent plate. However, once again the tensile strength of one weld (G/B/O) fell below the range specified for the parent plate.

For the corresponding cross-weld tensile specimens, no failures occurred in the weld metal, although the majority of specimens failed at the fusion boundary at tensile strength values which were below those of the all-weld-metal specimens, again indicating the presence of grain boundary defects. Only three failures occurred in parent steels. Both cross-weld tensile specimens from weld B/B/O failed at tensile strength values below those of the all-weld-metal tensile specimens. However, the other failure in parent steel, in weld L/B/O, occurred at a much higher tensile strength value (581 MPa), which was appreciably greater than the tensile strength of 548 MPa, measured in the corresponding all-weld-metal tensile specimen. Once again the differences in the weld beads which were included in the test specimen, and also differences in properties along the weld, may explain why the weld metal in weld L/B/O was able to sustain such a high stress in the cross-weld tensile specimens.

As noted earlier, the configuration of the welded specimens for the patch plate welds was such that failure would be expected to occur in the parent plate, unless the welds contained gross defects. For all the ferritic steel welds, fracture occurred in the parent plate, with maximum stresses ranging from 493 to 516 MPa. Failure at substantially lower loads occurred in welds S/P/V and S/P/O, deposited with electrode S. The maximum stresses, evaluated by dividing the maximum load by the sum of the throat areas of the two underwater fillet welds, ranged from 108 to 397 MPa. These two welds had sufficient integrity to allow the machining of tensile specimens, but defects in the welds were sufficient to induce failure through the weld throats at lower stresses than the maximum stress supported by the parent steel in the panels welded with ferritic steel electrodes.

Charpy Data

Charpy transition curves for the sub-size specimens from weld metal and HAZs are presented in Fig.6 and 7. For the weld metal of the vertical butt welds, Fig.6(a), the ranking shows some dependence on temperature, but generally increases in the order G, L, D, H and B. Toughness values are low, ranging from 18 to 30J at 0°C, which reflects the high weld oxygen levels (and therefore high inclusion contents) as well as the presence of porosity in the welds. The weld deposited with the stainless steel electrode was not tested, as the severe cracking prevented the machining of test specimens.

For the weld metal of the overhead welds, Fig.6(b), the ranking was similar to that of the vertical welds, with the weld deposited with electrode B clearly and consistently showing the best toughness and that deposited with electrode G the worst. The overall range at 0°C was lower than for the vertical welds, namely 11 to 28J. Once again, specimens could not be machined from the severely cracked stainless steel weld.

The HAZ toughness for the vertical welds, Fig.7(a), again showed the highest toughness for electrode B and the lowest for electrode G, possibly reflecting some influence of weld metal toughness in weldments with inclined fusion boundaries. However, the ranking for the other electrodes differed from that of the corresponding weld metal samples, with the HAZ of electrode D welds being only marginally tougher than welds produced with electrode G.

The HAZ toughness data for the overhead butt welds, Fig.7(b), reveals that electrode B clearly gave welds with the toughest HAZ. Absorbed energy values ranged from 26J to 58J; there was no consistent trend with increasing temperature, probably as a consequence of the notches in different specimens sampling different proportions of weld metal, coarse-grained HAZ and grain-refined HAZ. The HAZ toughness of welds deposited with the remaining electrodes was considerably lower; absorbed energy values ranged from 6J to 21J, with the HAZ toughness of welds deposited with electrode D showing similar behaviour to those from weld B.

DISCUSSION

Handleability and Weld Soundness

The series of trials of commercial MMA wet underwater welding electrodes has shown clearly that, for positional welding, there are appreciable differences in the behaviour of the electrodes which were included in the trials. Also, it is clear that the achievement of sound welds with a reasonable profile is more difficult for overhead than for vertical welding. The normal requirement for repair welding is for fillet welding, in order to attach temporary patches. The deposition of multiple-pass fillet welds appeared to place lower demands in the handleability of the electrodes than did the deposition of the butt welds, as weld appearance and soundness were generally better for the fillet welds than for the corresponding butt welds. This was especially true for electrode S, where extensive cracking occurred in the butt welds, which had uneven profiles, in contrast to the reasonably smooth profiles and slightly greater integrity of the fillet welds. Also, the overhead fillet weld deposited with this electrode was uncracked, whereas the two butt welds were both extensively cracked. Among the differences between the welds in the different configurations, the fillet welds were less highly restrained, and this difference would have reduced the risk of cracking.

The risk of cracking occurring at the fusion boundary always exists when an austenitic stainless steel weld metal is deposited in contact with a C-Mn steel, as a narrow band of martensite is formed all along the fusion boundary. Its formation is predicted by the Schaeffler diagram, Fig.8,

which shows that a tie line from an approximately 312 stainless steel composition to that of a C-Mn steel with minimal Cr content and Ni content, i.e. a point at the lower left corner of Fig.8, must cross the martensite region. Such martensite is brittle, and is the preferred path for hydrogen-induced cracking to occur, either during or (shortly) after welding.

Overall, the best handleability was obtained with electrodes B, H and L. Weld quality, in the butt welds deposited with these electrodes, was generally good, although weld L/B/O had an uneven profile, and a large crack was revealed in the radiograph of this weld. Also fine-scale weld metal and HAZ cracking was found in the metallographic section from weld B/B/V. Weld quality was poorer in the overhead butt welds G/B/O, D/B/O and S/B/O, and also in the vertical butt weld S/B/V.

Weld Metal Chemical Composition and Microstructure

For the ferritic steel welds, the coarsest as-deposited microstructures were found in the vertical and overhead butt welds deposited with electrodes G and D. Compared with the other ferritic steel welds, these welds have lower C, Si and Mn levels than the other welds, with the exception of welds L/B/V and L/B/O. These leaner compositions are consistent with the coarser as-deposited microstructures observed in welds G/B/V, D/B/V, G/B/O and D/B/O. The near absence of any fine-scale intragranular ferrite, despite rapid cooling, is thus attributable to the leaner compositions of these deposits. Whilst they have the leanest Ti levels, even the lowest Ti levels in the present welds are higher than the minimum levels required for the intragranular nucleation of ferrite (8) in welds deposited in air. Therefore, it is the leaner Mn content of electrode L welds which is largely responsible for their slightly coarser microstructures. A sufficient level of alloying is required, in order to achieve some degree of microstructural refinement in the as-deposited microstructure, and such refinement is associated with improved Charpy toughness.

With increasing alloying comes an increased risk of weld metal hydrogen-induced cracking, as observed in the elctrode B vertical butt welds, the level of weld metal hydrogen generated by electrode B may have been higher than that from the other deposits, as B/B/V was the only ferritic steel butt weld in which HAZ hydrogen-induced cracking occurred. Also, it will be noted that the welds produced with this electrode had the highest strength of any of the deposits, and high weld strength can increase the risk of HAZ hydrogen-induced cracking.

The microstructures of the stainless steel welds can be largely understood by reference to the Schaeffler diagram, Fig.8, where the compositions corresponding to those of the capping passes on the butt welds S/B/V and S/B/O are plotted. In both the butt welds and the fillet welds, the microstructures in the early passes reflect higher dilution, and contain lesser amounts of ferrite and increasing amounts of martensite.

Mechanical Property Data

For the ferritic steel deposits, the strength data follow a simple pattern, as shown in Fig.5, where the yield and tensile strength values are plotted as a function of IIW CE. The clear trend is one of increasing yield and tensile strength with increasing hardenability, as characterised by IIW CE (which is given in Table 1). Thus, the lowest strength deposits are those produced with electrode D, and those with the highest strength were produced with electrode B.

The butt weld hardness data show a broadly similar trend, Fig.4, but with greater scatter, particularly for the overhead butt weld data, Fig.4(b). The reason for this greater scatter is not clear, but it may reflect some averaging by sampling a range of microstructural regions in the tensile tests.

The butt weld Charpy toughness, Fig.6, largely reflect the increase in strength and hardness, and the microstructural refinement, associated with increasing IIW CE. The exception to the trend is electrode D, which had the lowest IIW CE, but for which the toughness was only slightly lower than that of electrodes B and H. The most likely reason for this difference in ranking is the comparatively low nitrogen content (~0.005) of the butt welds produced with electrode D, which was even lower than that in the butt welds produced with electrodes B and H.

The absolute levels of toughness achieved for the ferritic steel butt welds at sub-zero temperatures are moderately low. However, it should be recognised that sub-size specimens were tested. Toughness values appropriate to full size (10mm square) Charpy specimens are obtained by doubling the absorbed energy values and by changing the temperature by ~+20°C (9). Thus, with the exception of the butt welds produced with electrode G for the vertical welds and G and L for the overhead welds, Charpy toughness values correspond to greater than, say, 27J at -10°C, if measured values at -30°C are considered. The same argument applies to the HAZ toughness data, Fig.7, although here it is butt welds produced with electrodes D and G which give HAZ toughness below this toughness criterion.

General Comments

Assessing the overall performance of the various electrodes, the best handleability was found with electrodes B, H and L, which generally gave the welds with fewer or smaller defects, and the best surface appearance. Some lack of penetration in the root was observed in weld B/B/V, deposited with electrode B, and in the butt welds produced with electrode H. However, it will be noted that this electrode was welded DC +ve throughout the weld, and penetration in the root would undoubtedly be increased by welding the root passes DC-ve, as is commonly done for root pass welding in air with ferritic steel electrodes.

Cracking was detected in one of the radiographs of the overhead weld deposited with electrode L, and fine-scale cracking was observed in the metallographic section from weld B/B/V, deposited with electrode B. Also of note is the low toughness of welds deposited with electrode L.

Thus, taken overall, the electrode which gave the most satisfactory performance was electrode H. While the welds were not entirely free from minor defects, reasonable sub-zero toughness was achieved in butt welds produced with this electrode. Thus, it may be used not only for temporary repairs but possibly also for permanent repairs and installations, as long as appropriate consideration is given to other issues such as the effect on the fatigue performance of the structure.

CONCLUSIONS

1. The handleability of the six commercial electrodes evaluated in the programme differed, with electrodes coded B, H and L generally showing the best handleability, with that of electrodes G, D and S being less good.

2. Handleability was better for vertical than for overhead welding, and was also better for fillet welds than for butt welds.

3. Weld soundness was poorer than is normally achieved for welding in air, with the butt welds containing pores and worm-holes. Both surface appearance and the incidence of defects reflected the differences in handleability; slight lack of penetration in the root was common. Electrode S butt welds showed extensive fusion boundary cracking, and cracks were also observed in the radiographs

of overhead butt welds deposited with electrodes L, G and D. Fine-scale cracking was observed, in both weld metal and HAZ, in the vertical butt weld deposited with electrode B.

4. The fillet welds generally showed a small amount of porosity, with welds H/P/V and B/P/V showing lack of fusion in the root, weld S/P/V showing some cracking, and weld G/P/O showing no reportable defects.

5. Extensive cracking prevented the extraction of specimens for mechanical testing from the butt weld panels welded with electrode S, the stainless steel electrode.

6. For the weld metal of the ferritic steel butt welds, strength and hardness increased with increasing IIW CE.

7. For the weld metal of the ferritic steel butt welds, Charpy toughness generally improved in the order G, L, D, H and B, with absorbed energy values at 0°C, for the half-size specimens, ranging from 18 to 30J for the vertical welds and from 11 to 28J for the overhead welds. HAZ toughness values were generally higher than for the weld metal, but reflected the weld metal behaviour, largely because they sampled some weld metal.

8. Electrodes coded B and H gave the best handleability and mechanical properties. However, fine-scale cracking was observed in the vertical butt weld deposited with electrode B, and thus electrode H is recommended as giving the best all round behaviour. The poorer handleability and the higher incidence of weld defects for electrodes D, G and S precludes further use. As the butt welds produced with the stainless steel electrode (S) showed extensive cracking, this electrode is not recommended.

ACKNOWLEDGEMENTS

The assistance, co-operation and support provided at TWI North by Messrs J Sheppard and P Bosten is acknowledged with gratitude. The vital work of depositing the welds under water was carried out by Messrs. D. Scicluna and A. Baird, whose skill and knowledge of their craft contributed greatly to the success of the welding programme. The assistance and advice of the manufacturers of some of the electrodes is also gratefully acknowledged. Assistance has also been provided by colleagues at TWI, Abington, particularly Messrs. R. Banham, M. Tiplady and W. Hedley, and Mrs. W. Martin. Discussions with colleagues, particularly Messrs. P Woollin, T G Gooch and P H M Hart are also acknowledged.

REFERENCES

1 West T C, Mitchell G and Lindberg E, "Wet welding electrode evaluation for ship repair", Weld. J. 1990, 69(8), 46-56.
2 Szelagowski P, Stuhff H and Loebnel P, "Properties of wet welding joints", Proc. 21st Annual Offshore Technology Conference, Houston, USA, 1989, OTC paper 5890, pages 77-78.
3 Pokhodnya I K, Gorpenyuk V N, Kononenko V Ya, Ponemarev V E and Maksimov S Yu, "Special features of arcing and metal transfer in underwater welding with a self-shielding flux-cored wire", Paton Welding Journal, 1990, 2(9), 1-4.
4 Phillips M K, Findlan S J and Childs W J, "Underwater wet welding for the repair of reactor pressure vessel internals", Codes and standards and applications for design of pressure vessels and piping components 1991, Symposium during 1991 Pressure vessels and piping conference, San Diego, USA, 23-27 June 1991, R. F. Sammataro, G. A. Antaki, K. R. Rao, and J. F. Staffiera, Editors; Pressure Vessels and Piping, 210(1), 27-31.

5 Ellis M D B and Gooch T G, "The availability of manual metal arc underwater welding consumables", TWI confidential report 620724/1/94, November 1994, for the Ministry of Defence.
6 ANSI/AWS D3.6–93, 1993, "Specification for underwater welding".
7 Widgery D J: "New ideas in submerged arc welding", Trends in steels and consumables for welding, The Welding Institute, 1978, 217–229.
8 Evans G M: "The effect of titanium in SMA C–Mn steel multipass deposits", Weld J. Res. Suppl. 1992, 71 (12), 447s–454s.
9 Towers D L: "Charpy requirements for sub–size specimens", The Welding Institute Research Bulletin 1978, 19(8), 224–227.

Table 1 Chemical analyses of the weld metal and of the 8mm thick parent steel plate, compared with the requirements of the specification NES791 Part 3 ISS2 1987 (Admiralty B quality).

Identity/weld code	Element, wt%															
	C	S	P	Si	Mn	Ni	Cr	Mo	V	Cu	Nb	Ti	Al	N	O	IIW_{CE}
Plate*	0.15	0.006	0.016	0.22	1.37	0.02	0.02	0<0.005	<0.005	<0.005	<0.002	<0.002	0.040	0.0070	0.0011	0.38
Specification	≤0.19	≤0.040	≤0.040	0.10 to 0.35	1.20 to 1.70	–	–	–	–	–	–	–	–	–		–
H/B/V	0.08	0.008	0.019	0.34	0.42	0.03	0.03	0.005	0.02	0.01	0.006	0.011	0.004	0.006	0.113	0.16
B/B/V	0.09	0.011	0.018	0.44	0.62	0.02	0.03	0.005	0.02	0.02	0.009	0.018	0.005	0.006	0.083	0.21
L/B/V	0.08	0.014	0.011	0.35	0.27	0.08	0.02	0.01	0.01	0.07	0.006	0.018	0.004	0.013	0.115	0.14
G/B/V	0.06	0.035	0.022	0.12	0.38	0.02	0.01	<0.005	0.01	0.01	<0.002	0.011	0.005	0.016	0.138	0.13
D/B/V	0.06	0.014	0.019	0.12	0.28	0.03	0.01	<0.005	0.01	0.02	0.002	0.008	0.005	0.005	0.088	0.11
S/B/V	0.12	0.013	0.018	0.51	0.78	8.2	26.6	0.30	0.08	0.08	<0.01	0.02	–	0.076	0.111	–
H/B/O	0.10	0.008	0.018	0.32	0.42	0.03	0.03	0.005	0.02	0.01	0.006	0.015	0.004	0.006	0.117	0.18
B/B/O	0.10	0.011	0.018	0.59	0.72	0.02	0.03	0.005	0.02	0.02	0.012	0.018	0.005	0.005	0.070	0.23
L/B/O	0.09	0.013	0.011	0.36	0.25	0.08	0.02	0.01	0.01	0.07	0.009	0.020	0.005	0.013	0.110	0.15
G/B/O	0.06	0.026	0.022	0.11	0.39	0.03	0.01	<0.005	0.01	0.02	<0.002	0.005	0.004	0.013	0.109	0.13
D/B/O	0.06	0.011	0.019	0.18	0.34	0.03	0.02	<0.005	0.01	0.02	0.004	0.012	0.005	0.005	0.103	0.13
S/B/O	0.13	0.015	0.021	0.45	0.81	6.4	19.5	0.24	0.07	0.07	<0.01	0.01	–	0.063	0.081	–

Sn, Co <0.005 except L/B/V and L/B/O, Sn, Co = 0.01; D/B/V, C. ~0.32* and D/B/O, Co ~0.33*

As, Pb, Zr <0.005, B, Ca <0.0003 – Except welds S/B/V and S/B/O, for which these elements were not determined. Also, the Ca level of the plate was not determined.

* Above the calibration range.

+ IIW CE = C + Mn/6 + (Cr+Mo+V)/5 + (Ni+Cr)/15

TWI analyses S/95/173, S/95/237, O/N 95/50 and O/N 95/75

Note that the small size of the sound region of the sample from weld D/B/V allowed only one spark analysis to be made, rather than the usual two.

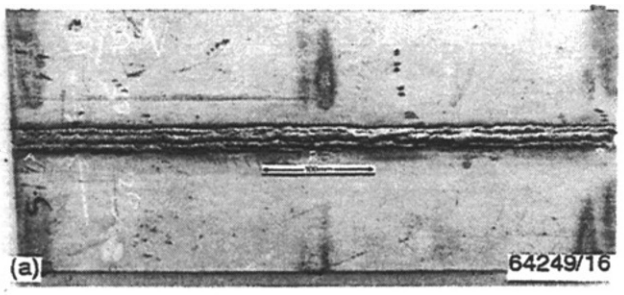

Fig. 1. Photographs of butt welded panels
(a) Vertical weld B/B/V.

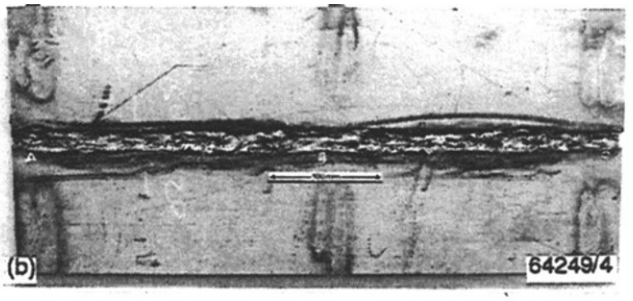

(b) Overhead weld S/B/O.

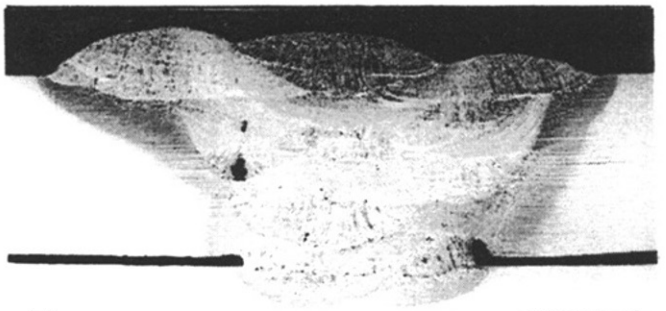

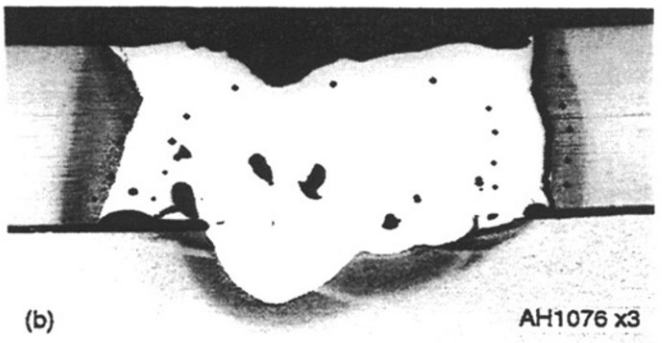

Fig 2. Transverse sections of selected welds
(a) Vertical butt weld B/B/V
(b) Overhead butt weld S/B/O
(c) Overhead patch weld D/P/O

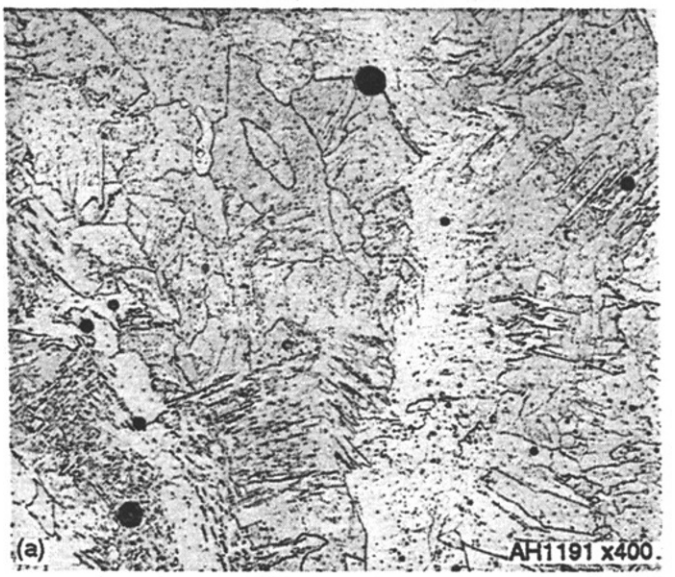

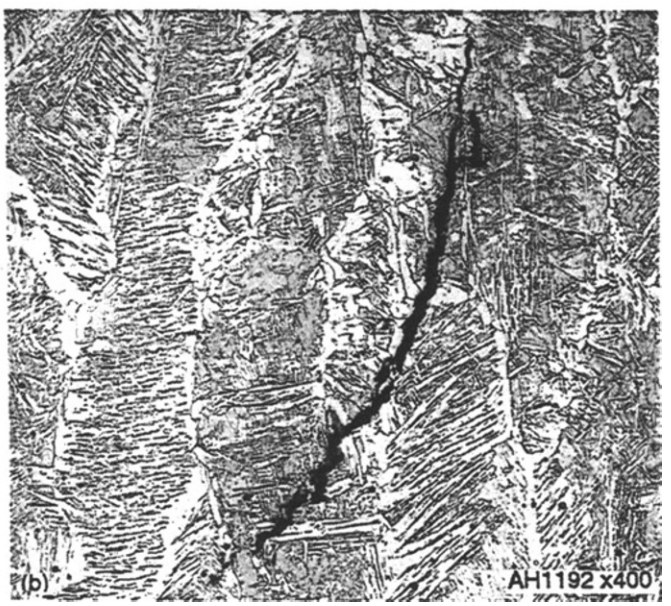

Fig. 3. Optical micrographs of as-deposited weld metal
(a) Weld D/B/V (b) Weld B/B/V

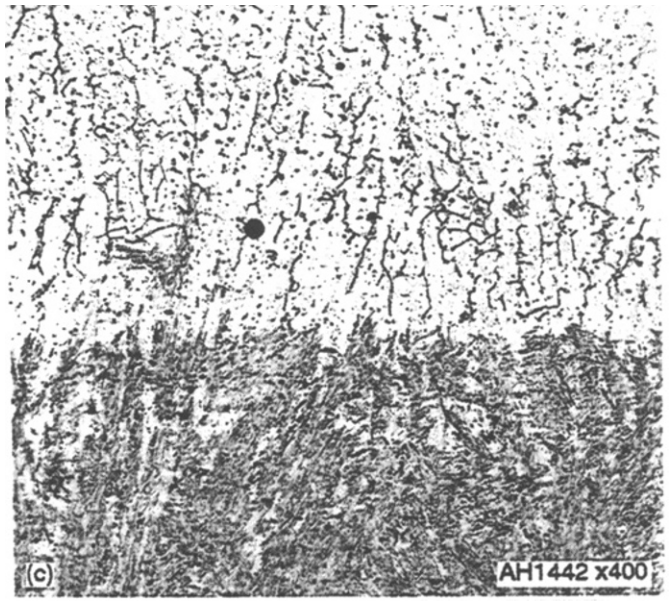

Fig. 3. continued
(c) Weld S/P/O

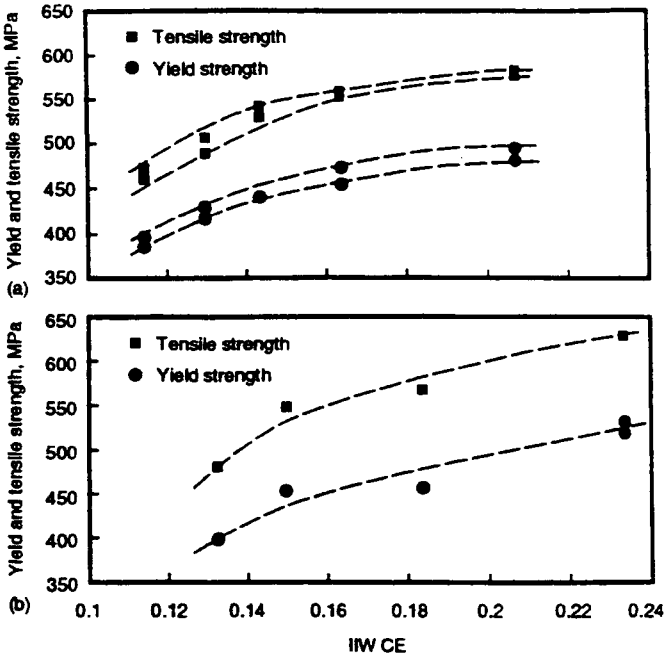

Fig. 5. Yield and tensile strength as a function of IIW CE.
(a) Vertical butt welds
(b) Overhead butt welds

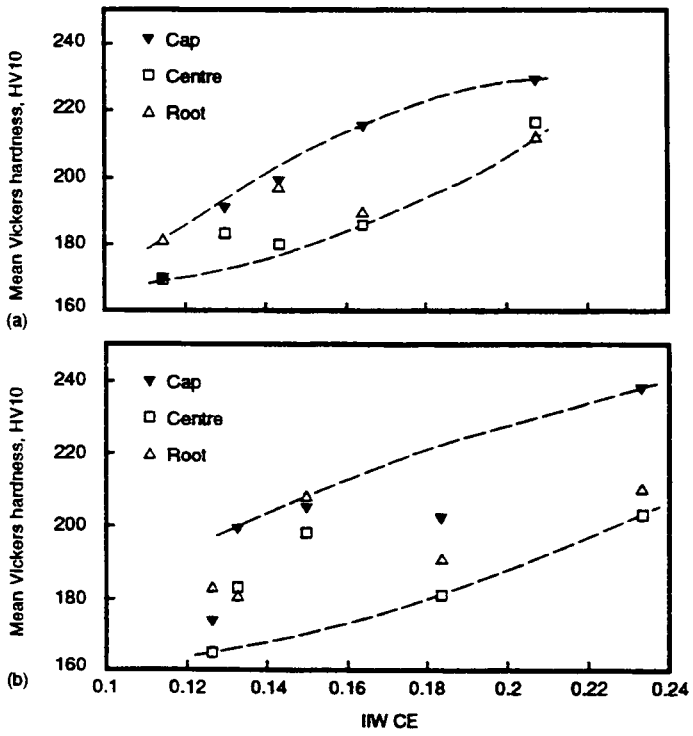

Fig. 4. Mean hardness data as a function of IIW CE
(a) Vertical butt welds
(b) Overhead butt welds

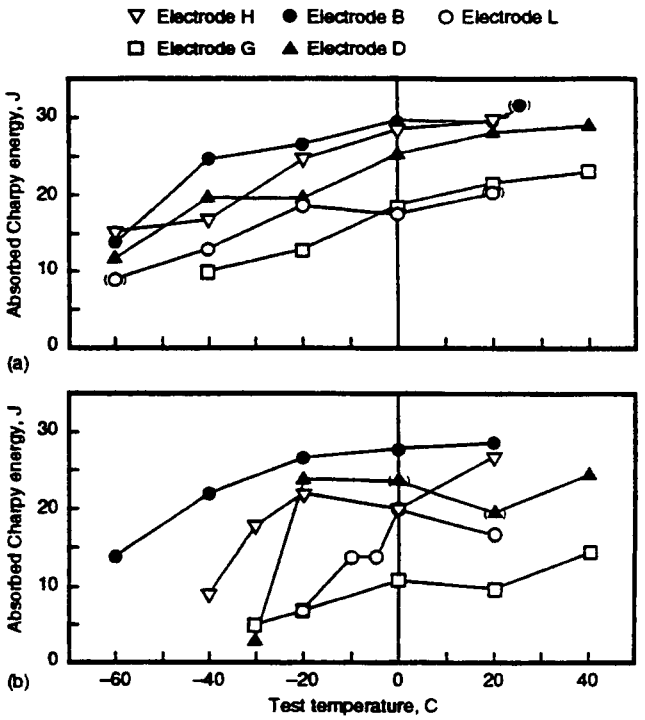

Fig. 6. Weld metal Charpy toughness data. Data points in brackets, indicate specimens with defects on the fracture surfaces.
(a) Vertical butt welds (b) Overhead butt welds

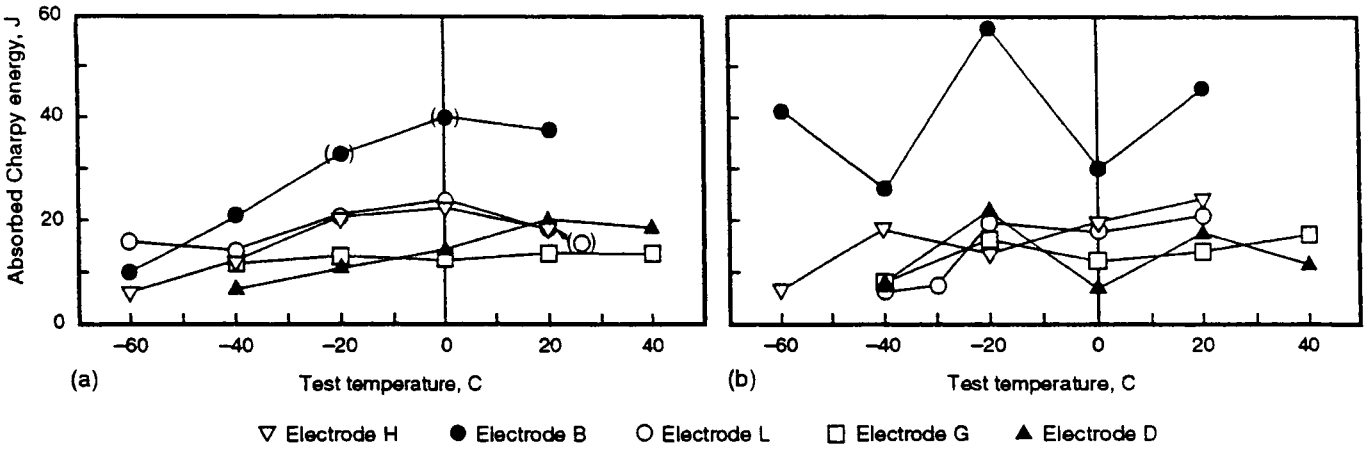

Fig. 7. HAZ Charpy toughness data. Data points in brackets indicate specimens with defects on the fracture surfaces.
(a) Vertical butt welds (b) Overhead butt welds

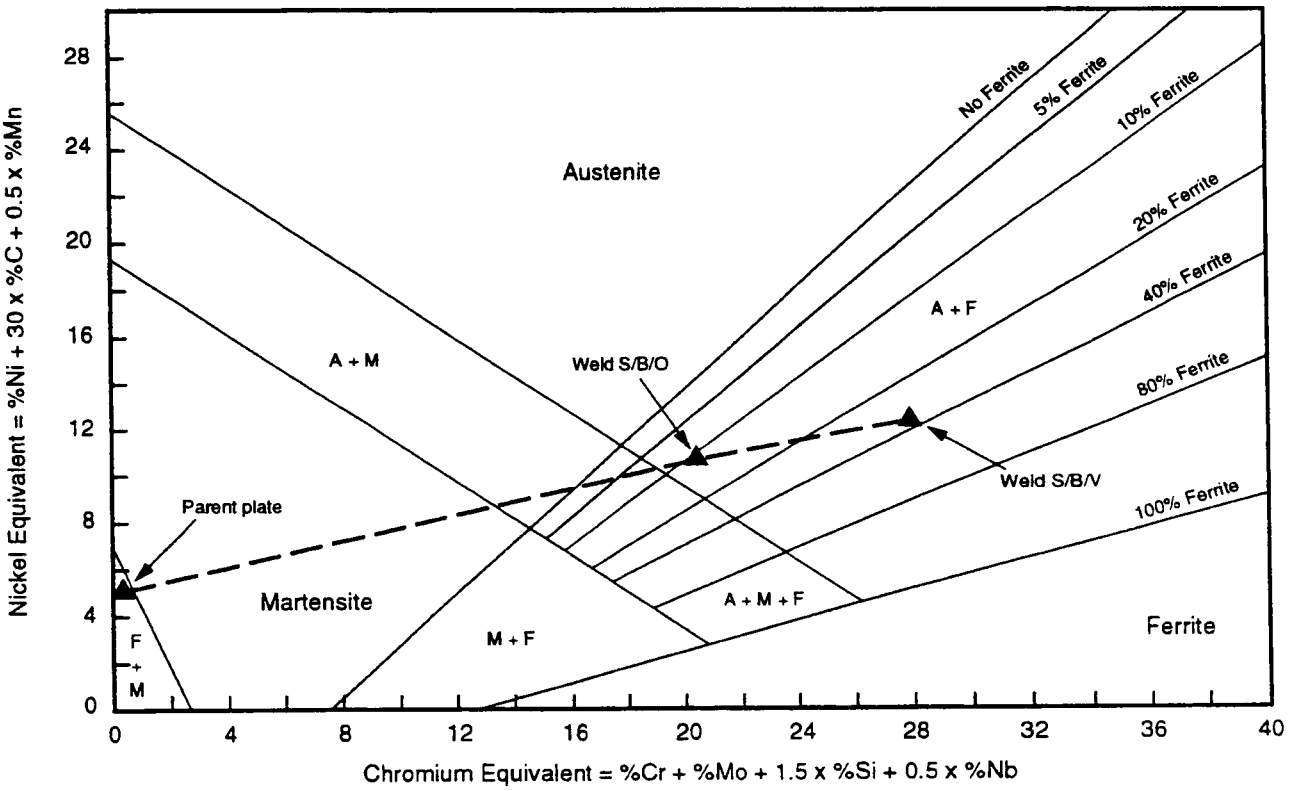

Fig. 8. The Scaeffler diagram, showing a tie-line joining the points corresponding to the compositions of welds S/B/V and S/B/O, welded with electrode S, to a point representing the parent steel composition. Note that the tie-line crosses the martensite region.

Technological peculiarities of wet semi-automatic welding with flux-cored wire

Yu Ya Gretskii and I M Savich, E O Paton Electric Welding Institute

If the arc welding is performed directly in water, the environment influences essentially on arc burning stability, consumable melting and molten metal transfer character, weld metal chemical composition, structure and properties formation. Every of above factors defines to a certain extent the quality of welded joint. The data in this respect of underwater flux-cored wire welding are presented.

Bead formation. It is known that the structure failure under dynamic loading begins, as a rule, from the places of weld-base metal transition. The smoother this transition, the higher the fatigue strength of weldment. In air welding, to increase the weldment fatigue strength it is recommended the local mechanical or argon-arc treatment of the weld boundaries. Under underwater conditions, performing of such treatment are either difficult or impossible at all. In this connection, at underwater welding obtaining the welds of favourable shape becomes of important, and the quality of consumables and possibility to effect at the expense of technological parameter variation are the only measure for solving this problem.

Below the data of investigation of welding regime parameter variation influence on bead appearance and weld shape at different salinity and excessive hydrostatic pressure are presented.

Bead-on-plate was performed with rutile type flux-cored wire of 1.6 mm in dia. in air, fresh water and synthetic water of 30‰ salinity. Welding variety was in the range Iw=120...260 A and Ua=25...37 V, Vw=5...25 m/h, reverse polarity.

It has been found that the regularities obtained in air arc welding are of the same character in underwater conditions, too. With current rising, penetration (h), width (B) and reinforcement (a) of welds increase. Rise of voltage gives rise of the weld width and the penetration and decreases the reinforcement. The influence of welding speed is that the higher the speed, the lesser all these sizes of deposited beads. The underwater welds are on the whole narrower, have some smaller penetration depth and reinforcement than the welds performed in air, all other factors being the same (Fig.1).

The observed decrease of bead sizes is believed as being the result of excessive base metal cooling by surrounding water.

As to influence of water salinity, it is possible to explain in such a way. The presence of salts of natrium, potassium, calcium, magnesium vapours which enter the vapour-gas bubble gives widening of arc column. As the result, the arc pressure on welding pool decreases and, in turn, bead wide rises, but penetration depth becomes smaller.

To determine the effect of hydrostatic pressure on weld parameters the beads were performed under conditions simulating the depth up to 60 m. As it has been found, the water depth influences negligibly. In doing so, bead wide slightly decreases, at the same time, both penetration depth and reinforcement slightly increase.

Arc stability. Peculiarities of arc burning and metal drop transfer in underwater flux-cored wire welding were studied employing the specialised microcomputer-based analyser. Welding was performed by means of an automatic device using the commercial flux-cored rutile wire PPS-AN1 type in a special high-pressure chamber filled with fresh water. Diving down to depths 0.5, 10, 20 and 50 m was simulated by changing pressure in the chamber. Welding in air was also performed for comparison. The character of metal transfer was estimated by the duration of short-circuits (τs.c.) and their frequency (fs.c.) The peculiarities of arc burning were analysed by the histograms of arc voltage and welding current by the method of stepwise processing of multimodal distribution (1).

Figure 2 shows the effect of the diving depth (h) on short-circuit duration and frequency. As seen from the data presented, the diving depth affects these factors to a considerable degree. The short-circuit duration drastically increases with the diving depth and reaches maximum at h=10 m. The short-circuit frequency also drastically grows, i.e. the share of molten metal transferred into the welding pool at short-circuits increases, the share of time related to short-circuits amounting to 24% of the total welding time.

The information required for the deeper insight into the underwater process can be obtained by the analysis of arc voltage and welding current histograms (Fig.3). It can be seen, that in welding in air the spread of the arc voltage and welding current values is small (Fig.3,a,b).

This is the evidence of the high stability of the process. But the situation changes even at the 0.5 m depth. As the depth increases, there appear the characteristic disturbing arc extinctions, this being indicated by the two new distribution regions clearly defined in the arc voltage histograms. The left distribution region in Fig.4,c shows voltage at the moments of short-circuits, the right one - the voltage spikes caused by inductance of power source and welding circuit at the moments of arc extinction, while the middle one - voltage during arc burning. Arc extinctions are indicated also by the distribution region in the current histograms within the area of the zero current values (Fig.3,d,f,etc).

It is rather difficult to estimate quantitatively the share for arc extinctions; but, considering the areas of different regions of histogram Ua, one can notice that the region corresponding to voltage Ua.b. diminishes with the increase in the diving depth. As compared to welding in air, particularly for the 50 m depth, the area of the Ua.b. voltage distribution decreases by 4 times. Thus the "net" time of arc burning is drastically shortened due to short-circuits and extinctions and at the 50 m depth it amounts to 25-30% of total welding time, this inevitably affecting the weld formation and the process productivity.

Therefore, behaviour of welding arc and character of electrode metal melting in underwater welding greatly differ from those observed in welding in air.

Water vapours forming the basis of a vapour-gas bubble inside which the arc burns, should dissociate at a high temperature into hydrogen and oxygen. They, being present in

the arc gap, can greatly affect the arc stability and the character of molten metal transfer; however, the effects of these components are different. Thus, being a surface-active element, oxygen should decrease the surface tension coefficient of metal drops and, hence, cause their refinement. Hydrogen that possesses the high thermal conductivity and ionisation potential should cause the arc column contraction and, accordingly, promote the increase in electrodynamics force which, in this case, influences the drop on the arc side and retains it at the electrode tip; i.e. in the end , it should coarsen the drops being transferred. Besides, oxidation of iron greatly increases with the diving depth (rise of pressure), this being indicative of oxygen fixing and, accordingly, of the increase in hydrogen partial pressure in the arc zone.

The important factor that affects the wet underwater welding process stability is the dynamics of the vapour-gas bubble formation. If the bubble persists (in overhead welding on a plane), the process is stable enough. In other spatial positions there occur the periodic collapses of the bubble (i.e. detachments) that can take place during the prolonged short-circuits, the arc extinction or during the arc burning. When the bubble collapses, the pool and the arc gap are rapidly cooled by an ambient water and the contact of wire with the pool is required to excite the arc.

Therefore, short-circuits of two kinds are observed at large depth: short-circuits caused by the electrode metal drop growth and short-circuits associated with the displacement of an electrode wire tip at the moment of arc extinction before the contact with the base metal surface. Here, the metal drop at the electrode tip can have small sizes. The share of short-circuits of the second kind increases with the increase in depth.

The main cause of the increase in the number of short-circuits and arc extinctions with the depth is the reduction of the vapour-gas bubble sizes. In this case the more contracted arc should have the higher voltage gradient in the column. Allowing for the fact that power source provides the constant arc voltage (29...30 V), the length of the arc column should be smaller at the higher voltage gradient. This can result in the lower mean value of short-circuit durations after exceeding of the certain critical diving depth, it being confirmed by the results shown in Fig.2.

Flux-cored wire. The available flux-cored wire for underwater welding type PPS-AN1 is rutile based one. It permits to obtain welds of satisfactory quality when welding in all spatial positions. True, performing butt welds directly in overhead position is connected with some difficulties even for high-skill diver-welder. That is why it is desirable to prefer the overlap joints allowing to avoid performance of welding in strictly overhead position. With this connection, it is necessary to take into account this peculiarity working out technological recommendations.

The comparatively small diameter of flux-cored wire helps a diver-welder to reach favourable bead appearance, Fig.4. The optimum size of wire diameter is considered to be of 1.6 mm according to practice experience. It permits to have welding pool of such dimensions when it is not difficult to avoid flowing down of liquid slag and due to that to protect welds from excessive porosity (let note that flux-cored wire considered is self-shielding one). In addition, the wire of small diameter is handy in operation because of flexible welding hose.

The commercial flux-cored wire PPS-AN1 which have been manufactured up to date provided the obtaining weld metal with tensile strength up to 450 MPa. So long as the weld metal is not alloyed and does not practically contain carbon, it is possible to consider such value of strength index as sufficiently high. The said level of weld metal strength is reached mainly at the expense of peculiarities of structure formation under conditions of accelerated cooling. The typical microstructure is distinguished by refined grains of polygonal ferrite. The non-metallic inclusions are mainly small-dispersed iron oxides and distributed uniformly. The big inclusions are found comparatively seldom and their sizes do not exceed 23 μm. Typical chemical composition of metal deposited with flux-cored PPS-AN1 wire is presented in Table 1, the microstructure is shown in Fig.5.

Table 1. Chemical compositions of weld metal

	Element, wt%					
Steel	C	Si	Mn	Ni	S	P
09G2	0.05	0.03	0.27	0.06	0.02	0.022

Sea-water corrosion rate. Necessity to perform underwater repair of ships afloat demanded for evaluation of underwater weld resistance to corrosion. Tests were performed in synthetic sea water using welded joints of low-carbon structure steel with manganese content of 1.7%. The profilogram of the tested specimen is given in Fig.6. It is evidence of high corrosion resistance of both weld and HAZ metals (2). There are the reserves for further increase of welded joints corrosion resistance at the expense of additional weld metal alloying with copper and nickel (3).

Mechanical properties. Long time applied commercial flux-cored wire PPS-AN1 provided the sufficient level of strength of joints by welding low-carbon steels with yield point up to 350 MPa. But the level of weld ductility did not meet the class "B" requirements as specified in the AWS D3.6 document. The possibility for further increase weld metal mechanical properties especially for plasticity, were exhausted. Evidently, this task could be solved by means of alloying.

Nickel is regarded to be the one of the elements favourably influencing both strength and ductility of metal. This effect of nickel proved to be true in the case of underwater flux-cored wire welding as well. Corresponding investigations showed that alloying of weld metal with nickel leads to appearance of acicular ferrite and, simultaneously, to refining of polygonal ferrite grains. Increase of nickel content more than 2.5% results in formation of zones with structure of lath martensite (especially in root part of weld).

Such structure alterations result in corresponding changes of mechanical properties.

Tensile and bend testing of welded joint were performed in accordance with AWS D3.6-93 Specification. They have shown that the said way is sufficiently effective for increasing both ductility and strength of underwater welds, the bend angle rising especially intensive when alloying with nickel up to 1.5%, Fig.7. Increase of nickel content above 2.5% results in decrease of bend angle because of low-carbon lath martensite formation.

These investigations showed the possibility to obtain the bend angle value as high as 180 degrees when testing the welded samples in accordance with class A requirements of AWS D3.6 Specification, Fig.8.

As to strength characteristics, they reach maximum values at nickel content about 3% (Fig.9). It should be noted that it is impossible to provide maximum values of weld metal strength and ductility simultaneously. Proceeding from the understanding, that the ductility is more critical factor as compared to strength under underwater condition, the nickel content in the weld metal can be restricted to 2.5%.

Therefore, the reached level of weld metal mechanical properties is believed to be sufficient for satisfactory performance of repair and current works on underwater structures made from mild and low-alloyed steels with tensile strength up to 500 MPa. As to FCA welding steels of more high strength level, the assessment of weldment quality is in direct dependence from the requirements of customer, because the welds will be less strong than base metal. Besides, such steels are sensitive to HAZ metal crack formation and the question of weldment fitness-for-service is carried to the fields of weldability and search of suitable constructive solutions for increasing an operational reliability of weldments.

References

1 Pokhodnja I K et al: 'Some Peculiarities of Arc Burning and Metal Transfer in Wet Underwater Self-Shielding Flux-Cored Wire Welding', Avtomaticheskaya Svarka, No 9, 1990, p1

2 Ignatushenko A A et al: 'Mechanized Underwater Welding Using Austenitic Consumables', Proce IIW Intern Conf 'Underwater Welding'. Trondhaim, Norway, June 1983, p227

3 Gusachenko A I et al: 'Corrosion of Welded Joint of Hull Steel 09G2S Type and Possibility its Prewelding under Water', Avtomaticheskaya Svarka, No 11, 1987, p58

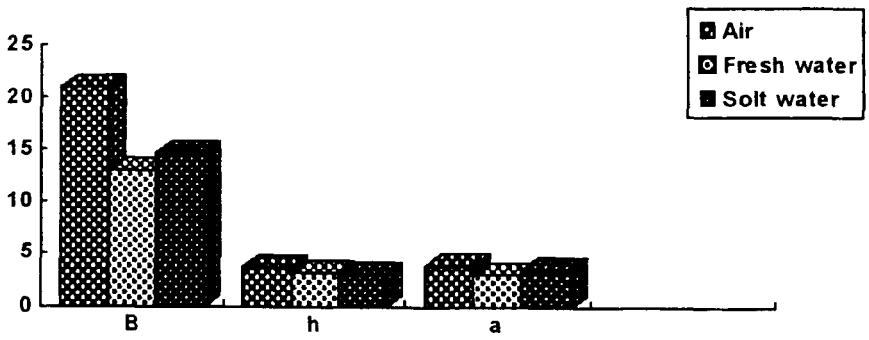

Figure 1 Influence of the environment on the bead shape: B - width of weld, h - depth oh penetration, a - reinforcement of weld

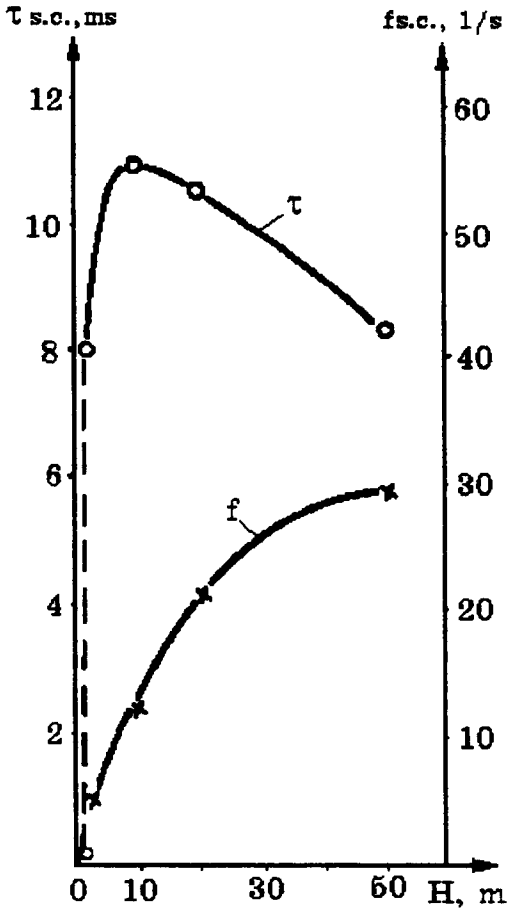

Figure 2 Effect of diving depth on duration τsc and frequency fsc of short-circuits

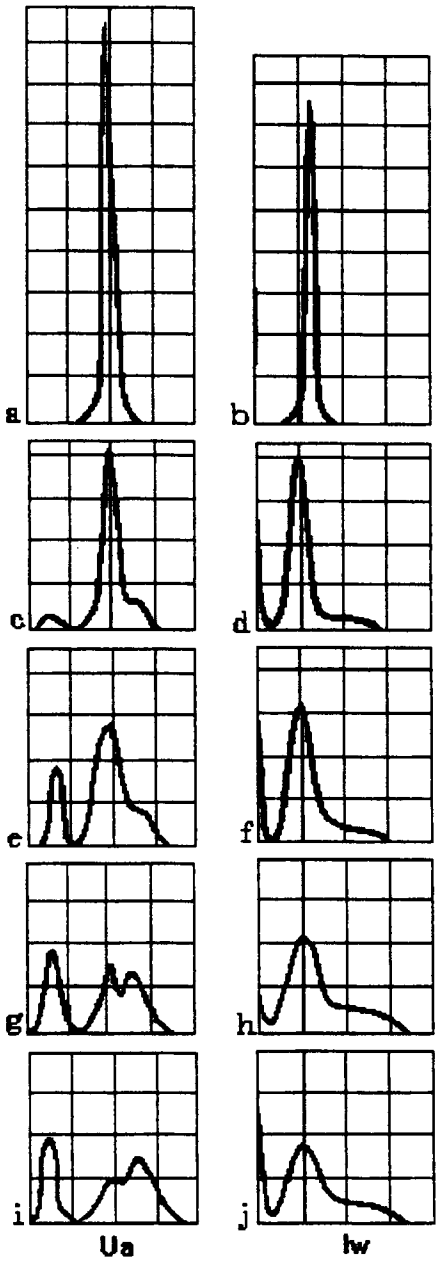

Figure 3 Histograms of arc voltage and welding current in welding at different depths: a,b - air; c,d - 0.5 m; e,f - 10 m; g,h - 20 m; i,j - 50 m

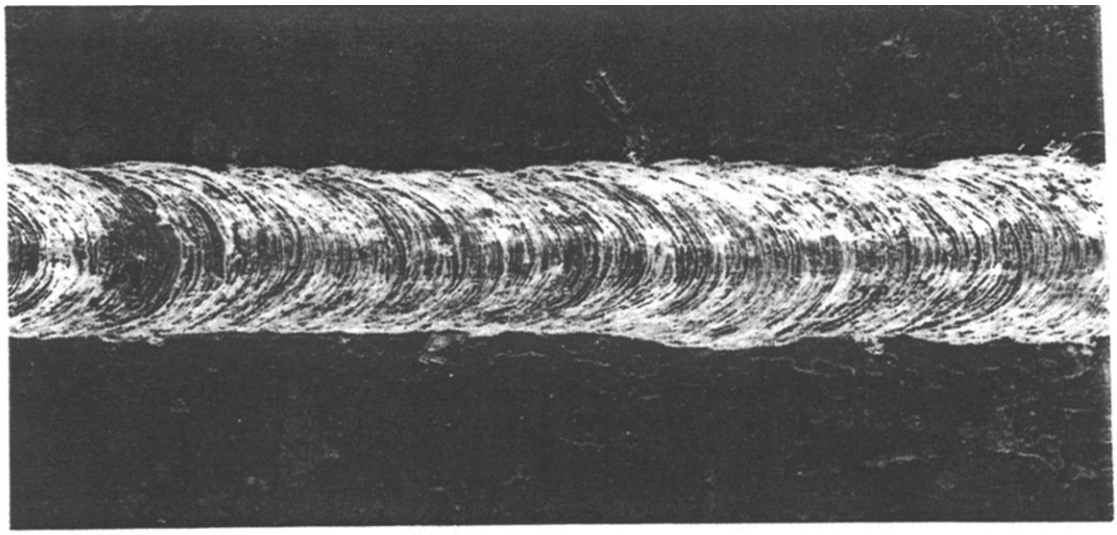

a

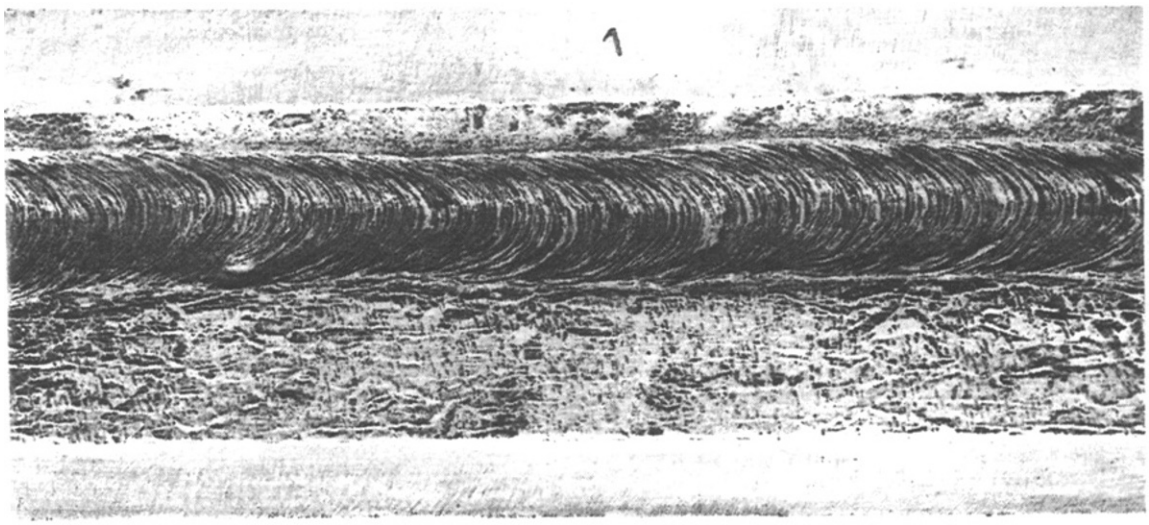

b

Figure 4 Bead appearance when welding with flux-cored wire PPS-AN1 type: a - butt weld, b - fillet weld

Figure 5 Typical microstructure of the weld metal (×320)

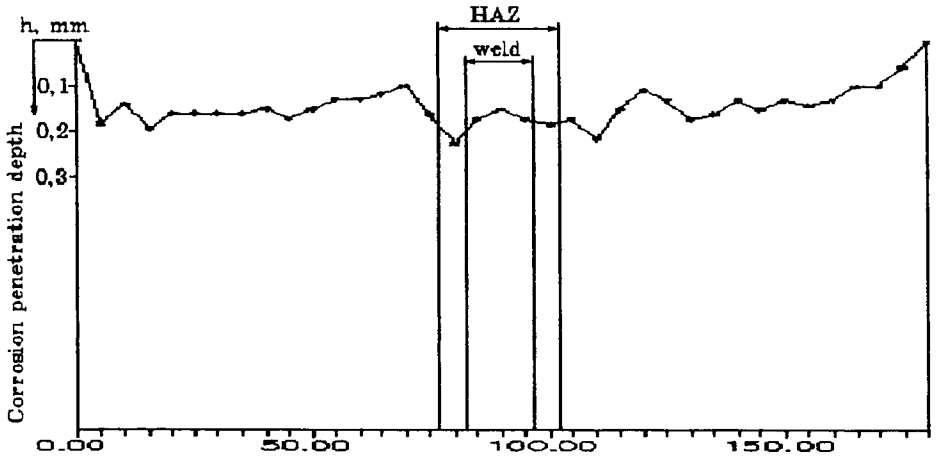

Figure 6 The profilogram of the specimen welded by flux-cored wire

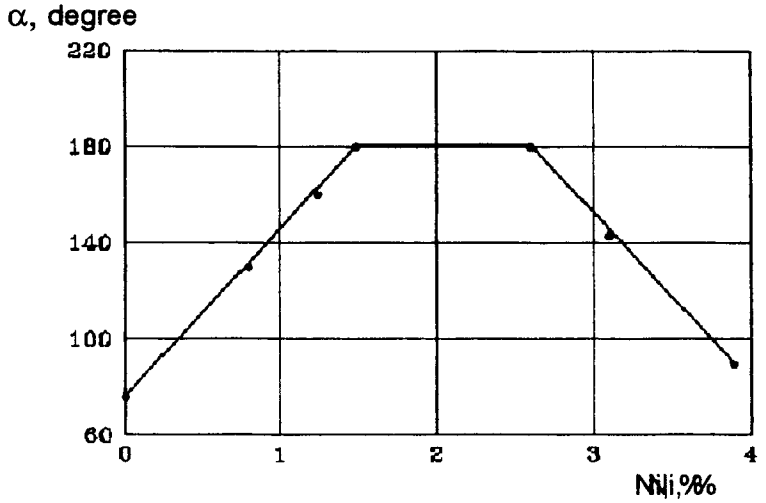

Figure 7 Influence of nickel content in the weld metal on the bend angle value

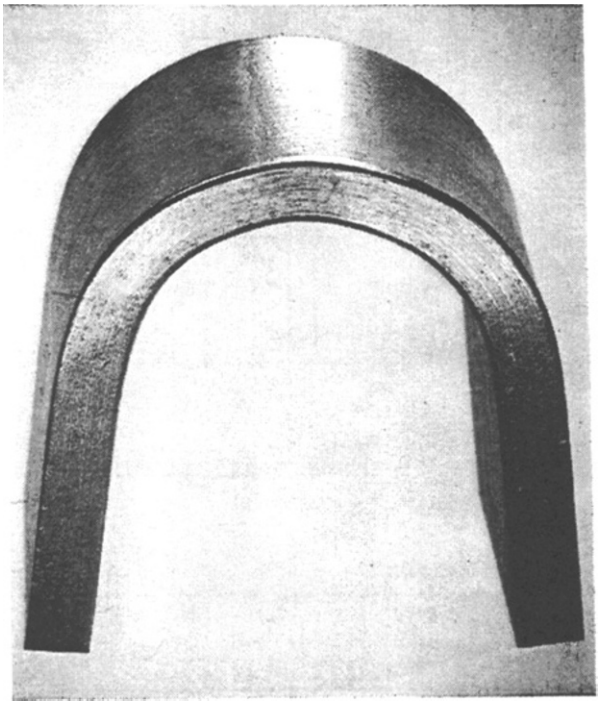

Figure 8 The sample after bend test

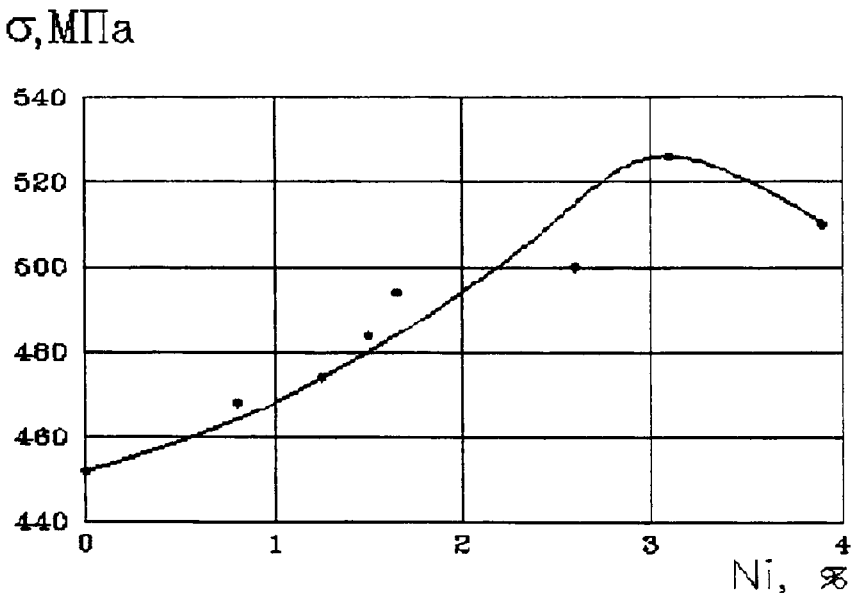

Figure 9 Influence of nickel content in the weld metal on the tensile strength

The experience of practical application of the underwater semi-automatic welding with flux-cored wire

I M Savich and V Ya Kononenko, E O Paton Electric Welding Institute

The results achieved in wet underwater flux-cored wire welding permitted the E.O.Paton Electric Welding Institute to put into practice the new technique still from 1970. Since that time, such experience had been accumulated which gives us the base to declare about reliability and prospectiveness of FCAW technique.

The 25-years experience of FCAW application on the former USSR territory is evidence of possibility to apply the method, at least, for restoration of wharfs, platforms, pipelines, ships, and other related applications. The wet flux-cored technique proved successful under the harshest of conditions.

The higher quality, versatility, manoeuvrability, and low cost of the wet flux-cored system combined with other advantages such as ease of diver-welder training give the user greater flexibility in design engineering, as well as a broader range of potential applications.

The satisfactory quality of wet welded joins is ensured when welding the mild and low-alloy structural steels with yield and tensile strength of up to 350 MPa and 500 MPa correspondingly and with carbon equivalent value up to 0.35. Chemical compositions of such steels and weld metal are given in Table 1, the welded joint mechanical properties are seen from Table 2. Analysis of these data shows that even at the slight alloying the weld metal has the sufficiently high level of both strength and ductility, the Charpy-toughness being higher than that at the negative temperatures. The some difference in the values of these characteristics of base and weld metal does not prevent from wide application of FCAW technique for repair aims because the constructive strength of the restored objects proved to be enough for the sufficient operational reliability.

Using the flux-cored wire method in question, it is possible to perform the welded joints in all spatial positions. At welding in overhead position, performing of overlap joint is preferable.

Hydrological conditions are of important for successful performance of underwater welding. The welding can be carried out in fresh and sea water if the visibility is not less than 0.15 m and water current velocity is not more 0.4 m/s. Otherwise, the protective measures must be applied.

The accumulated experience showed that the operation procedures of FCAW technique are run in by diver-welder comparatively easily and faster than in the case of MMA welding.

Pipelines. The technology of repair of gas- and oil pipelines having cracks foresees the defect place preparation with abrasive tool and following multipass welding up the groove.

Table 1. Chemical compositions of steels and weld metal

Steel	Place of analysis	Element, wt%							
		C	Si	Mn	Ni	Cu	Cr	S	P
St3	base metal	0.23	0.21	0.81	0.04	-	0.01	0.036	0.021
	weld	0.03	0.03	0.12	1.40	-	0.02	0.026	0.015
09G2	base metal	0.11	0.40	1.40	0.03	0.05	0.12	0.014	0.026
	weld	0.03	0.03	0.15	1.40	0.03	0.08	0.019	0.025
09G2C	base metal	0.10	0.70	1.50	0.05	0.04	0.06	0.018	0.024
	weld	0.03	0.04	0.17	1.40	0.03	0.05	0.020	0.023
14G	base metal	0.15	0.25	0.83	0.07	0.05	0.03	0.032	0.024
	weld	0.02	0.02	0.10	1.45	0.03	0.08	0.021	0.017
19G	base metal	0.20	0.23	0.86	0.04	0.04	0.03	0.028	0.027
	weld	0.02	0.04	0.11	1.43	0.03	0.02	0.026	0.025
14G2	base metal	0.16	0.21	1.29	0.03	0.03	0.04	0.027	0.029
	weld	0.02	0.03	0.12	1.48	0.04	0.03	0.025	0.027
A36	base metal	0.23	0.22	0.97	0.05	-	-	0.012	0.014
(USA)	weld	0.03	0.03	0.11	1.50	-	-	0.023	0.013

Table 2. Welded joint mechanical properties

Steel	Tensile Strength, MPa	Yield Strength, MPa	Impact Energy, J (-20°C)
St3	420...450	320...340	35...45
09G2	430...460	330...350	40...50
09G2S	430...460	330...350	40...45
14G	430...460	320...350	35...45
19G	430...470	330...360	35...45
14G2	430...470	330...370	35...50
A36 (USA)	420...460	320...350	40...50

Note: All samples were tested according with ANSI/AWS D3.6

At present of dent, the damages areas are removed. Appeared adges and surrounding surface of pipe are treated with abrasive tool. Using an installation contrivance, a patch is introduced into the pipe through the performed hole and then welded to pipe with butt multipass weld, Fig.1. In the case of corrosion defect of small sizes, it is possible to repair superimposing patch on faulty area and welding it with pipe surface performing fillet weld. In the case of the full rupture of pipeline, the repair technique, as a rule, includes installation the inner and external pipe shells. The samples simulating repair of the typical defects are shown in Fig.2.

In repairing of water-pipelines, the same technologies are used as in the cases of restoration of gas- and oil pipelines. But the experience is evidence of possibility to simplify the technique at the expense of application of two half-couplings which are welded together on water pipeline and welded to pipeline body with girths.

Since 1970 more than 70 gas-, oil-, and water pipelines across the water obstacle were restored using the FCAW system.

As the example, next case is described which took place in repairing the underwater passage of the gas pipeline across the Enisei river near the Dudinka.

The 325 mm dia. siphon (09G2S steel pipe) failed along the field joint in the place where it comes out of the deepened area near the right bank 100 meters from the water edge, 12 m deep. The type of failure is shown in Fig.3. The welded joint fracture in the HAZ extended for more than 270° around the pipe perimeter. A 150 mm long tearing of the wall along the axis in the base metal was observed, it being, evidently, due to the section rotation under the water current effect. The circular crack opening in the upper portion of the pipe was 20 mm, the sections in the tearing location were displaced relative to each other by 40-60 mm. The river bed relief in the zone of the siphon laying specified the complex spatial bending of the "river" and "bank" section axes in the region adjacent to the tear. The angles in the vertical and horizontal plane were, approximately, 10° and 7°, respectively, thus requiring a thorough alignment to ensure coaxiality. The repair technology (Fig.4) required the removal of the defective area of the siphon, fabrication and installation of the inner shell, its welding by two double pass inclined welds, weld testing by the working pressure P=3 MPa, installation of the external coupling preliminarily mounted on the "river" section, concentrically to the inner shell. The external coupling should also be welded under water by inclined welds, the water should be removed from the circular gap between the inner shell and external coupling, and the as-assembled unit should be tested by the working pressure of gas. A threaded hole is provided in the upper part of the external shell the purpose of which is to simplify the deposition of the sealing weld. This hole is necessary, because an intensive, concentrated in a small volume heat source causes an intensive vapour formation and pressure increase in the space between the inner and external shell, and this may hinder the deposition of the last, sealing portions of the circumferential weld. Other versions of the repair assembly were also considered: flange joint design of the inner shell with a bevel cut of end faces, the shell being rotated for 180° around the longitudinal axis after installation, and others. However, they were rejected because of a considerable bending of the axes of the "river" and "bank" sections, limited technical possibilities of installation equipment and short terms of the work performance.

The technical devices used in repair operations consisted of a 290 t barge carrying a self-contained electric power station of 100 kW power, pipe-layer, winches, divers' boat, tug boat and of draft mechanisms, located on the bank, etc.

According to the plan of repairs, the operation sequence was as follows.

After installing the machinery, deepening the river bottom, and welding equipment testing in site, the defective section of the pipe was removed. To simplify the inner shell installation and its welding on, the bevel cuts were made according to a template.

The semi-automatic underwater cutting with PPR-AN2 flux-cored wire was performed with A-1660 semi-automatic machine at the conditions, ensuring the high-efficiency and good quality of the surfaces, the cutting time amounting to 11 minutes.

The "river" pipe end was lifted by hoists along the vertical approximately by 3/4 of the diameter, the external shell was moved over it, and an inner shell with a rest mounted on it was introduced into it. After alignment of the fact cross-sections of the pipes, the inner shell was installed in the place specified in the repair scheme by the axial force and welded by two-pass circumferential welds in the conditions, given in Table 3. After performing the root weld, the slag crust was carefully removed.

It should be noted, that in underwater mechanised welding, the same as in air, the weld deposition in the overhead position requires from the diver-welder a certain amount of training and skill. Here, the welding of the overhead regions of the weld was hindered by the inconvenience of the welder position under the pipe. There was no possibility of preparing the trench of s required depth, since the bottom in site was made up by rocks with pebble-like and silt inclusions. However, despite of the inconvenient position and periodical impairment of visibility, due to pileup winds, the high-quality of weld performance was achieved, and the welds were accepted after the first test by the working pressure. The semi-automatic welding efficiency is 3-4 times higher than that of the manual electric-arc underwater welding. The average welding rate is 6-8 m/h. with 10-12 mm weld leg.

Table 3. Semi-automatic welding and cutting conditions.

Conditions		Main parameters					
Operation kind	Steel grade, thickness, mm	Arc voltage, V	Current, A	Welding (cutting) rate, m/h	Power source, polarity	Wire grade, diameter	Spatial position
Semi-automatic welding	09G2S 10-12	32-34 30-32 27-28	240-260 200-220 160-180	12 8 4-8	PSG-500 reverse	PPS-AN1 1.6 mm	flat vertical overhead
Semi-automatic cutting	09G2S 10-12	38-39 37-38 37-38	400 380 380	20 16 12	PSG-500 straight	PPR-AN2 2.0 mm	flat vertical overhead

After welding on the inner shell, and weld testing under the working pressure by the axial force, created by the on-shore draft mechanism through a system of simple devices, the external shell was moved over to its position specified by the repair scheme. It had been preliminary oriented in such a way, that the large generatrix was located below. The welds, fixing the external shell were also made under conditions, given in Table 3. After performing the inclined welds, the upper threaded hole was plugged, and a weld was made around it, and the holes in the lower part of the shell were used for removing the water from the circular space between the external and internal shells.

In winter the gas supplied to the underwater passage is down to the temperatures of -40° C and lower. This makes higher demands not only of the strength and ductility properties of the welds themselves, but also of the design of the repair assembly as a whole. A rather thick layer of ice is formed on the outer surface of the pipe. An air cushion is provided in the circular space between the shells to prevent the possible defreezing and depressurization if the assembly. The air cushion is created by air supply from the surface under the pressure up to 0.5 MPa through one of the holes, located on the lower generatrix of the external shell, the water having been removed from the space for about 60-70% by volume. After the water removal the holes 5 have been plugged (Fig.4).

The experience of E.O.Paton EWI and CIS-companies which use the FCA welding and cutting techniques relates to restoration of river pipeline passages at the depths down to 20 m. The maximum diameter of repaired pipes was 1020 mm, the inner operating pressure being up to 4 MPa.

As a rule, the repair work are performed in the areas of intensive navigation. In this connection, the most of these works were performed in the winter time. All the auxiliary

equipment were installed on ice directly over damaged area of pipeline (Fig.5). Usually, the duration of restoration including removing of faulty area, mechanical treatment, adjustment of patch, welding and quality inspection, was 4...10 days.

Ship afloat. The most often defects of ship hulls are divided conditionally into surface (for example, corrosion defects, slight tears, dents, and so on) and through (for example, cracks, holes, and so on). In the cases of first type, cleaning out of faulty surface up to sound metal and subsequent welding up are sufficient. The some schemes of preparation are given in Fig.6. In the cases of through damages, the border metal of holes is removed up to plane surface and the crack edges are cut out up to V-groove, both ends of crack are drilled (Fig.7). As to holes, they are repaired using patches which are prepared on air. If the hole is of big dimensions, the patch is assembled from several parts which are joint together with butt welds.

With the aim to decrease of hull deformation, the welding of patch with hull is performed sectionally, the separate weld sections being performed in turn on opposite sides. If the access to inner side of patch is available, the back weld can be made.

For the first time the semi-automatic flux-cored arc welding was applied in salvaging the motor ship "Mozdok" sunk in the Odessa port. The mentioned ship got a 7 x 14 m breach as a result of collision and submer-creating hazards for normal navigation in this region.

The ship salvaging was performed by the combined methods: using lifting pontoons and creating the positive floatability of the hull by pumping polystyrene into the holds. It was necessary to ensure complete tightness of the brought-in patch and of the ship cargo hold covers to prevent the leakage of polystyrene pumped into the holds. The semi-automatic underwater welding allowed to perform a large volume of welding jobs in a short time. The vertical overlap welds, 30-12 m deep, Fig.8, and the welds in the vertical and flat position 12 m deep, were made in two passes. The total length of welds was 100 m. There were no problems of polystyrene leakage after a through sealing, and the ship was lifted by the time fixed.

Since that time more than 200 ship-repairing and ship-rising works were carried out on the base of FCA welding technology.

For the time being two companies apply at the former USSR territory the worked out by Paton EWI technology the most widely - EO ASPTR of Baltic Sea Steamship line (St.-Petersburg) and Scientific-production enterprise "Shelf" (North region, Murmansk). These companies have a high skill diver-welders and the necessary equipment. The main types of works of first organisation is repair of ship hulls, screw propellers and rudders. Within the last 10 years the EO ASPTR carried out more than 76 big repair work using FCAW-technique.

The character of works carried out by "Shelf" company is connected with specificity Murmansk's region. These works are, mainly, hermetization of underwater part of ship hulls, the restoration of integrity of hulls damaged with underwater stones or with blocks of ice, repair of screw propellers and rudders. The following figures give an idea of volume of works accomplished. At hermetisation of cruiser's "Nevskii" hull, the dimension of patches reached 3600×1800 mm, the length of welds was in general more than 300 m. In restoration of merchant ship "V.Arsenjev" heavy damages as the result of hitting

against stones the 8 patches measuring from 880×780 mm up to 1800×760 mm with the total perimeter length of 42 m were welded on. After examination of restored ship, the Register gave permission for dispatch of the laded ship from Murmansk to Vladivostok through the North Sea Way.

Besides ship restoration works the SPE "Shelf" has experience in repairing moorages and floating docks.

The accumulated experience of practical application of FCA welding technique shows the possibility and expediency of its utilisation in the next cases:

- repair of ship hulls with navigation and corrosion damages;
- hermetization of ship hulls before transportation to place of ship liquidation;
- hermetization of Kingston's shafts for repair and substitution of fittings;
- installation of protective casing around screw propeller;
- substitution of protectors;
- restoration of raders;
- repair of floating docks and moorages;
- ship rising.

In a number of cases the semi-automatic underwater welding application permitted to considerably reduce labour consumption for the repair jobs and shorten repair terms, the semi-automatic underwater welding technology being used for such operations, which cannot be called underwater welding ones in the initial meaning of this notion, for these are usually performed in open water reservoirs.

In one of the integrated chemical works of the country an emergency repair was performed of the siphon of the recycling system of water supply for the main production. A 60 mm diameter hole was formed in 800 mm diameter pipe, made of low-alloy 09G2S pipe steel, as a result of insufficient cathodic protection and abrasive action of water, which contained a suspension of hard particles. A large volume of earth-moving was required for an exact location of the defect and its elimination. The defect was removed with semi-automatic underwater welding. An operation (technological) access hole was cut out in the pipe surface in the area of the expected fracture. The diver, entering the water-filled pipe by the access hole revealed the defect 20 m from the access hole. A special light-weight small-sized semi-automatic machine for the underwater welding was introduced into the pipe, and an oval-shaped patch was welded on. A noticeable efficiency was achieved at the expense of reducing the volume of the preparatory operations and of completely eliminating the earth-moving. The short terms of the work performance should be especially noted, since the whole work took only several hours.

The semi-automatic underwater welding application in emergency cases and in case of emergency repair in distant industrial regions gives such important advantages as mobility and a possibility of a fast mobilisation of the equipment, high speed of the operation performance due to a high efficiency of the process, moderate expenses for the welding performance and very high economic efficiency.

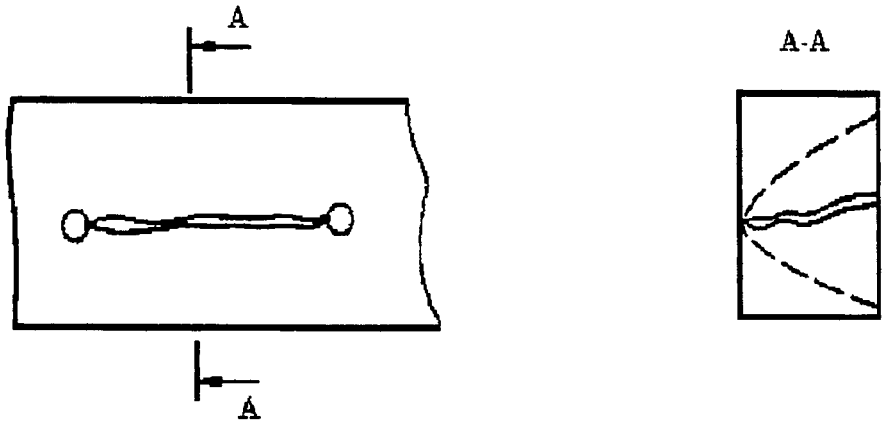

Figure 7 Edge preparation of through crack

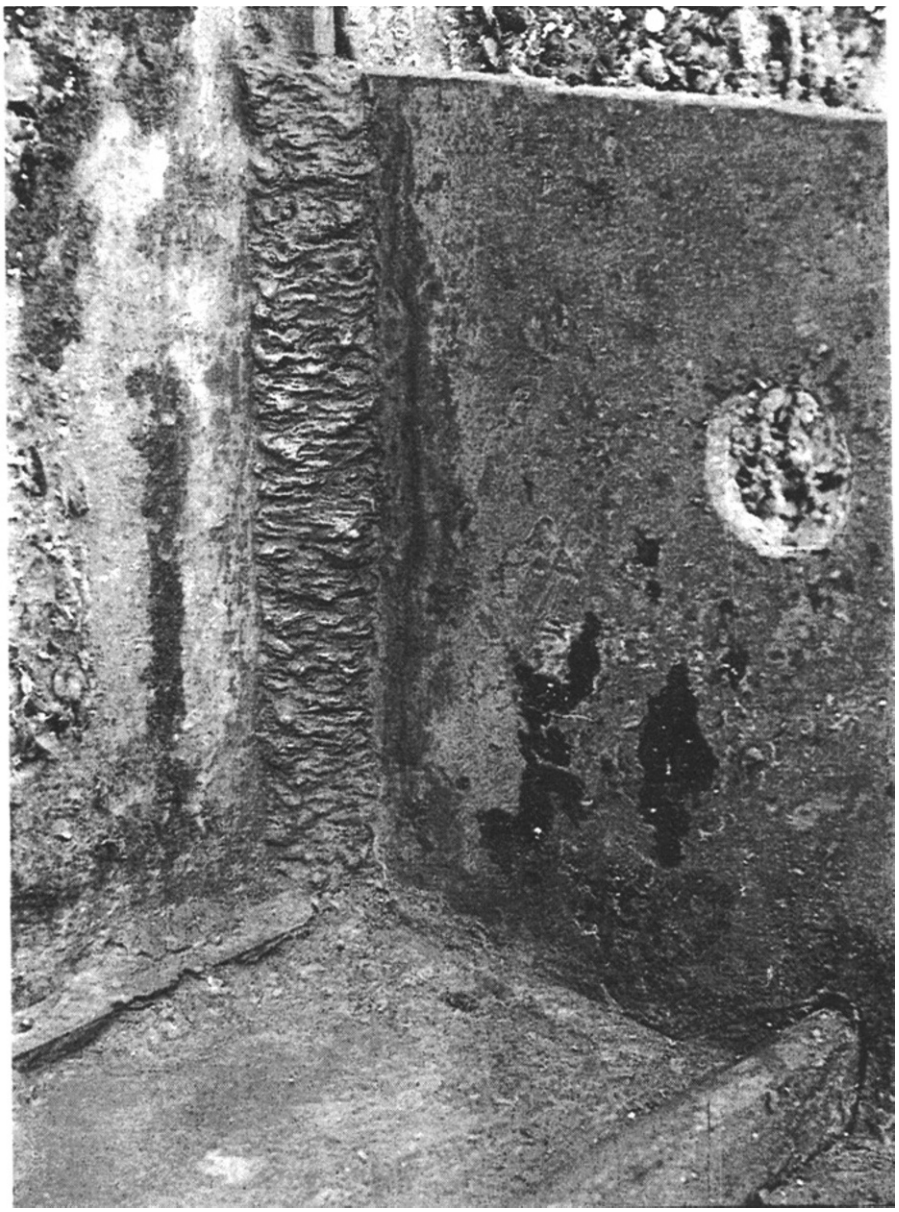

Figure 8 Fillet weld of ship structure element performed with flux-cored wire PPS-AN1 type in vertical position

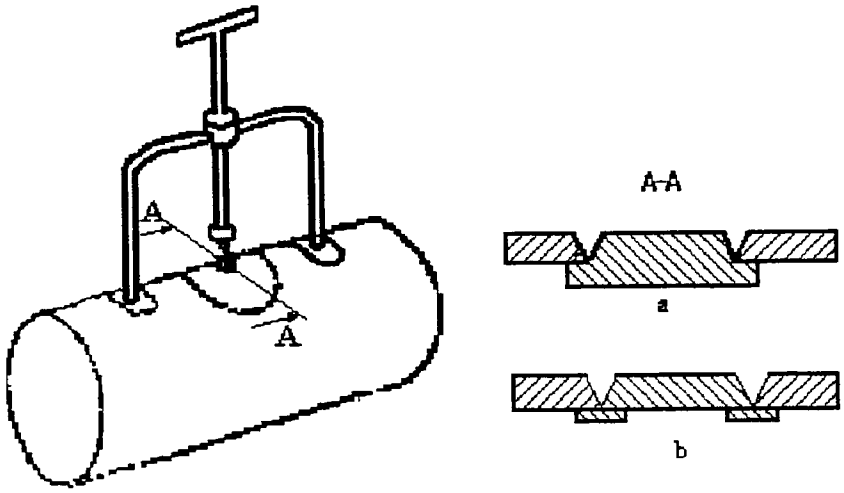

Figure 1 Installation of the patch on the tube

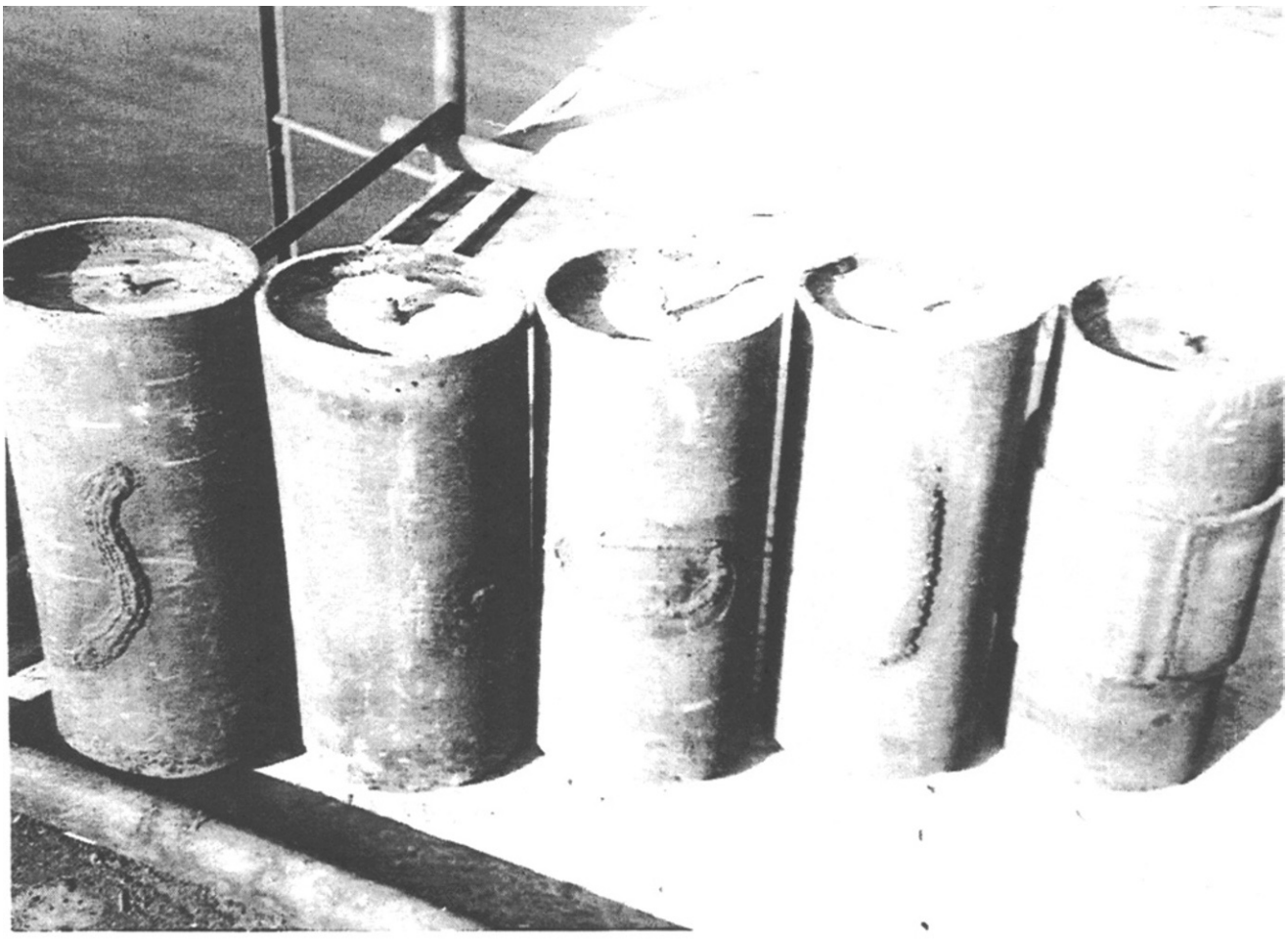

Figure 2 The samples simulating repair of the typical defects of pipelines after testing under inner pressure of 5 MPa

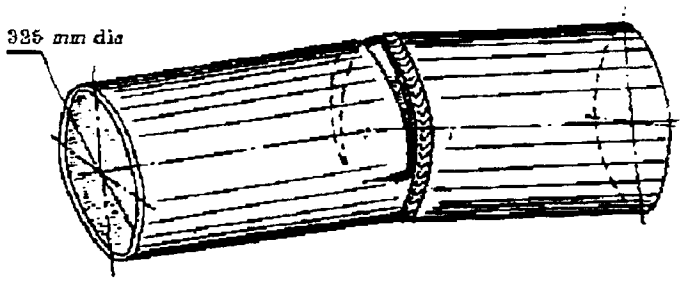

Figure 3 Scheme of pipeline field joint fracture

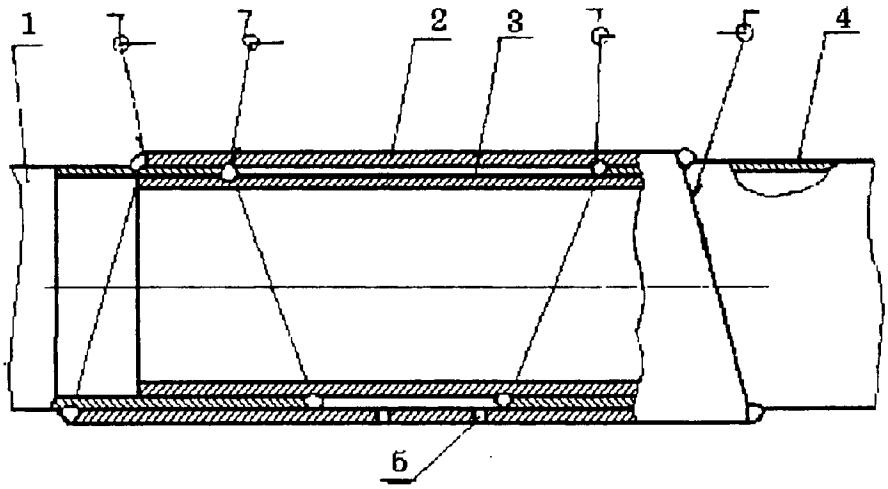

Figure 4 Repair assembly scheme: 1 - pipe end from the fairway side,
2 - external shell, 3 - inner shell, 4 - pipe end from the bank side,
5 - holes for water removal from circular space between the external and inner shells

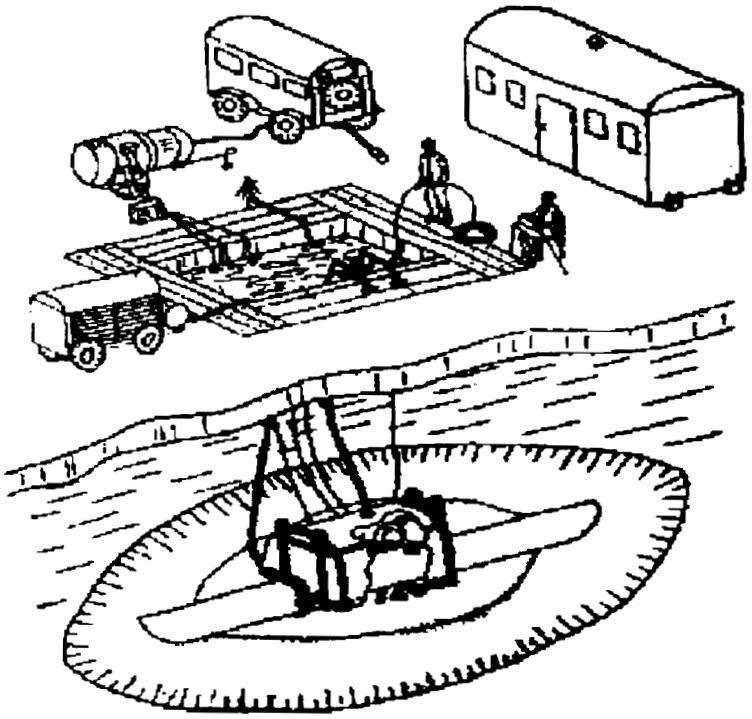

Figure 5 Technological scheme pipeline repair in winter

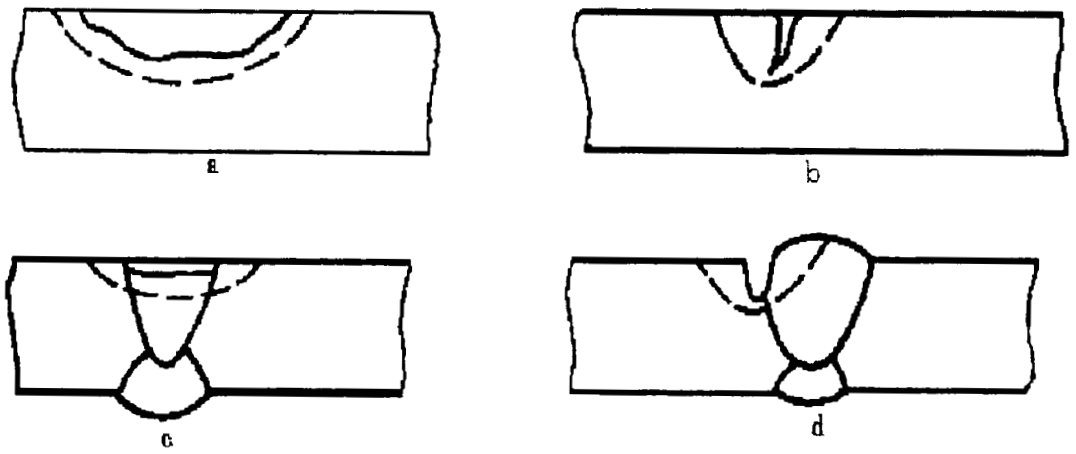

Figure 6 Edge preparation of non-through surface defects:
a - corrosion cavity, b - non-through crack, c - corroded weld,
d - corroded fusion zone

Study of peculiarities of underwater flux-cored wire arc cutting without additional supply of oxygen

Yu Ya Gretskii and Yu N Nefedov, E O Paton Electric Welding Institute

Arc ignition and discontinuity of its burning are important technological factors influencing stability of cutting process, consumption of electrode materials and electrical energy, and defining of edges quality at underwater semi-automatic and mechanised arc cutting.

Earlier performed investigations of arc discharge under water were concerned with short arc of small current density (not more than 125 A/mm^2) and relatively low voltage (only up to 40 V) (1). In this case, the deteriorations of arc burning are mainly connected with transfer of electrode material drops and periodical collapses of vapour-gas bubble in which the arc burns. Contrastingly, the deterioration of arc burning at underwater cutting arise mainly because of all the time changing in arc length in the cut cavity. The above said reasons of instability of short arc (i.e. transfer of drops and periodical vapour-gas bubble collapses) become of secondary importance. In this respect, the investigations for defining the conditions under which the long arc burns stabely have been performed.

The bursting length and burning through capacity of arc have been adopted as basic criteria in evaluation of arc stability, the burning through capacity of arc being the time necessary for cutting a hole in metal of definite thickness.

It is known that the larger is current value, the higher is possibility of arc to be stretched (2). But the primary experiments on ignition of arc and its further burning under water have shown, that the regularity, being true for arc burning in air, is not sufficient for arc discharge existing under water, especially if the arc is long. So, it is impossible to apply the known flux-cored wires developed for underwater welding and commercial solid wires developed for MAG welding of steels at forced operating regimes of cutting (current density is more than 125 A/mm^2) due to impossibility of long arc burning. The worse results have been obtained using the wire of solid cross-section.

This fact seems to take place owing to absence of reasonable quantity of strongly arc stabilising elements in the wire composition. Apparently, in the case of arc cutting with solid wire, the small volume of vapour-gas bubble also adversely affects process stability. While the possibilities of flux-cored wires for varying chemical composition are sufficiently wider, the solid wires have not been applied in further experiments.

Stable ignition and the longest arc length permitting to have conditions for stable arc discharge (bursting arc length) were observed during comparative underwater testing of experimental flux-cored wires with the charge core on the carbonate (gas forming) base and with additions of compounds having ionising effect, such as barium

hydroxide $Ba(OH)_2*8H_2O$ and natrium metasilicate Na_2SiO_3 (Fig.1). These results have been obtained at the current density of 150...200 A/mm^2 and the value of short circuit current of 530 A, excessive hydrostatic pressure Pex being of 0.1 MPa (the operating depth was of 10 m).

The bursting arc length decreases with an increase in excessive hydrostatic pressure (Fig.2) This phenomenon is observed by any wire chemical composition if the arc burns from tip of wire. But, if the wires for underwater welding gave the value of bursting arc length of 12...15 mm at P_{ex}=0.6 MPa, then wires with barium hydroxide in their charge provided values bigger by 8...10 mm.

The positive results of experiments on the long arc stabilisation for underwater environment obtained at high values of current density demonstrate the wide possibilities in variation of technological parameters of cutting with the aim to increase in burning through and arc cutting effectiveness.

The arc burning through capacity is considered to be space of time from arc ignition to full burning through of metal. This parameter was established to be sufficiently dependent on both hydrostatic pressure (Fig.3a) and thickness of metal being cut (Fig.3b). With growth of pressure, the time of burning through decreases if cutting current is constant. This is connected with increase in arc power at the expense of both growth of arc voltage gradient and increase in current density in arc column and, in turn, with heat energy concentration.

Therefore, physico-chemical condition of arc discharge existing under water can to be under control at the expense of charge wire composition changing. The gas-forming ingredients (including oxygen-forming components) create not only vapour-gas bubble around the arc and oxidise the molten metal, but form the plasma jet which has the active gas-dynamic effect on molten pool promoting the burning through of metal plate being cut.

With the aim of successful solving of tasks connected with working out of new electrode materials and equipment for FCA cutting without additional supply of oxygen as well as for an increase in efficiency of this technological process, it is necessary to have the data with regard to mechanism of FCA cutting, character of cutting process proceeding, and influence of thickness metal being cut, excessive pressure and other factors on technological productivity.

Direct observation of cutting arc is made difficult by opaque vapour-gas bubble forming as result of water and wire charge decomposition and fluctuating around arc. What is why our investigations of FCA cutting mechanism were ground on analysis of different indirect factors, such as cut shape, distance between cut edges, arc voltage Ua, cutting current Ic etc. (3-6). This data are not enough for full understanding of the phenomenon. But, definite conception has been formulated.

So, it has been observed that with an increase of arc voltage the shape of cut changes from nearly rectangular with almost parallel edges (Fig.4a) to barrel-looking (Fig.4c). In doing so, the distance between cut edges decreases from of 2-3 wire diameter to one diameter. This fact gave the grounds to consider that the wire tip position of relatively to surface of metal being cut depends on cutting conditions.

Simultaneously, the lateral surface of flux-cored wire is continuously coming nearer to edges of cut cavity with velocity that is equal to velocity of cutting (Fig.6). The short circuit between wire and edges would be as natural result. But, the expected short circuit does not happen because the arc passes from first inter electrode space ("wire tip - molten metal") to second space ("wire lateral surface - cut cavity edge"). The last position of arc is more preferable as to expenditure of energy. In such conditions the arc burns through the tube of flux-cored wire. As the result, the new wire tip appears and the arc comes back to first space again (Fig.6). This cycle repeats periodically.

It is possible to give a great deal of facts supporting the assumed mechanism of FCA cutting process.

Firstly, at high wire feeding rate, the discharges of burned out wire pieces of small length (2...5 cm) are observed, these pieces having a traces of melted off lateral surface.

Secondly, the oscillograms U_a and I_c have a specific areas characterised with sharp decrease in arc voltage and corresponding increase in cutting current (Fig.7).

Thirdly, increase in base metal thickness, wire feeding rate, and excessive pressure of water environment and decrease in cutting velocity must, in accordance with above described mechanism of FCA cutting, aggravate the role of effect of wire tip submerging into cut cavity and, accordingly, reinforce the left part of arc voltage histogram. It is really observed in practice.

From the point of view on FCA cutting mechanism, it is possible to explain the shown earlier variety of cut shapes. So, under conditions when wire tip is out cavity (high arc voltage, small thickness metal being cut, low excessive pressure), cutting is performed with arc flame. In this case, cut edges are relatively parallel (Fig.4a). The cut width is proportionate with three or more diameters of wire. The histogram of arc voltage is single-modal.

When negligible submersion of wire tip into cut cavity, the cut shape becomes evidently conical at the expense of gap narrowing to two wire diameters on arc side (Fig.4b). The histogram of arc voltage is two-modal with feebly marked left part. The narrowing of upper edges is connected with decrease in efficiency of their melting. This is also in accordance with described mechanism of FCA cutting. Anode spot through which main part of energy for melting of metal enters the plate being cut is in upper edges area only during short time when the arc passes on to inter electrode space "lateral wire surface - cut cavity edges".

Still less of energy enters area of upper edges at significant submersion of wire tip into cut gap (large thickness metal being cut; high wire feeding rate and excessive pressure; low arc voltage). The gap between upper edges reduces up to value equal approximately to one wire diameter. The cut shape approaches to barrel-looking (Fig.4c). The arc voltage histogram has clearly-expressed two-modal type.

At very short arc (low arc voltage, high excessive pressure), even negligible moving off of anode spot from wire tip will give rise to sharp instantaneous increase in arc voltage, sufficient decrease in cutting current and, accordingly, decrease in melting

rate of wire tip. The possibility of passing of the arc on lateral surface of wire grows. Under such conditions, the gaps between both upper and lower edges become lesser.

The data obtained on mechanism of underwater FCAC allow to develop the monitoring procedure for the cut process based on continuous analysis of the arc voltage histogram and the parameter's variation coefficient in order to maintain the optimal conditions of cutting. But, it is incorrectly to found such algorithm only on analysis of histogram form because both single-modal and two-modal histograms, according to FCA cutting conditions, can correspond to normal proceeding of process. True, the first type used to be very seldom at cutting. At the same time, the form of histogram is always single-modal at the absence of a cut.

Such algorithm suggests determination firstly of form of arc voltage histogram for definite FCAC conditions which correspond to optimal proceeding of cutting process (with burning through) and to insufficient one (without cut). Then, the departure of arc voltage histogram form from optimal one will show a breach of process.

In addition, it is necessary to define also the coefficient of arc voltage variation (K_v^u). Note, its value will be considerably higher for two-modal histogram than for single-modal one. Therefore, the more high values of the coefficient will be corresponded, as a rule, to normal proceeding FCAC process (Table 1).

The understanding of the underwater FCAC mechanism opens the new possibilities for optimisation of this method. For example, now it is clear, that increasing in the wire feeding rate can not give the equivalent rising of cutting velocity because of burning through of wire periodically with arc acting on lateral surface of wire. The cutting velocity can even reduce. It is possible to specify the requirements to power sources for underwater flux-cored arc cutting.

CONCLUSIONS.

1. As the result of statistical analysis of underwater flux-cored wire arc cutting electric parameters, shapes of cut and other characteristics of this process, disclosed has been the its mechanism consisting in that the flux-cored tip is, mainly, in cut cavity where it moves following to lengthening arc up to moment of critical nearing of lateral wire surface with cut cavity edges after that the arc passes on new more short inter electrode space; the wire tube is burned through with arc, and the arc passes again into former inter electrode space "wire tip-liquid metal" being on the line of wire axis.

2. Burning of arc by turns in two inter electrode spaces, of considerably different extent, leads to formation of two-modal arc voltage histogram in which the either mode corresponds to arc burning in one of them.

3. The conditions at which the wire tip does not enter the cavity are created when thickness of metal being cut is small, arc voltage is increased and excessive pressure of water is low. In such case, the arc voltage histogram is single-modal.

Table 1. Influence of technological parameters of underwater FCAC on the variation coefficient K_v^u at Ic=450...600 A, Ua=50...55 V, Vwf=350 m/h

Vc, m/h	Pex, MPa	δ, %	K_v^u,%	Histogram form	Presence of cut
14	0.1	20	36.4	two-modal	yes
16	0.1	20	32.2	two-modal	yes
18	0.1	20	22.4	one-modal	no
14	0.1	20	40.6	two-modal	yes
14	0.3	20	35.0	two-modal	yes
14	0.6	20	23.5	one-modal	no
14	0.1	15	30.8	two-modal	yes
14	0.1	20	27.6	two-modal	yes
14	0.1	30	25.8	one-modal	no

Note: Ic=450...600 A, Ua=50...55 V, Vwf=350 m/h

4. At FCA cutting, the degree of wire tip submersion into cut cavity rises with increase of base metal thickness, flux-cored wire feeding rate and excessive pressure and with decrease of arc voltage and cutting velocity.

5. The cut shape is defined with extent of submersion of wire tip into forming gap: the deeper submersion, the narrower cut cavity in area of upper edges.

6. The obtained data and formulated conception of FCA cutting mechanism allow to develop an algorithm of operative control of this process grounded on continuous analysis of arc voltage histogram shape and value of variation coefficient of arc voltage with the aim to maintain optimal cutting technological parameters.

REFERENCES

1 Lebedev V K et al: 'Calculation of Basic Characteristics of Arc in Underwater Mechanised Welding', Underwater Welding and Cutting, 1980, p29
2 Leskov G I: 'Electric Welding Arc', Mashinostroenie, 1970, p87
3 Danchenko M E et al: 'Underwater Flux-cored Wire Arc Cutting', Avtomaticheskaya Svarka, No 4, 1988, p59
4 Danchenko M E et al: 'Effect of the Depth of Underwater FCAC on the Process Technological Parameters', Avtomaticheskaya Svarka, No 1, 1989, p48
5 Danchenko M E and Nefedov Yu N: 'Underwater Flux-cored Wire Arc Cutting with Semi-automatic Machine', Avtomaticheskaya Svarka, No 1, 1990, p70
6 Danchenko M E and Nefedov Yu N: Choosing of Optimal Parameters of FCAC Process', Avtomaticheskaya Svarka, No 11, 1991, p64

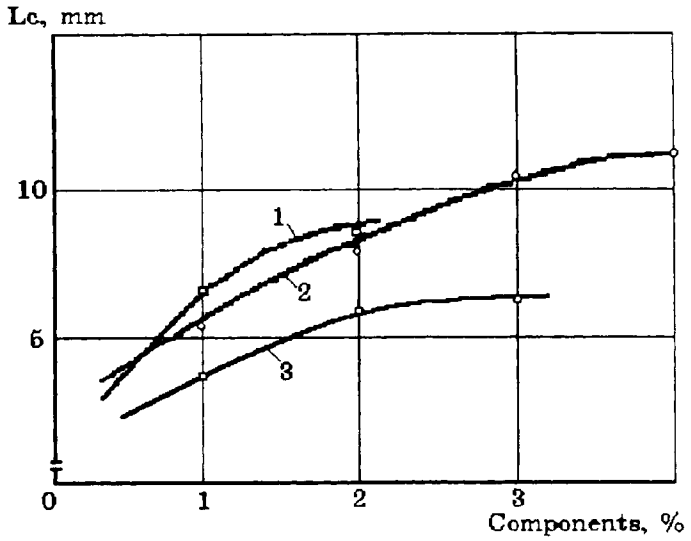

Figure 1 Influence of flux-cored wire charge components on bursting length of cutting arc: 1 - Na_2SiO_3, 2 - $Ba(OH)_2*8H_2O$. Current of short-circuit - 830 A; open circuit voltage - 65 V; wire dia - 1.6 mm; excessive pressure - 0.6 MPa

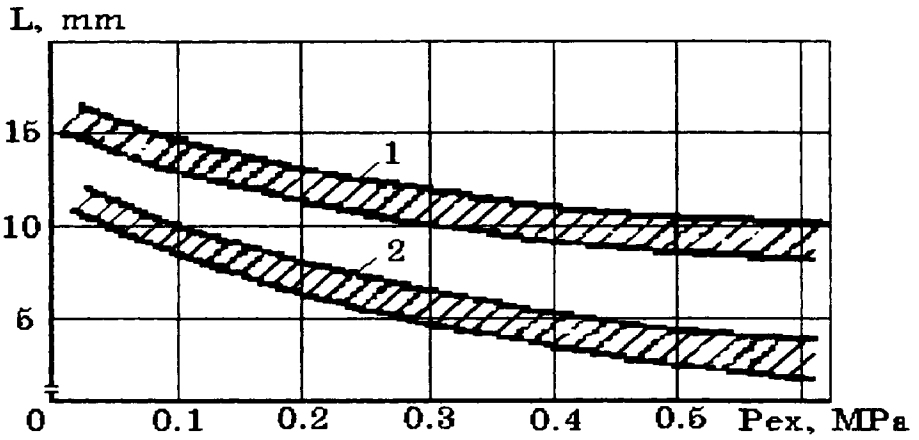

Figure 2 Bursting arc length values depending on hydrostatic pressure: 1 - wire PPS-AN1 type (for underwater welding), 2 - experimental wire

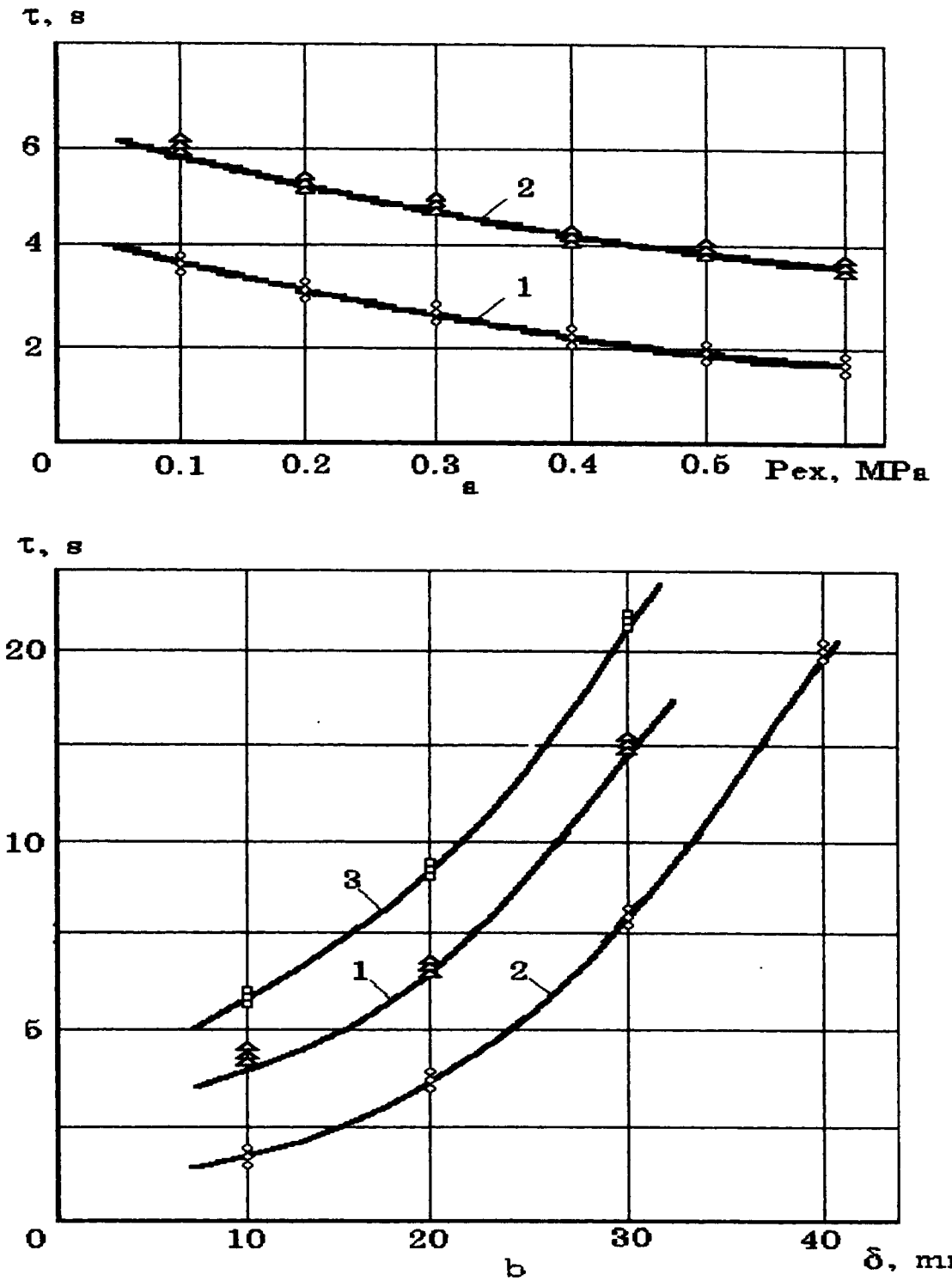

Figure 3 Dependence of burning through capacity of arc on hydrostatic pressure at steel thickness of 20 mm (a) and on thickness of metal being cut at hydrostatic pressure of 0.1 MPa (b): 1 - wire dia - 2.4 mm, Ic=600 A, Ua=45...50 V; 2 - wire dia - 2.0 mm, Ic=470 A, Ua=40...50 V

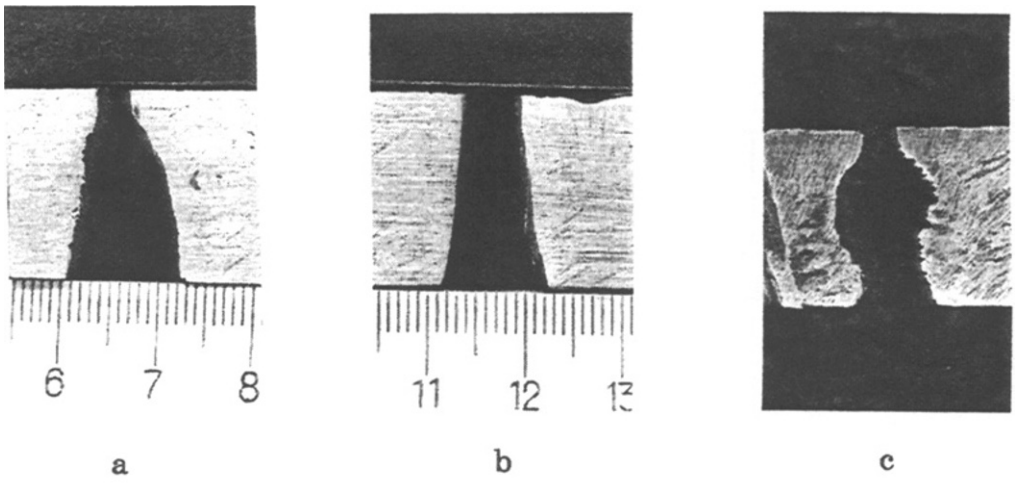

Figure 4 Typical shapes of cut cavity

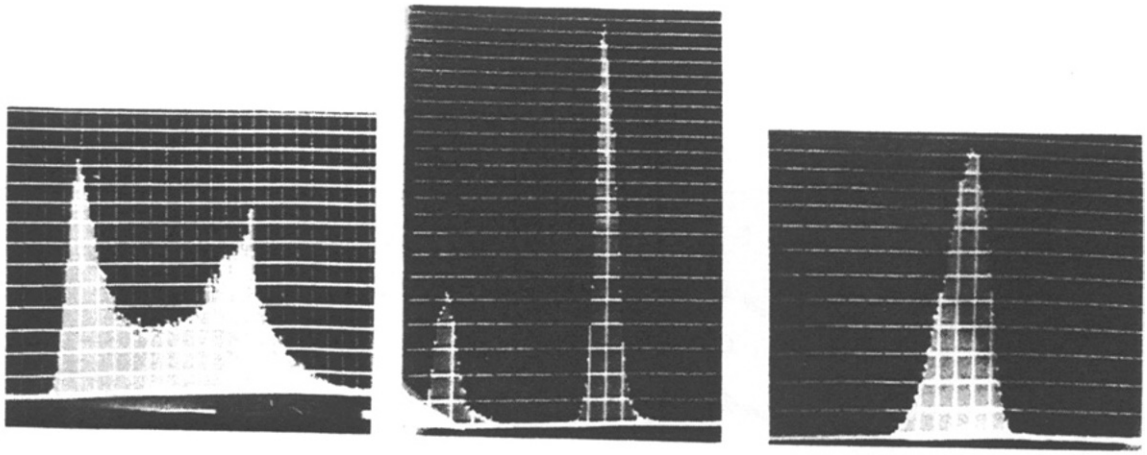

Figure 5 Typical forms of arc voltage histogram at underwater FCAC (a) and at underwater arc welding with (b) and without (c) short-circuits

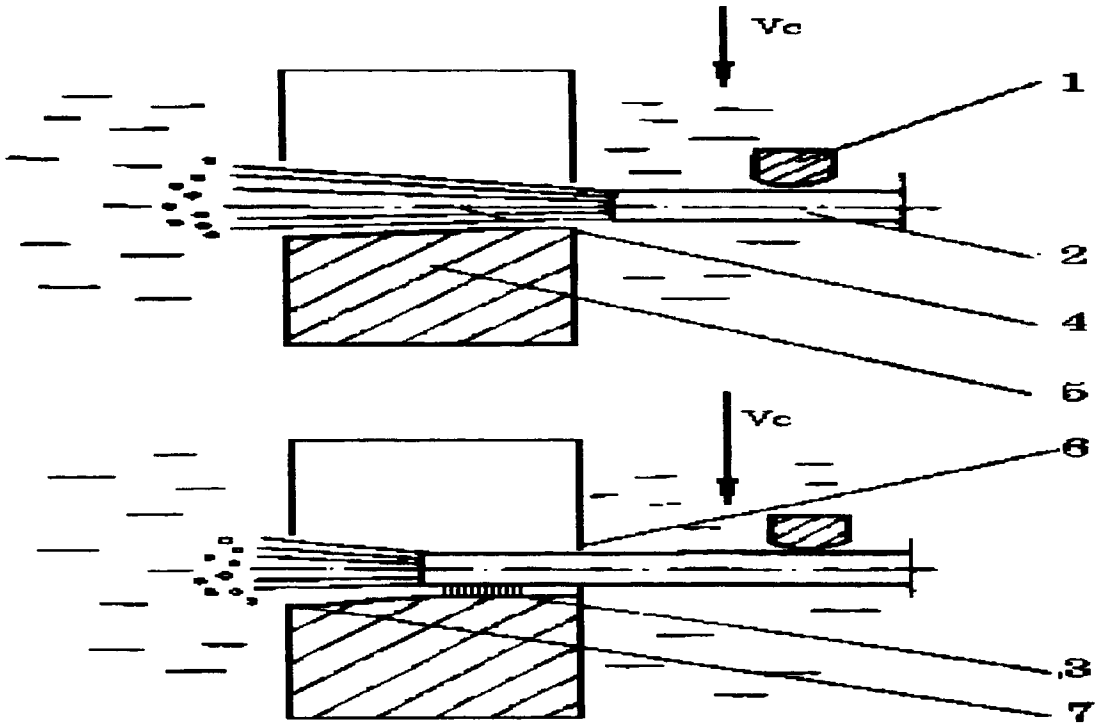

Figure 6 To explanation of underwater FCAC mechanism: 1 - current feed, 2 - flux-cored wire, 3 - inter electrode space "wire tip - liquid metal", 4 - metal being cut, 5 - upper edges of cut cavity, 6 - inter electrode space "lateral surface of wire - edges of cut cavity", 7 - lower edges of cut

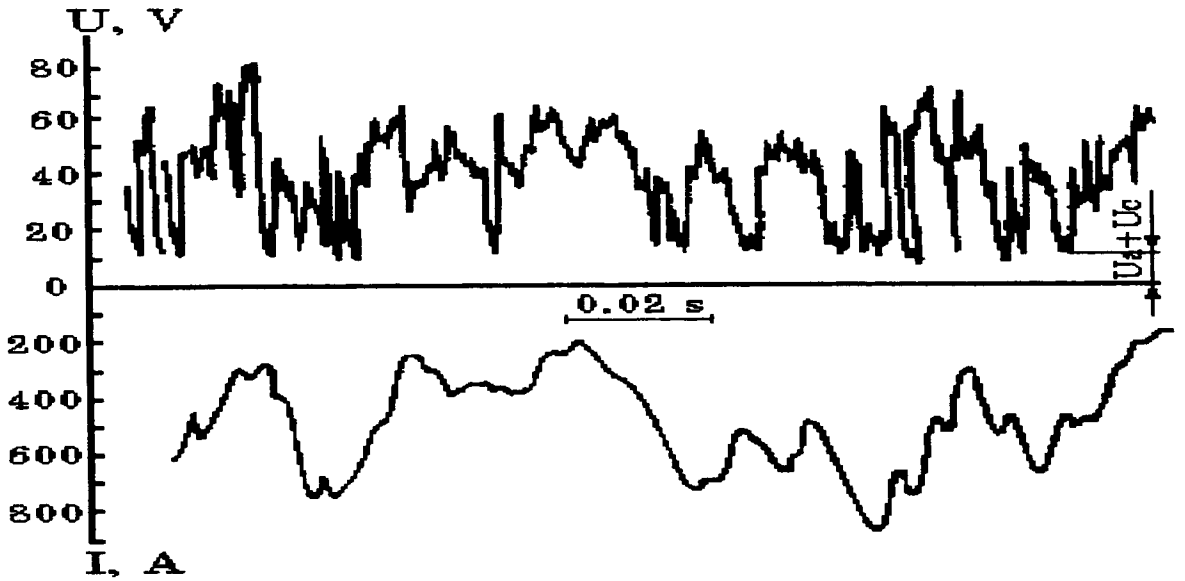

Figure 7 Oscillograms Ua and Ic of underwater FCAC at wire feeding rate of 350 m/h, wire dia of 2.4 mm, cutting current of 600...650 A and arc voltage of 50...55 V

Technology and experience of application of underwater flux-cored wire arc semi-automatic cutting

Yu N Nefedov and M E Danchenko, E O Paton Electric Welding Institute

One of the actual tasks defining the development of underwater technique is improvement of existing underwater cutting methods, creation of new electrode materials and high efficient cutting process of metals and non-metals. Arc cutting methods have a key position in these attempts. They are based mainly on application of stick electrodes combining with oxygen supply to arc burning zone (1,2). The heat of both the electric arc and exothermic reaction of base metal and metallic electrode in the oxygen environment is used for heating metal being cut.

For the time being, the method of underwater electric-arc cutting steels with stick electrodes is the most-used one. For performance of manual oxy-arc cutting the expensive equipment is not needed. Nevertheless, this technique has a number of disadvantages, such as high oxygen consumption (0.20...0.35 m^3 per running metre of cut), comparatively low productivity because of high time waste for burning through all base metal thickness in the beginning of process, strong overheating of electrodes and closely associated with that increased consumption as well as often changes of stick electrodes in operation. As the depth of submerging increases, the efficiency of using of stick electrodes comes down. Furthermore, the application of this technique for cutting non-ferrous metal and high-alloyed steel is practically impossible.

To eliminate above said disadvantages of the known cutting methods, to increase the process capacity, and to improve diver's labour conditions, the fundamental researches on metallurgical and technological peculiarities of underwater arc cutting have been performed at E.O.Paton Electric Welding Institute including study the physical characteristics of electric arc burning under water up to depth of 60 m. Among them, the next researches can be mentioned:

- study of flux-cored wire cutting (FCAC) mechanism (3);
- assessment of hydrostatic pressure effect on technological parameters of process (4-7);
- choice of optimal underwater cutting parameters (6-8);
- study of the effect of power source characteristics on process parameters (9).

On the base of these investigations the new method of underwater arc cutting - semi-automatic/mechanised flux-cored wire arc cutting (FCAC) - has been worked out.

Absence of additional oxygen supply into arc zone and continuity of cutting performance are important peculiarities of the technique (10). The high cutting through capability and arc burning stability are provided at the expense of flux-cored wire composition. Gas- and oxygen forming components, besides their action as liquid metal oxidisers and vapour-gas bubble creators, form plasma jet. The letter exerts active gas-dynamic pressure on liquid metal due to that burning through of base metal is accelerated.

Flux-cored wires for underwater cutting must meet a number of technical requirements defining possibility and expediency of their application for steel of different thickness in the wide range of operating depths. The main requirement of metallurgical character is intensive oxidising of molten metal in cut cavity. The technological requirements determine necessity to provide the stable burning of arc and quality formation of cut edges. From economic point of view, the wire must distinguish in minimum expenditure of electrode material and energy to provide the technical-economic efficiency of their application comparing with stick electrodes. Therefore, the components of flux-cored wire charge must be as strong oxidiser, gas-forming and arc stabilising compounds.

This understanding was the base of our activity in working out of flux-cored wires for cutting. Three groups of charge composition was investigated. Every of them differed with own primary effect on cut metal in cut cavity oxidising, gas-dynamic or exothermic. These systems were evaluated in the context of possibility to provide high efficiency of technological process. According to that, three type of wire have been created and introduced into practice (Table 1).

Table 1. Characteristic of flux-cored wires for underwater arc cutting of steels without additional supply of oxygen.

Flux-cored wire type	Basic system of components	Thickness of base metal, mm	Cutting rate, m/h	Purpose
PPR-AN1	gas-forming	10...20	8...20	For large volumes of work at depth up to 30 m
PPR-AN2	oxidising	10...20	8...24	Special works at depths up to 30 m
PPR-AN3	exothermic	10...40	6...26	Works at the depths up to 60 m

The productivity of process (velocity of cutting) have been taken as the main criterion of assessment of technological efficiency of the process provided the arc burns stably.

The system with high degree of gas-forming is based on application of carbonates. True, the extent of metal oxidation with carbon dioxide is lower than that with oxygen. But application of this system is attentive due to its manufacturability of wire making as well as non-scarcity and cheapness of components.

Oxidising system is more effective than gas-forming one. But, its possibilities are limited with intensification of steel wire tube burning at excessive oxygen emission.

The main advantage of the system on the base of exothermic effect comparatively with two above said systems is increase in burning through capability of arc by 10...15 per cent. This advantage becomes especially apparent with rise of hydrostatic pressure. Besides, in shallow water the system allows the cutting current to be decreased without considerable losses in productivity of process.

Determined have been the optimum expenditures of electrode materials and electric energy per running metre of cutting for every above said basic systems. The comparative characteristic of these specific indices for different operating depths is given in Fig.1.

As it is evident from data given, to use the wire with exothermic system is most effective for deeper depths. The most high expenditures of electric energy are at gas-forming system because cutting is performed at forced regimes (Ua=50 V, Ic=500 A) with aim to ensure the full decomposition of carbonates in the arc burning zone.

The wires of small diameter (2.0...2.4 mm) are more preferable for semi-automatic FCAC, because they allow to use a light-weight holder which is more convenient for underwater application (6).

Plots Ia=f(Vwf) shown in Fig.2 indicate that the intensity of current growth decreases with the increase in wire feed speed, particularly for the small diameter wires.

When the 2.0...2.4 mm dia. wires are used, the up to 30 mm thick low-carbon steels can be cut by FCAC; however, the said wires are more reasonable to be used for underwater cutting the 15...20 mm thick metals at cutting speed not less than 10...15 m/h (Fig.3).

The significant improvement of the arc cutting capacity is observed when the 3 mm dia. wire is used. In this case, however, the heavier holder should be used and this makes the work of a diver-cutting operator much more difficult.

The most important factor affecting the technological parameters of the FCAC process is hydrostatic pressure. As found by investigations of the FCAC optimum parameters for carbon steel specimens, to improve the cutting efficiency with the growth of depth it is necessary to keep up the maximum cutting current and arc voltage values for the wire diameter selected which would provide the best factors of the cut cavity shape and dimensions.

With the increase in hydrostatic pressure the arc voltage grows following a curve which is characteristic of the changes in arc column electric field strength under water (5) (Fig.4).

When arc voltage increases by 10...20% above the minimum value that provides the stable FCAC process, the wire cutting capacity increases with the simultaneous improvement of the cut cavity geometry. However, the further increase in arc voltage causes degradation of the FCAC performance due to the longer arc and the anode (reference) spot wandering in the cut cavity (4). As found by oscillography of the FCAC process parameters, the cutting arc stability deteriorates with the increase in hydrostatic pressure, as evidenced by step disturbances appearing on current and voltage oscillograms. However, this does not exert the significant effect on the FCAC technological parameters.

Optimum parameters of operating cutting regimes have been chosen for wires in dia of 2.0...2.4 mm. For semi-automatic cutting of the up to 10 mm thick steels at the depth up to 30 m it is rationally to use the flux-cored wire of 2 mm diameter. When increase of metal thickness up to 20 mm at the depth up to 60 m it is more reasonable to use the flux-cored wire of 2.4 mm dia. For these wire diameters, the range of the operation regime has been established according to cutting current and wire feeding rate (Fig.5). At the cutting current values higher curve A, intensive burning out of wire tube occurs. At the cutting current values bellow curve B, the stable arc burning process is practically impossible. The shaded area between A and B curves corresponds to those values of current at which edges of cut have satisfactory quality and high productivity of process is provided (Fig.6).

Besides basic dependence of cutting velocity on operating depth and base metal thickness, the important technological characteristics of FCAC process are specific indices of electrode wire and electric energy expenditures:

$$q_w = K_1 V_{wf} \frac{Q}{V_c}; \quad q_e = K_2 \frac{P_a}{V_c},$$

where qw and qe - the wire and electric energy expenditure per one running metre of cut, in kg/m and kWh/m, respectively; Vwf - wire feeding rate, m/h; Q - mass of one metre of wire, kg; Vc - cutting velocity, m/h; Pa - arc power, kW; coefficients K_1 and K_2 have been estimated by calculation, K_1=1.04, K_2=0.9. As seen, these specific indices include the basic technological parameters of cutting and, therefore, they can be as criteria of effectiveness FCAC process assessment.

Some data in respect of these indices are given in Table 2.

Table 2. Some economic data concerning to underwater flux-cored arc cutting with wire PPR-AN1 type.

H, msw	δ, mm	dw, mm	Ic, A	Ua, V	Vc, m/h	qw, kg/m	qe, kW*h/m
10	10	2.0	470	40	20.0	0.333	0.940
		2.4	620	45	25.0	0.365	1.116
	15	2.0	460	43	12.0	0.554	1.648
		2.4	600	47	20.0	0.455	1.410
	20	2.0	460	45	8.0	0.831	2.531
		2.4	600	50	15.0	0.606	2.000
20	10	2.0	450	42	18.0	0.369	1.050
		2.4	610	47	23.0	0.396	1.246
	15	2.0	460	45	10.0	0.665	2.070
		2.4	580	49	18.0	0.505	1.578
	20	2.0	440	47	6,0	1.108	3.446
		2.4	580	52	13.0	0.699	2.320
30	10	2.0	440	44	16.0	0.416	1.210
		2.4	570	49	20.0	0.455	1.396
	15	2.0	440	47	8.0	0.831	2.535
		2.4	560	51	16.0	0.568	1.785
	20	2.0	420	49	4.0	1.662	53145
		2.4	560	54	10.0	0.910	3.024

Note: 1. Base metal - low-carbon structural steel St 3.
2. Wire feeding rate - 350 m/h.

The underwater FCAC technique has also the certain peculiarities. In semi-automatic cutting the wire extension should be small, the best wire position - at lead angle. Here, there is practically no flash at the lower cut edges. Cutting speed

is greatly affected by a spatial position of a metal sheet to be cut. The highest speed can be achieved at its vertical position and at downward cutting. The speed in flat position is by 10...15% and in overhead position is by 15...20 % lower than that in vertical position. Such decrease in the speed can be accounted for by the fact that in flat cutting the vapour which forms in the cut cavity decreases pressure of a cutting jet on molten metal and disturbs arc stability in the cut cavity. In overhead position the counteraction is exerted mostly by gravitational forces under the effect of which molten metal and oxides rush towards the cutting jet. The similar decrease in the speed by 10...20% is observed during cutting under sea water, as compared to cutting under fresh water.

The speed of cutting low-carbon and low-alloy steels is practically similar. Austenitic steels can be cut by 10...15% faster, this being explained by the higher concentration of the cutting jet heat energy due to the lower thermal conductivity of metal. The speed of cutting aluminium is 1.5...2 times as high as that of cutting low-carbon steel of the same thickness, this being related mainly to the great differences in melting points. At the same time, the speed of cutting copper is by 2...3 times lower, though the difference in melting points is effective as well. In the latter case, the great effect is exerted by the high thermal conductivity of copper.

Adjustment of cutting technological parameters is performed at the expense of choice corresponding external volt-ampere characteristic of power source. By them, it is necessary to take into account a large distance between power source and operating place that results in application of electric cables of big length (about 150 m at the depth of 60 msw). The significant power losses appear, in some cases they being of 40% of cutting arc power. Therefore, the power sources should have a open circuit voltage increased by 15...20 V. With this aim, it is possible to use commercial welding power sources having rigid or gently falling external volt-ampere characteristic. In the second case, the steepness of the characteristic could be adjustment in the range of 0.025...0.030 V/A.

The E.O.Paton Electric Welding Institute widely uses the new cutting technology in real conditions. A number of unique works are performed when salvage of ships, repair of oil and gas pipelines, restoration of bridges, clearing of river-beds, repair of sea moorages and so on.

CONCLUSIONS.

On the base of investigation results obtained at E.O.Paton EWI the new underwater flux-cored wire semi-automatic arc cutting method has been developed and is widely used in restoration of underwater steel structures and salvage situation. The method is distinguished with absence of additional supply of oxygen to arc burning zone and intended for cutting of carbon and high-alloyed steels, non-ferrous metals and alloys in thickness up to 40 mm at the operation depths up to 60 m both in fresh and sea water. Three types of flux-cored wires (with oxidising, gas-dynamic and exothermic character of influence on melting metal) had been developed. Their application is always profitable.

REFERENCES

1 Uzilevskii Yu A et al: 'Underwater Cutting of Structural material (Review of Foreign Scientific-technical Literature), Avtomaticheskaya Svarka, No8, 1984, p49

2 Danchenko ME and Lappa A V, 'Underwater Cutting with Stick Electrodes, Avtomaticheskaya Svarka, No 8, 1993, p35
3 Danchenko M E et al: 'Peculiarities of Underwater Cutting Process with Flux-Cored Wire', Avtomaticheskaya Svarka, No10, 1993, p15
4 Danchenko M E et al: 'Hydrostatic Pressure Influence on Technological Parameters of Underwater Arc Cutting with Flux-Cored Wire', Avtomaticheskaya Svarka, No 1, 1989, p48
5 Lebedev V K et al: 'Calculation of Base Arc Characteristics in Underwater Mechanised Welding', Underwater Welding and Cutting of Metals, Kyiv, E.O.Paton EWI, 1980, p29
6 Danchenko M E et al: 'Underwater Arc Cutting with Flux-Cored Wire', Avtomaticheskaya Svarka, No 4, 1988, p59
7 Danchenko M E and Nefedov Yu N: 'Underwater Flux-Cored Wire Cutting, Proce Int Conf 'Welding Under Extreme Conditions', IIW, Helsinki, Finland, Sept 1989, p141
8 Danchenko M E and Nefedov Yu N: 'Choice of Optimal Parameters of Underwater Flux-Cored Wire Arc Cutting Process', Avtomaticheskaya Svarka, No 11, 1991, p61
9 Lebedev V K et al: 'Influence of Power Source Characteristics on Parameters of Underwater Arc Flux-Cored Wire Cutting Process', Avtomaticheskaya Svarka, No 1, 1988, p41
10 M.E.Danchenko and Yu. N. Nefedov: 'Underwater Cutting with Flux-Cored Wire Using Welding Semi-automatic machine', Avtomaticheskaya Svarka, No 1, 1990, p70

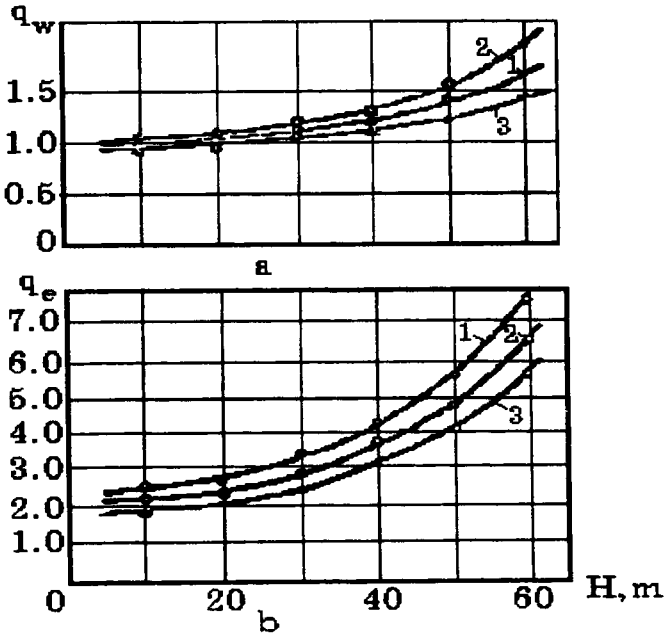

Figure 1 Dependence of flux-cored wire expenditure q_w (a) and electric energy q_e (b) per one running metre of cut on operation depth at the systems gas-forming (1), oxidising (2) and exothermic (3). Base metal thickness - 20 mm, wire feeding rate - 350 m/h, cutting current - 450...530 A, arc voltage - 40...55 V

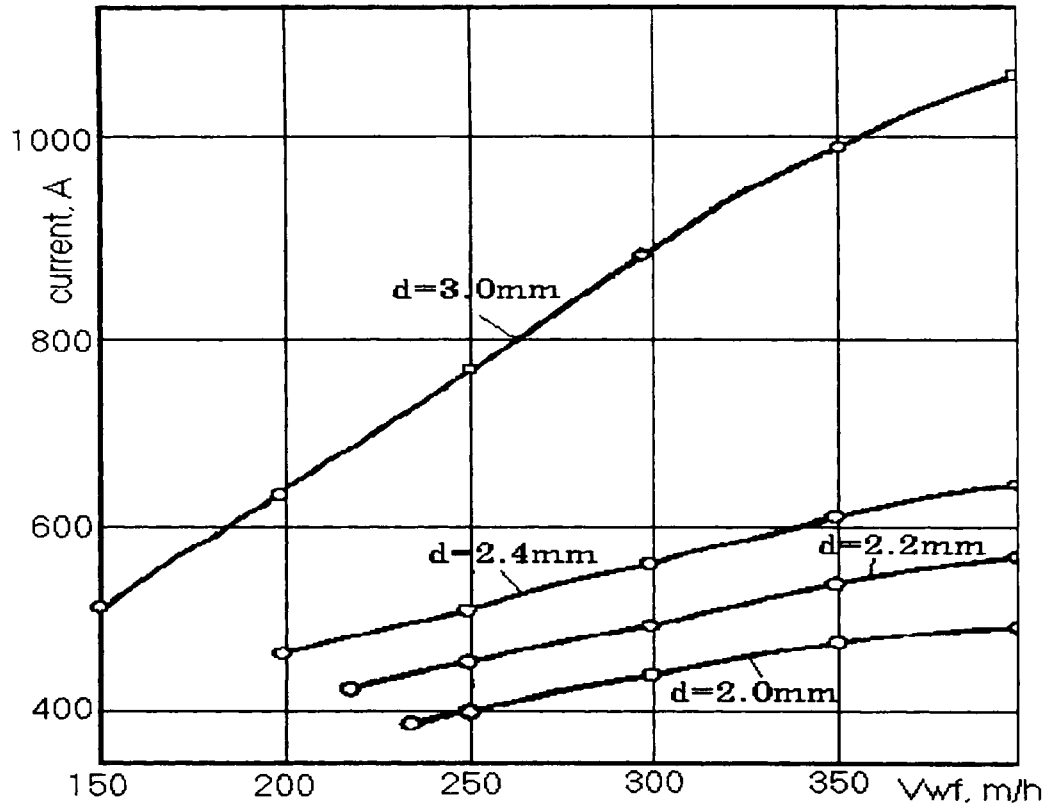

Figure 2 Relationship between cutting current and electrode wire feed speed (operation depth 0.3 m): wire dia - 2.0, 2.2, 2.4, 3.0 mm

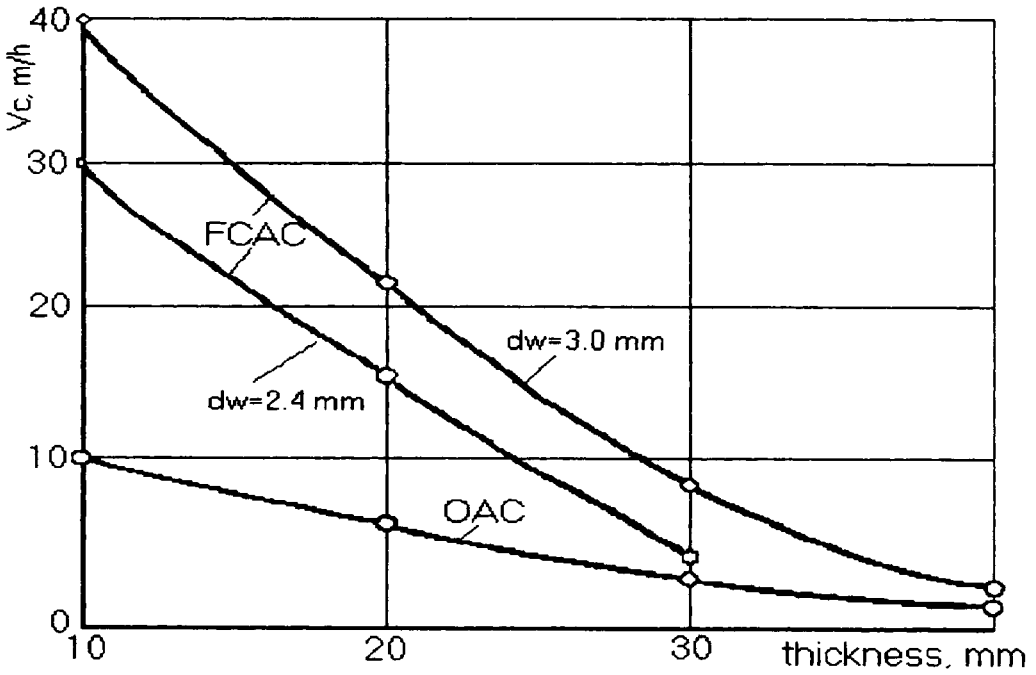

Figure 3 Relationship between underwater cutting speed and thickness of sheet being cut (St3) in FCAC (Vwf=350 m/h) and OAC

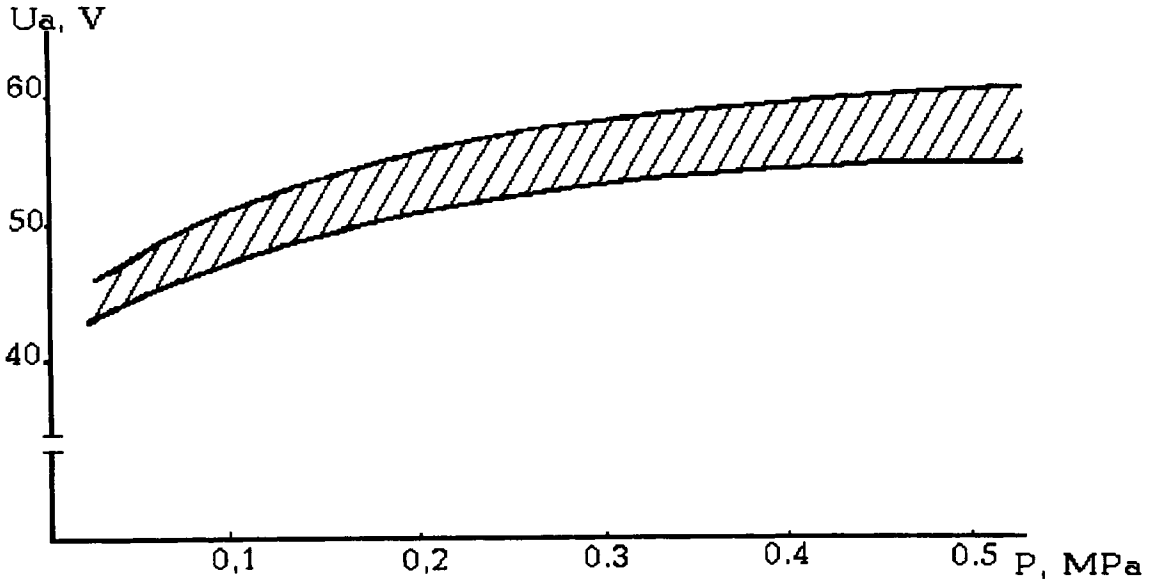

Figure 4 Effect of hydrostatic pressure on the voltages which provide stable arc burning

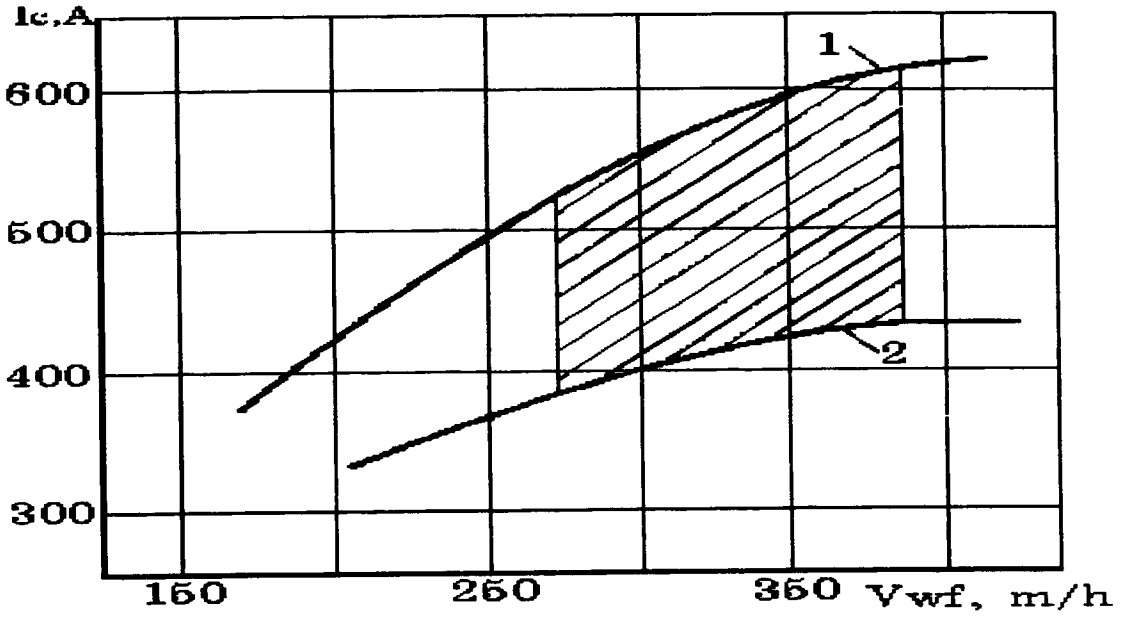

Figure 5 Dependencies of the cutting current on flux-cored wire feeding rate at operation depths from 10 m to 60 m:
1 - P=0.1 MPa, 2 - P=0.6 Mpa

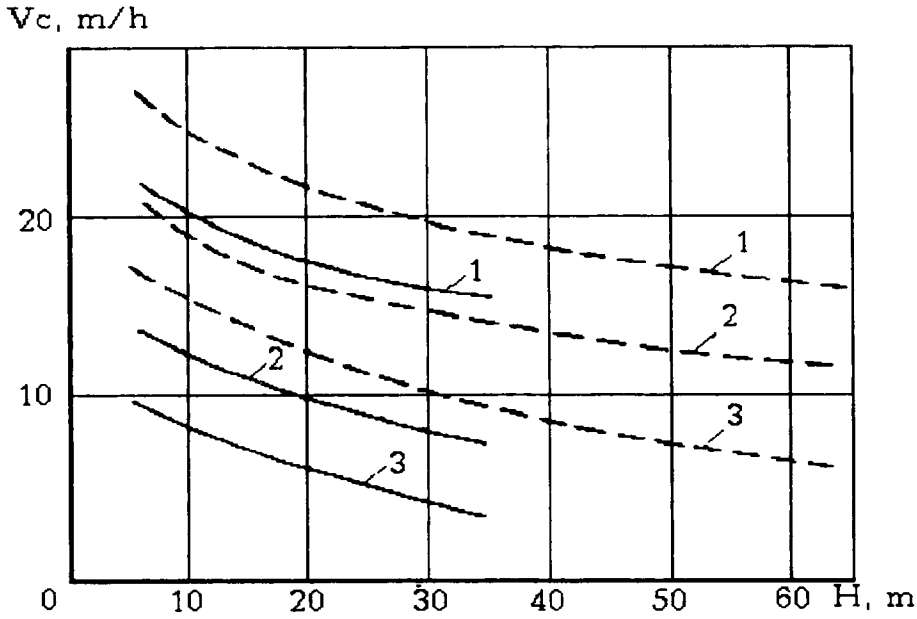

Figure 6 Dependence of cutting speed Vc on operation depth H:
1 - thickness of metal 10 mm; 2 - thickness of metal 15 mm;
3 - thickness of metal 30 mm;
——— wire dia 2.0 mm; -- -- -- - wire dia 2.4 mm

Underwater FCA wet welding

W Lucas, TWI
M A Cooper, Ministry of Defence, UK

INTRODUCTION

Underwater welding and cutting can be carried out using either dry (hyperbaric) or wet welding techniques. As a special habitat is not required, wet welding offers the advantages of low equipment costs and versatility in that the operations are only limited by access to the welder. Wet underwater welding is, therefore, the preferred technique in repair situations. In Europe and the USA, wet welding is carried out using the manual metal arc (MMA) process using special electrodes which have a water-proof coating. The limitations of MMA wet welding are as follows:

- As welding is intermittent due to the length of the rod, production rates are low.

- Direct contact with water causes rapid solidification of the weld pool which can result in a poor weld bead profile, and the rapid cooling of the weld metal and heat affected zone (HAZ) can produce low toughness, especially in low alloy steels.

- The large amount of hydrogen and oxygen generated by the arc reduces the toughness and ductility of the welds.

The E. O. Paton Institute has recently developed a new generation of wet welding and cutting techniques based on the self-shielded flux cored arc (FCA) process. The FCA wires have been developed specifically for operating in contact with water and the novel wire feed system can be completely immersed in the water. When employed in either cutting or welding operations, the FCA process offers the potential for significant productivity benefits from the use of a continually fed wire compared with MMA where the rod electrodes must be changed at frequent intervals. Furthermore, it is claimed that the combination of the flux formulation and wire composition produces the desired slag-gas forming reactions which will not only improve the weld bead profile but also reduce the pick up of hydrogen and oxygen in the weld metal.

The wet underwater FCA welding and cutting techniques have been employed quite widely in member countries of the former Soviet Union in applications such as for the repair of ships, pipelines and offshore structures. However, there is little experience in the Western Europe and the USA of the FCA process, the properties of the consumables and the operating performance of the equipment. As the FCA process appears to offer substantial benefits for cutting and welding operations, a series of welding trials were carried to evaluate the FCA process (consumables and equipment) with the intention of substantiating the claims for wet underwater welding and cutting both with regard to the benefits in welding characteristics and productivity.

WELDING EQUIPMENT

TWI has recently installed a new facility at Abington for carrying out wet welding and cutting trials. The facility is being used for research and development purposes, for example, in equipment evaluation and consumable development. The facility has been designed to be versatile in that welding can be carried out either with the welder standing outside the tank or totally immersed inside the tank i.e. to represent more closely actual diving conditions; the maximum depth of water in the tank is 1.5.

FCA Wire Feeding System

The unique feature of the FCA wire feeding system, Fig 1, is that it has been designed to operate fully submerged with only the control panel required to be outside the tank with the power source. The wire feed container is filled with water to balance the hydrostatic pressure when operating underwater (at depths up to 40m). The drive motor and reduction gear is contained in a sealed unit which is filled with a dielectric liquid, to provide insulation from the water.

The wire is held on a small reel with a capacity of 3.5kg. If necessary, a new reel of wire can be fitted by the welder/diver whilst underwater.

Power Source

For welding and cutting, a conventional flat (voltage-current) characteristic power source is employed but it must have relatively high open circuit voltage of 60V for operating underwater. The maximum current is normally limited to 400A (60% duty cycle).

System Control

The system is controlled remotely from the welder/diver for safety reasons. The control console, Fig 2, contains the electronics for controlling the wire feed motor, circuit tests, parameter measurements and indicators. In a diving situation, the welder will instruct the equipment controller on the surface to switch on/off the power source and wire feed and to regulate the power source voltage and the wire feed speed.

WELDING PERFORMANCE

The stability of the FCA wire for wet welding is characterised by the behaviour of the arc and the formation and collapse of the vapour-gas bubble which surrounds the arc and weld pool. As the wire is essentially a rutile type, molten metal transfers from the wire to the weld pool by the short circuiting mode of metal transfer. When welding in the flat position, the process is stable with a relatively quiescent arc within a stable gas bubble. To achieve process

stability (stable metal transfer and gas shield) in welding, the preferred wire diameter for welding is 1.2mm which produces a deposition rate of typically 1 kg/hr in the vertical position and up to 2 kg/hr in the flat position. The slag which is formed on the weld bead, is relatively easily removed.

When welding in position, the arc/metal transfer and vapour-gas bubble are less stable. A characteristic feature is that the bubble will periodically detach itself from the wire tip, usually during a short circuit and the arc is momentarily extinguished. Joints in the vertical position are more difficult to weld and greater skill is required to produce satisfactory weld penetration and bead profile. The vertical-up position is recommended for these wires to minimise the risk of fusion defects but the welder may find it easier to produce a smoother bead profile in the vertical-down position.

As shown for fillet joints in 8mm thick plate, weld penetration is particularly good as shown for the root pass in the vertical position, Fig 3a. The final weld also shows good sidewall fusion with no indication of cracks or porosity, Fig 3b .

WELDING TIMES

Typical welding parameters for FCA and MMA welding of butt joint and fillet joints which were produced by PWI and TWI, are given in Tables 1 and 2, respectively. The FCA wire was 1.2mm diameter, C Mn steel (type PPS-AN2) and the MMA rod was 4.0mm diameter, C Mn steel (type EPS-AN1).

A breakdown of the time to weld 1m length of 14mm thick steel was produced by the Paton Institute for FCA and MMA wet welding a butt joint in the flat and vertical positions, Table 3. In the flat position, the FCA weld was completed in 5 passes whereas the MMA weld required 10 passes. The considerably longer (total) welding times for MMA, more than double that for FCA welding, resulted not only from the greater number of passes but also the additional time required for changing the electrodes and the deslagging operations. In the vertical position, the welding, or arcing, times are comparable but the additional time for electrode changing and deslagging substantially increases the total time required for MMA welding operations.

WELDING COST ANALYSIS

The comparative costs of wet underwater welding using the MMA and FCA processes are shown in Fig 4. The costs are based on the times required to weld butt joints in 14mm thick plate using a qualified diver/welder and skilled in the use of the FCA process. As deslagging the welds between runs was carried out manually, the use of a mechanised cleaning tool should substantially reduce the time recorded for this operation. The consumable and labour costs are estimated figures but based on typical costs in the UK.

The greatest cost was for MMA welding in the vertical position due to the larger number of passes. As the number of passes were lower in the flat position, the overall cost was reduced.

FCA welding gave a significant reduction in the welding costs primarily because of the continuously fed wire electrode. In comparison, when using the MMA process, the welder required almost a third of the total welding time to replace the electrodes and it should be noted that these times were produced under ideal welding conditions i.e. in a tank. There were also significant gains in applying the FCA process from using a slightly higher welding current, fewer weld passes and a reduction in the amount of cleaning.

FCA CUTTING

The FCA process can also be readily used for cutting operations. A 2.1 mm diameter wire is normally employed which generates a more forceful arc and gas 'jet'. The process appears to work equally well in the vertical - down and horizontal - vertical positions. However, when cutting in the vertical - up position, it was significantly more difficult to maintain the cut opening.

The typical appearance of the FCA cut in 8mm thick plate for the horizontal-vertical is shown in fig 5. The cut edge was reasonably square but with a rough surface.

APPLICATIONS OF FCA SYSTEM

The wet underwater FCA welding and cutting techniques have been employed quite widely in member countries of the former Soviet Union in applications such as for the repair of ships, pipelines and offshore structures. Unfortunately, as similar equipment has not been available commercially, there is little experience in Western Europe and the USA of the FCA process.

In the former Soviet Union, the FCA system has been employed in the repair of ships and dock structures. Relevant application areas include:

- Sealing of hulls damaged by underwater obstructions or icebergs
- Repair of corrosion damage
- Repair of screw propellers and rudders
- Floating dock repairs and harbour installations

Based on TWI's evaluation tests at Cambridge, there is no doubt that the FCA system offers a substantial advantage over conventional MMA for wet welding and cutting operations, especially in those situations where a large amount of welding/cutting must be carried out. Although the process was designed for manual welding, it opens up the possibility of remote operation using an ROV. However, the successful application of the process will depend upon the reliability of the system to ensure that the economic benefits, to be derived from continuous operation, can indeed be realised.

Table 1 Parameters for Underwater, Wet Welding Butt Joints in 14mm Thick Steel
(Data produced by PWI, Kiev)

PARAMETER	WELDING POSITION			
	FLAT		VERTICAL	
	FCA	MMA	FCA	MMA
Welding Current	170-180A	170A	140A	160-180A
Arc Voltage	32v	27v	26v	24v
Welding Speed	106mm/min	111mm/min	96mm/min	107mm/min
Number of Runs	5	10	5	12
Number of Rods		50		60
Weight Consumed			3.218kg	3.600kg
Weight Deposited			1.218kg	1.750kg

Table 2 Parameters for Underwater, Wet Welding Fillet Joints in 8mm Thick Steel
(Data produced by TWI, Cambridge)

PARAMETER	WELDING POSITION			
	FLAT		VERTICAL	
	FCA	MMA	FCA	MMA
Welding Current	139-151A	170A	127-132A	150A
Arc Voltage	26-32v	27v	27-29v	28v
Wire Feed Speed				
Welding Speed	manual	manual	manual	manual
Number of Runs	3	3	3	3
Deposition Rate	1.98kg/hr	1.07kg/hr	1.9kg/hr	1.14kg/hr

Table 3 Breakdown of Time to Weld 1m Length of 14mm Thick Steel
(Data produced by PWI, Kiev)

TYPE OF OPERATION	TIME, mins			
	FLAT POSITION		VERTICAL POSITION	
	FCA	MMA	FCA	MMA
Welding	47 (5)	90 (10)	104 (5)	112 (12)
Slag removal	38	72	41	95
Electrode changing	None	30	None	36
TOTAL	85	192	145	243

( ) Number of runs

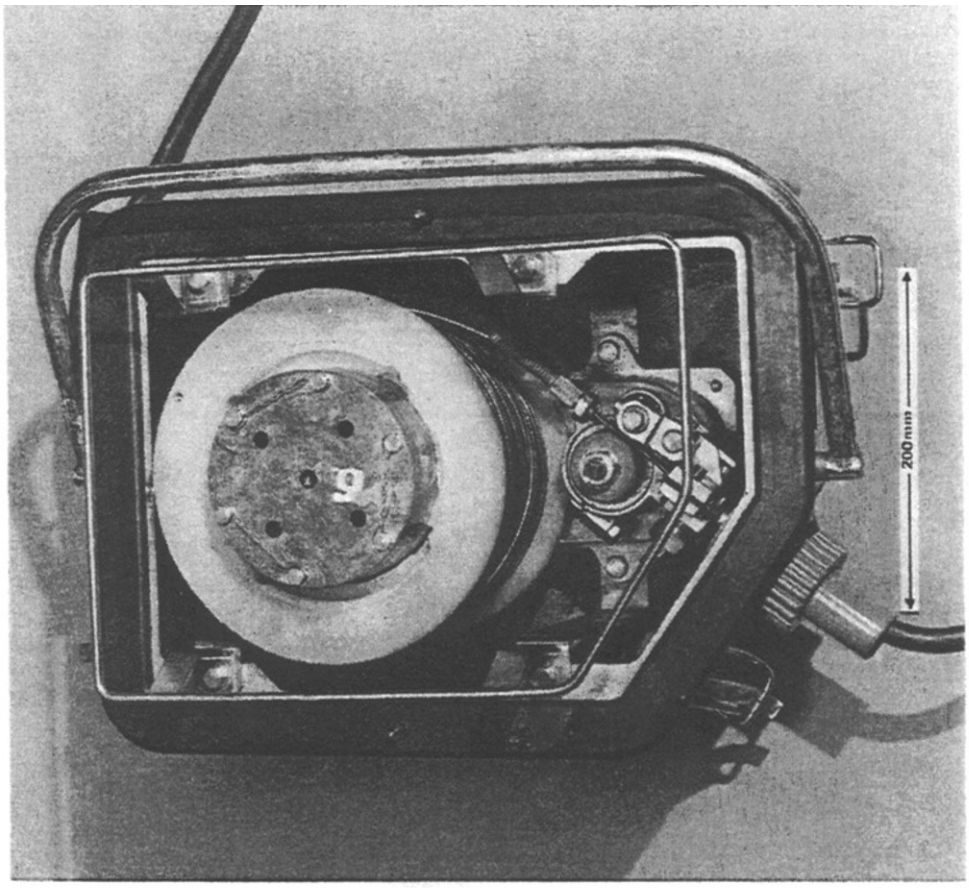

010, 066/4

Fig 1 FCA wire feeding system for wet welding

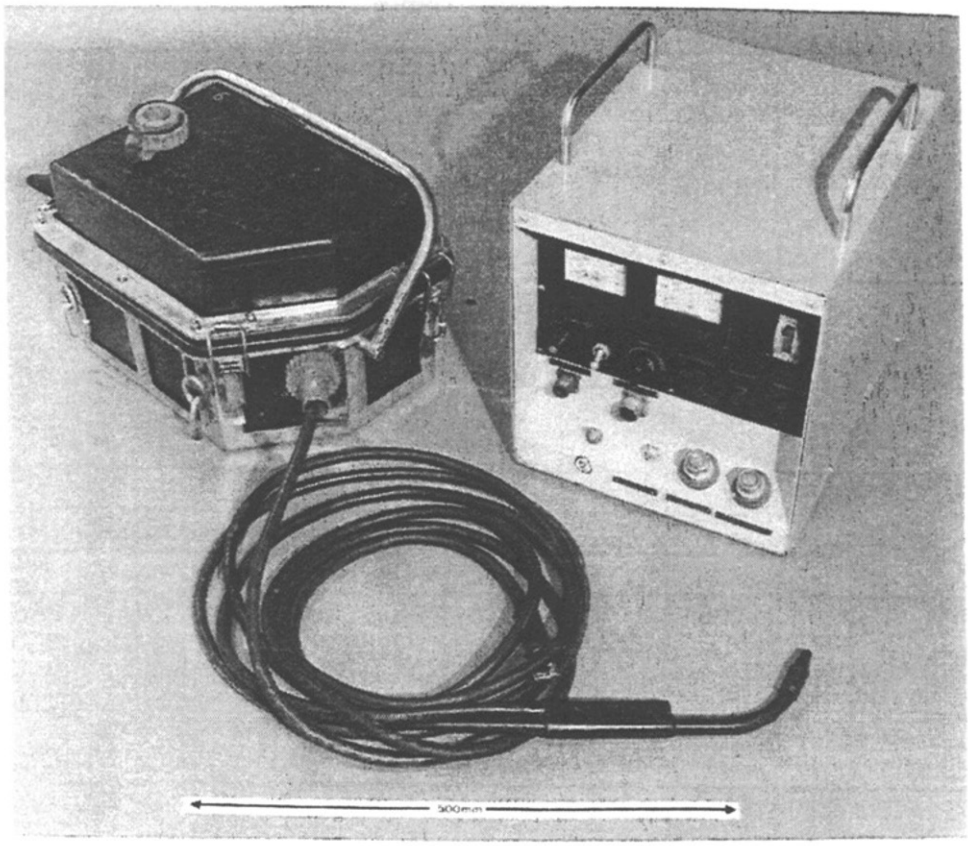

010,066/9

Fig 2 FCA wire feed system, welding gun and control console

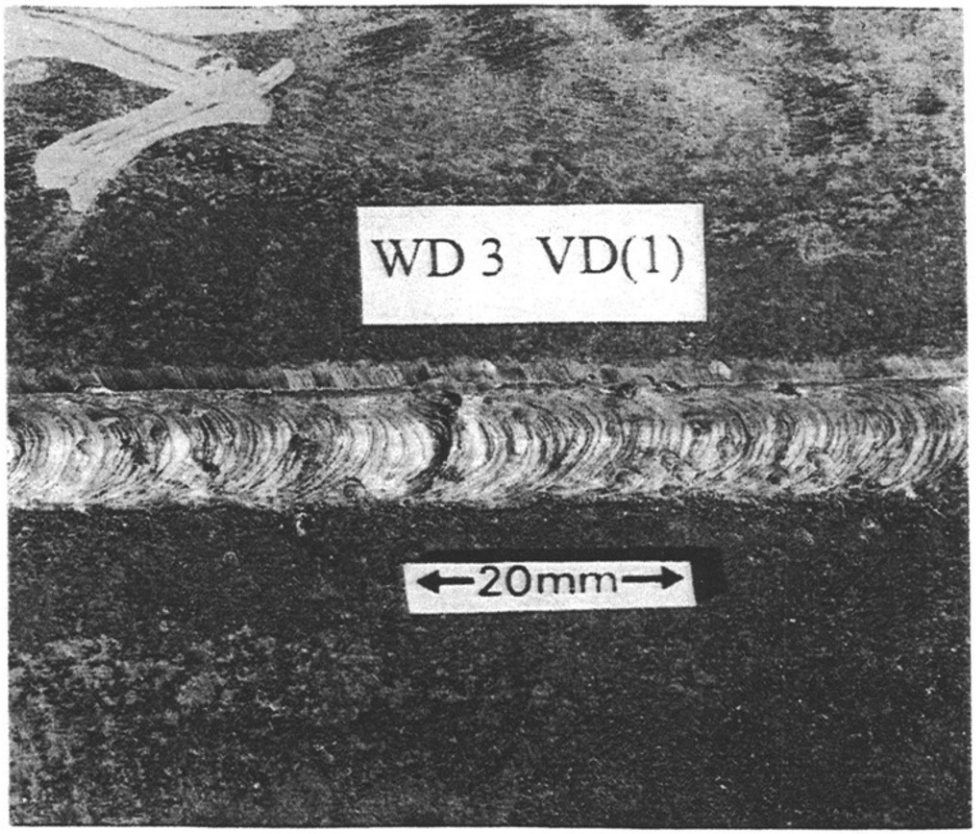

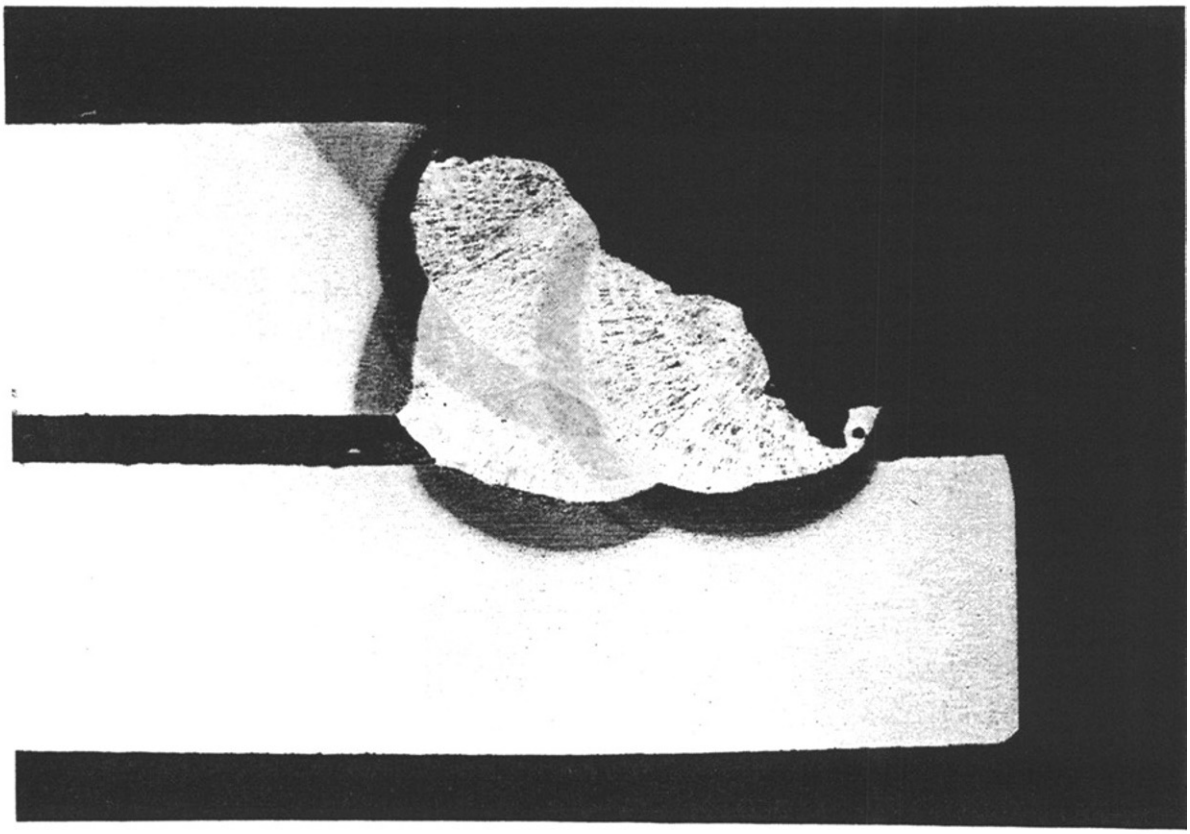

Fig 3 FCA wet weld in 8mm thick, C Mn steel plate welded in the vertical down position

a) general appearance of root pass

b) cross section through complete, 3 pass weld

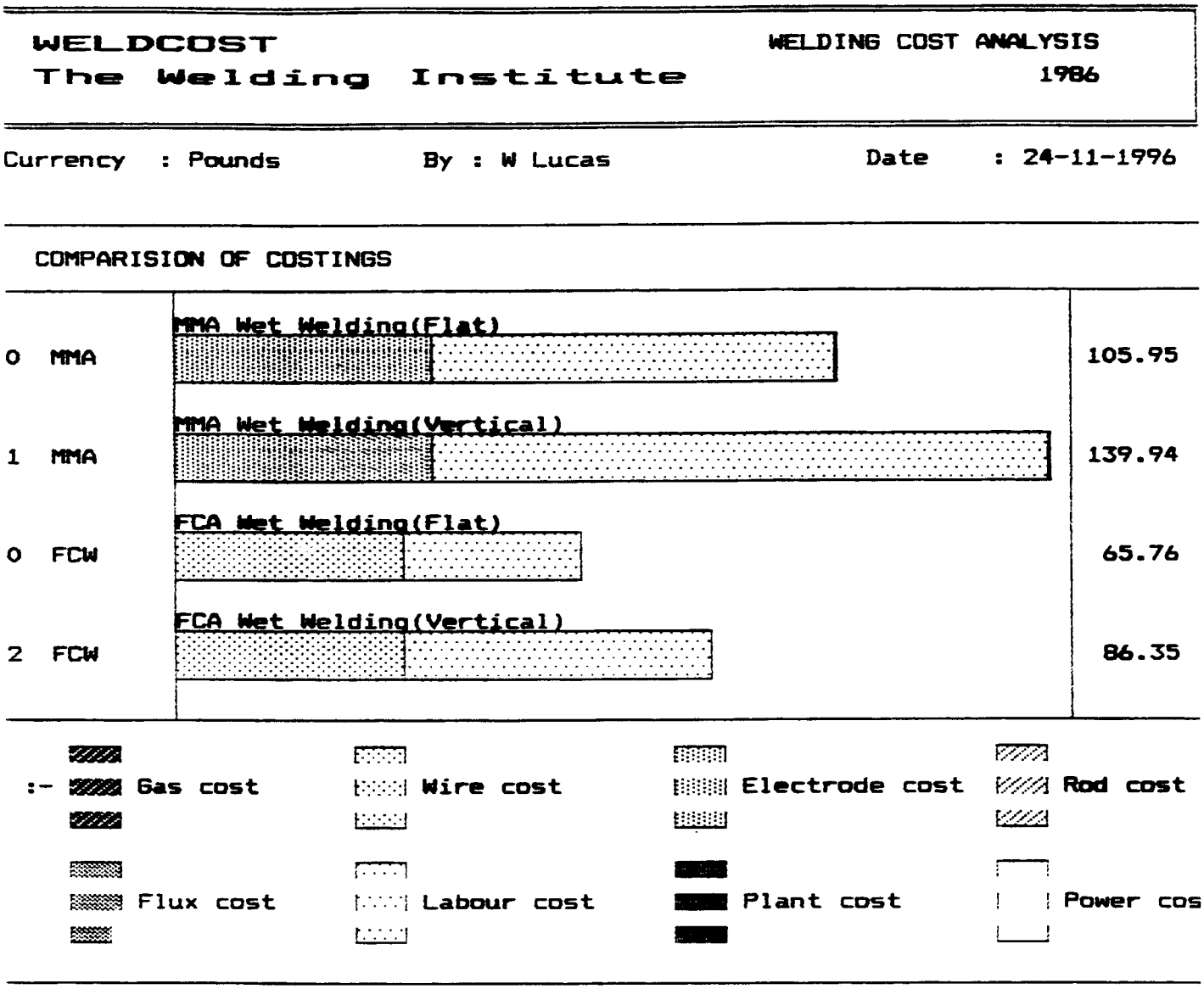

Fig 4 Comparative costs for FCA and MMA wet welding of 14mm thick plate

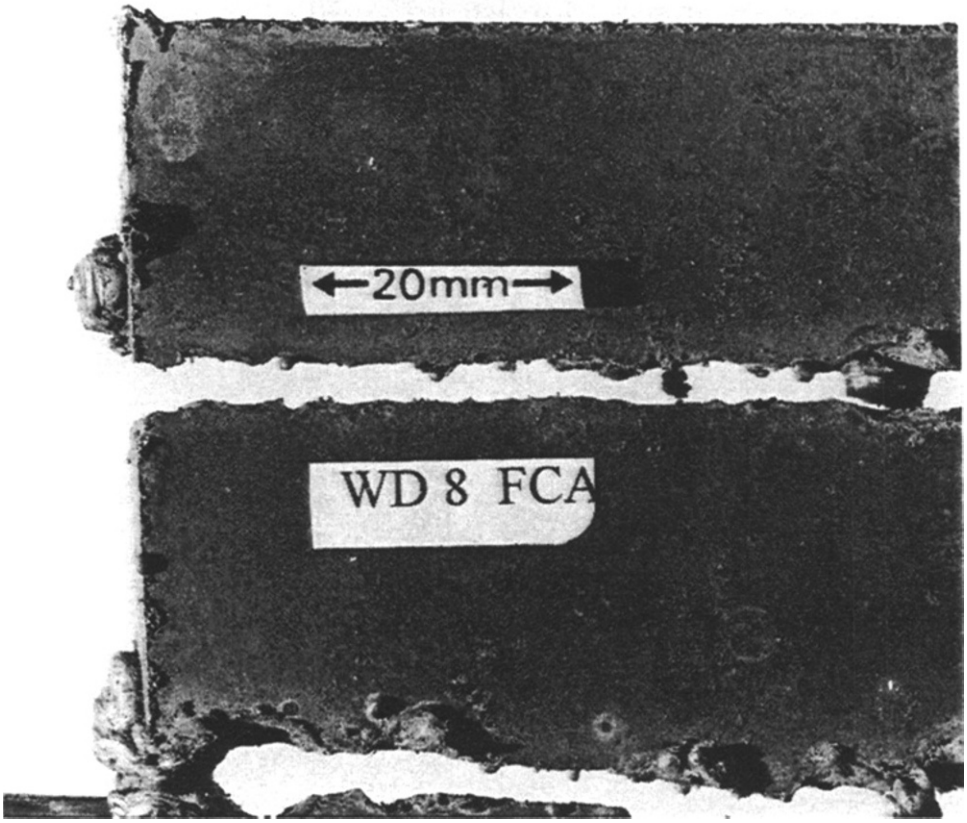

Fig 5 Appearance of FCA cut in 8mm thick C Mn steel which was cut in the horizontal-vertical position